Oregon State University | College of Forestry

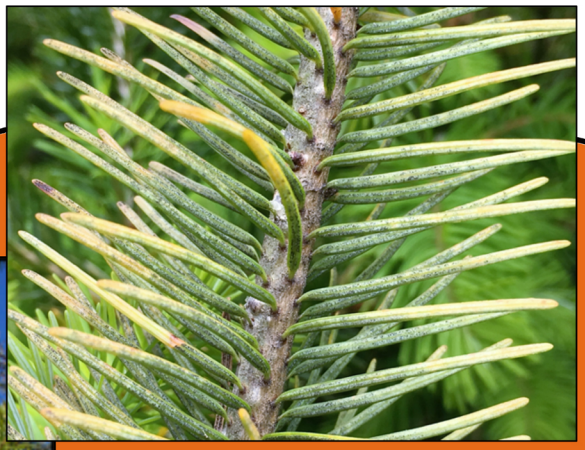

2018

ANNUAL REPORT

SWISS NEEDLE CAST COOPERATIVE

Members of the Swiss Needle Cast Cooperative

Bureau of Land Management

Cascade Timber Consulting

Greenwood Resources, Inc. Lewis & Clark Tree Farms, LLC

Oregon Department of Forestry

Starker Forests

Stimson Lumber

USDA Forest Service

Weyerhaeuser Corporation

Swiss Needle Cast Cooperative Staff

Dave Shaw – Director and Associate Professor of Forest Health

Gabriela Ritóková – Assistant Director

Edited by Gabriela Ritóková and David Shaw

Table of Contents

SNCC Income Sources and Expenditures: 2018

Income

Membership dues	80,000
Oregon State Legislature	95,000
Carry-over	113,341
Total 2018 Income	**$288,341**

Expenditures

Salaries and wages	149,706
Travel	8,211
Operating expenses	4,666
Materials and Supplies	1,558
Indirect Costs	21,338
Total 2018 Expenditures	**$185,479**

Balance	**$102,862**

SNCC Background and Organization

A major challenge to intensive management of Douglas fir in Oregon and Washington is the current Swiss needle cast (SNC) epidemic. Efforts to understand the epidemiology, symptoms, and growth losses from SNC have highlighted gaps in our knowledge of basic Douglas-fir physiology, growth, and silviculture. The original mission of the Swiss Needle Cast Cooperative (SNCC), formed in 1997, was broadened in 2004 to include research aiming to ensure that Douglas-fir remains a productive component of the Coast Range forests. The SNCC is located in the Department of Forest Engineering, Resources and Management within the College of Forestry at Oregon State University. The Membership is comprised of private, state, and federal organizations. Private membership dues are set at a fixed rate. An annual report, project reports, and newsletters are distributed to members each year. Our objective is to carry out projects in cooperation with members on their land holdings.

SNCC Mission

To conduct research on enhancing Douglas-fir productivity and forest health in the presence of Swiss needle cast and other diseases in coastal forests of Oregon and Washington.

SNCC Objectives

(1) Understand the epidemiology of Swiss needle cast and the basic biology of the causal fungus, *Nothophaeocryptopus gaeumannii*.

(2) Design silvicultural treatments and regimes to maximize Douglas-fir productivity and ameliorate disease problems in the Coast Range of Oregon and Washington.

(3) Understand the growth, structure, and morphology of Douglas-fir trees and stands as a foundation for enhancing productivity and detecting and combating various diseases of Douglas-fir in the Coast Range of Oregon and Washington.

Department of Forest Engineering, Resources & Management
Oregon State University, 280 Peavy Hall, Corvallis, Oregon 97331
T 541-737-4952 | **F** 541-737-4316 | http://ferm.forestry.oregonstate.edu/

February 2, 2019

To: Swiss Needle Cast Cooperative Members

From: David Shaw, Director, and Gabriela Ritóková, Assistant Director
Swiss Needle Cast Cooperative, College of Forestry, Oregon State University

Dear SNCC Members,

The Swiss Needle Cast epidemic in the PNW continues into 2018 but the aerial detection surveys (ADS) are noting significant drops in acreage observed, especially for Washington State. We believe the drops in ADS numbers for SNC in Oregon and Washington relate to the drought and dry early summers we have experienced since 2015. In British Columbia however, SNC is intensifying in some localized regions, especially in SW Vancouver Island and east of Vancouver in the low-elevation, and wet, Fraser River Valley sub-basins.

In case you have not heard, the scientific name for the fungal pathogen that causes Swiss needle cast has been changed from *Phaeocryptopus gaeumannii*, to *Nothophaeocryptopus gaeumannii*, and it was moved to a new family; the Mycosphaerellaceae, which includes some of the worlds' most important foliage diseases including Dothistroma needle blight of pines.

We are beginning to publish results from analysis of the first measurement of our SNCC Research and Monitoring Plot Network. The initial focus has been on associations between SNC and nutrients, climate factors, and how foliage retention and disease severity vary on the landscape. Other graduate student projects include Yung-Hsiang (Sky) Lan's dissertation chapter investigating how disease relates to canopy structure on young and old trees. In addition, Patrick Bennett completed a Ph.D. with Jeff Stone on the molecular ecology of *N. gaeumannii*, while Jonathan Burnett completed a Ph.D. with Michael Wing which included testing the utility of drones to survey SNC.

Currently, Andrew Russo, an MF student in Forest Engineering, Resources and Management is using GIS tools to explore patterns of the ADS-observed symptoms of SNC. His report, contained herein, has found no real eastward advance of ADS-observed SNC symptoms in the epidemic area of Oregon since 2000. In the more than 20-years of the aerial survey, his work shows that 75% of the symptomatic area has remained within ~15 miles of the coast.

We continue to monitor the Cascade Foothills of Oregon with both aerial detection survey (every-other-year), and annual monitoring of 37 plots on Weyerhaeuser, CTC, and small woodland owners plantations below 2,500 ft elevation. These plots show a lot of variability, but a number of stands are averaging under 3 years of needle retention.

The SNCC also continues to interact with a broad range of researchers, and leverage as much work on SNC as we can by collaboration with and education of the research community. Finally, Gabriela is leading the writing of a revision of the Silviculture Guide for SNC, which we hope will provide another resource for managers. Thanks to the SNCC membership for supporting the important work of the cooperative, we continue to keep the focus on Douglas-fir forest health.

Sincerely,

David C. Shaw

Gabriela Ritóková

2018 Swiss Needle Cast Aerial Survey

Sarah Navarro and Danny Norlander
Oregon Department of Forestry

Survey procedures

The observation plane flew at 1,500 to 2,000 feet above the terrain, following north-south lines separated by 2 miles. Observers looked for areas of Douglas-fir forest with obvious yellow to yellow-brown foliage, a symptom of Swiss needle cast (SNC). Patches of forest with these symptoms (patches are referred to as polygons) were sketched onto computer touch-screens displaying topographic maps or ortho-photos and the position of the aircraft. Each polygon was classified for degree of discoloration as either "S" (severe) or "M" (moderate). Polygons classified as "S" had very sparse crowns and brownish foliage, while those classified as "M" were predominantly yellow to yellow-brown foliage with slightly denser crowns than those classified as "S". The survey area extended from the Columbia River in Oregon south to the Del Norte County line in California, and from the coastline eastward until obvious symptoms were no longer visible. In 2018, we surveyed a portion of the west slope of the Cascade Range, from Lane County north through Clackamas County.

Oregon utilized the national standard Digital Mobile Sketch Mapper for the SNC survey in 2018. The system syncs the data directly to a national database housed in the USDA Forest Service and makes for an easily consumable and robust system for collecting aerial survey data. With this new system, the area is recorded in much the same way as the previous digital system, but incorporates some important changes, one being the metric used to record survey information. For defoliators such as SNC, we gain the area of the treed area affected in addition to the intensity of defoliation. This means that we can now record the intensity (severe or moderate) and the amount of the stand/polygon/area of interest that has damage. This is very useful for mixed stands where there may be a mix of host and non-host species.

Results

The survey was flown on May 3, 7, 23, 30, and June 5 and 7, 2016 and covered 3,359,099 acres in the Coast Range and 452,286 acres in the Cascade Range (figure 1). Bud break and SNC symptoms were on track this year, but was delayed mid-May due to weather, airplane maintenance, and USFS inspection of ODF aircraft. Despite this, symptoms remained visible to observers well after bud-break and into June.

The survey showed a slight decrease in the area of forest with symptoms of Swiss needle cast compared to the previous 5 years, the second decrease observed in six years. In the Coast Range we mapped 413,081 acres of Douglas-fir forest with obvious symptoms of SNC

(figure 2). As has been the case for the past several years, the easternmost area with obvious SNC symptoms was approximately 28 miles inland from the coast in the Highway 20 corridor, but most of the area with symptoms occurred within 18 miles of the coast. Figures 3 and 4 show the trend in damage from 1996 through 2016.

In 2018, as in 2016, we extended the survey south through Curry County to the Del Norte County line in California border even though few symptoms typically are observed south of Port-Orford. In Curry County we mapped only 40 polygons representing 1,860 acres with symptoms, most of them in the Port-Orford area. In Del Norte County, we mapped only 5 polygons representing 358 acres with symptoms.

In the partial survey of the Cascades Range (Lane, Linn, Marion, and Clackamas Counties), we mapped 7,219 acres of moderate SNC symptoms representing 158 polygons. A systematic survey was flown in 2018, like in 2016, in the Cascades Range in early June.

The SNC aerial survey provides a conservative estimate of damage because observers can map only those areas where disease symptoms have developed enough to be visible from the air. We know SNC occurs throughout the survey area, but discoloration often is not severe enough to enable aerial detection. The total area of forest affected by SNC is far greater than indicated by the aerial survey. The aerial survey does, however, provide a reasonable depiction of the extent of moderate and severe damage, and coarsely documents trends in damage over time.

Acknowledgements

The survey was conducted by the Oregon Department of Forestry Forest Health and Air Operations sections, and was funded by the Oregon State University Swiss Needle Cast Cooperative, the USDA Forest Service Forest, and the Oregon Department of Forestry. Chris Culp (Retired-OSP) and Dan McCarron (ODF) piloted the plane. Danny Norlander (ODF) is the survey coordinator and primary observer. Other aerial observers were Christine Buhl (ODF), Wyatt Williams (ODF) and Sarah Navarro (ODF).

Additional Notes

We appreciate any information regarding the accuracy or usefulness of the maps. If you have a chance to look at some of the mapped areas on the ground, please let us know what you observe. Please call Sarah Navarro (503-945-7394) or Danny Norlander (503-945-7395) if you have questions, suggestions, or comments.

The GIS data and a .pdf file can be accessed via the ODF web page at:
https://www.oregon.gov/ODF/ForestBenefits/Pages/ForestHealth.aspx
An online interactive ArcMap can be accessed via the Region 6 USFS web page at:
https://usfs.maps.arcgis.com/apps/MapJournal/index.html?appid=da5cda5003d24544b9231dbb8edf82fb

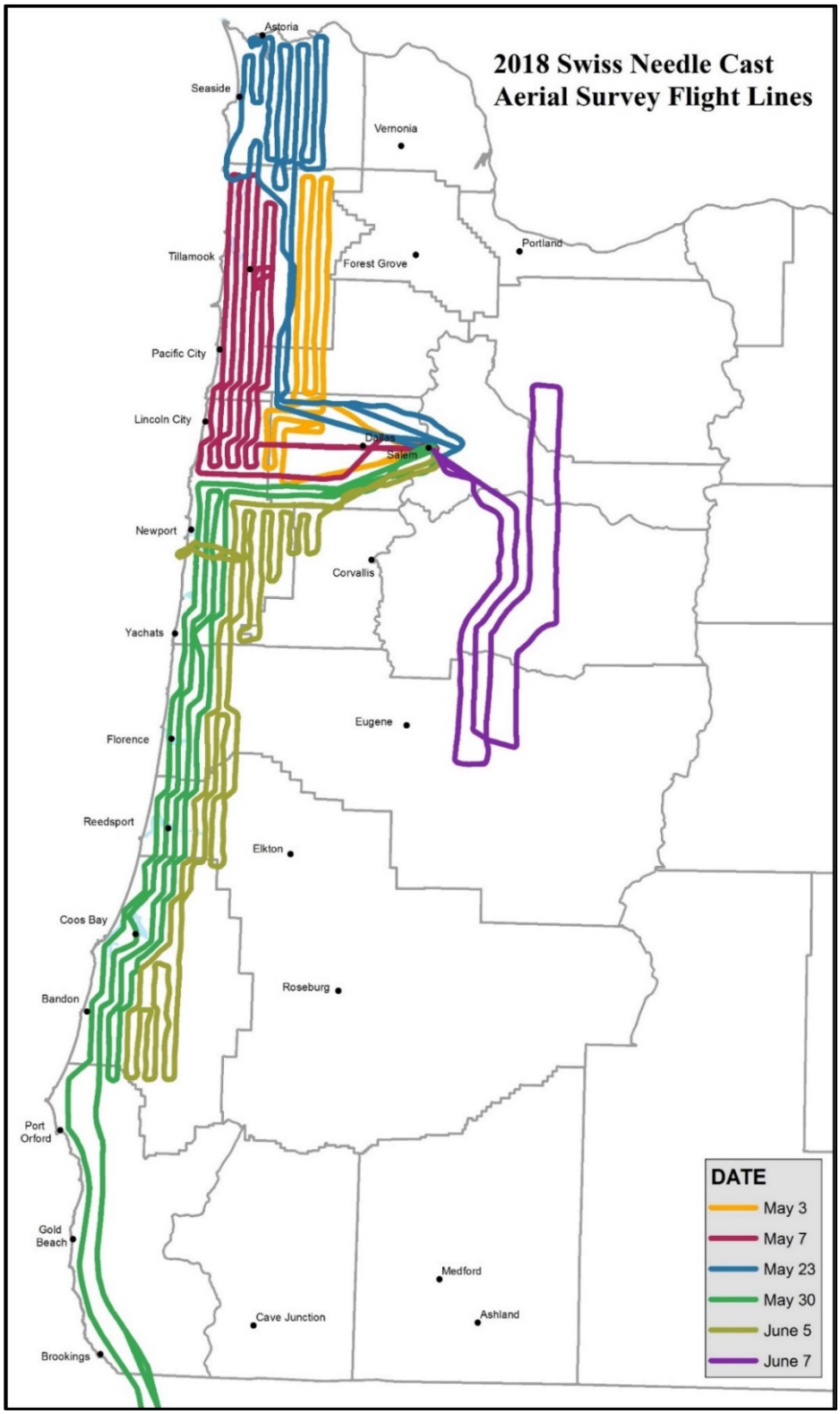

Figure 1. Area surveyed for Swiss needle cast symptoms, 2018. Flight lines are two miles apart.

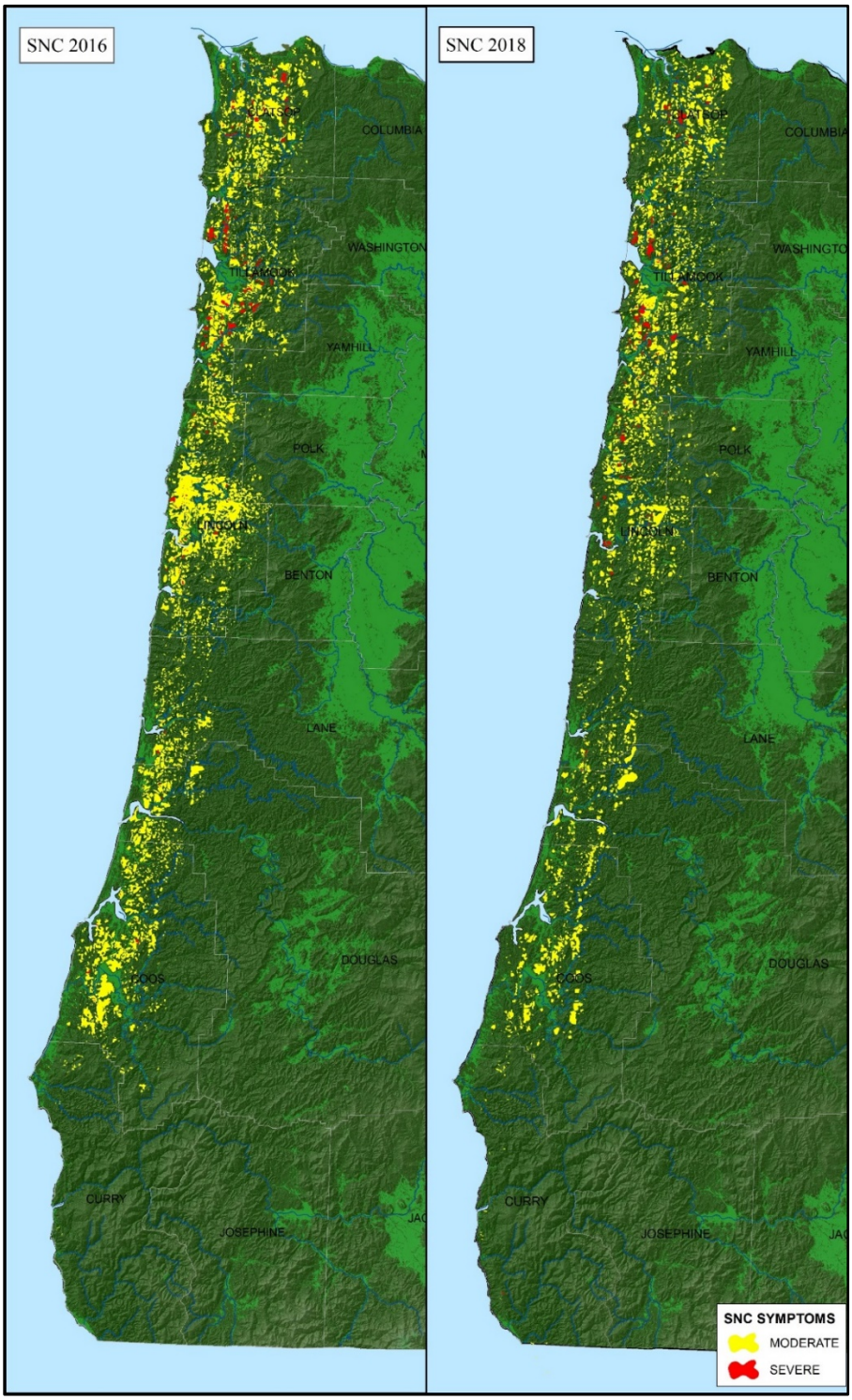

Figure 2. Areas of Douglas-fir forest with symptoms of Swiss Needle Cast detected in the 2016 and 2018 aerial surveys, Coast Range, Oregon.

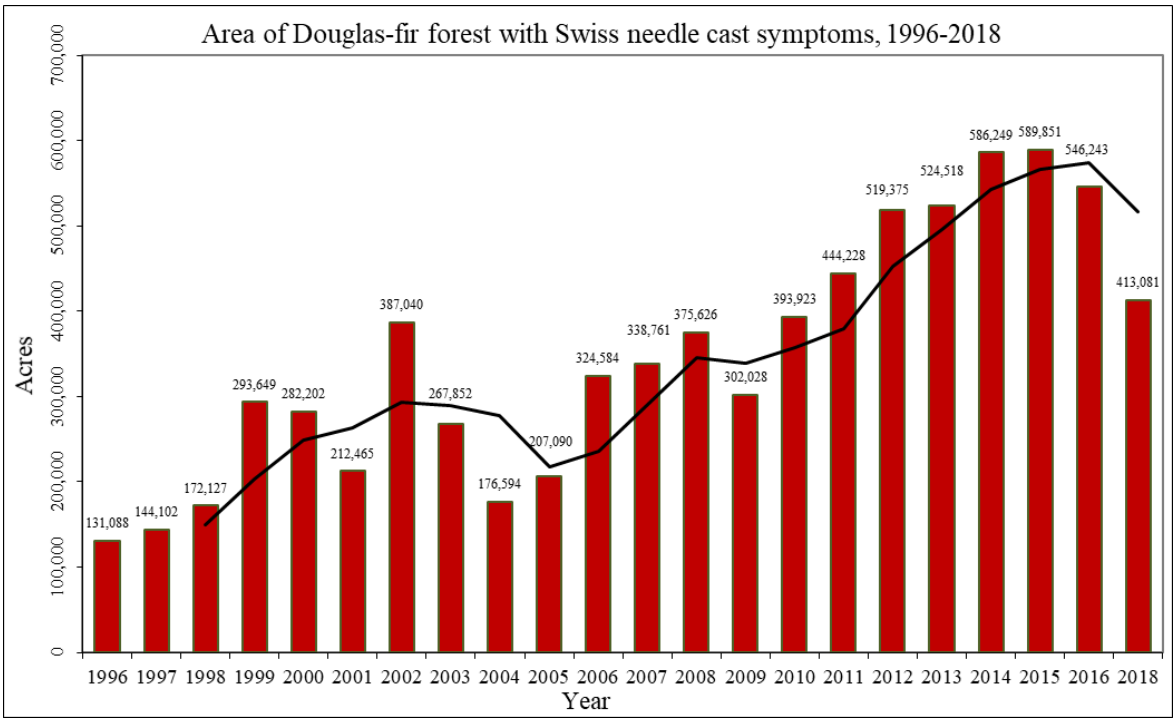

Figure 3. Area of Douglas-fir forest with SNC symptoms detected during aerial surveys conducted in April-June, 1996-2018 (2008 area estimated from partial survey consisting of 3 sample blocks). Trend line is 3-year rolling average. Coast Range, Oregon.

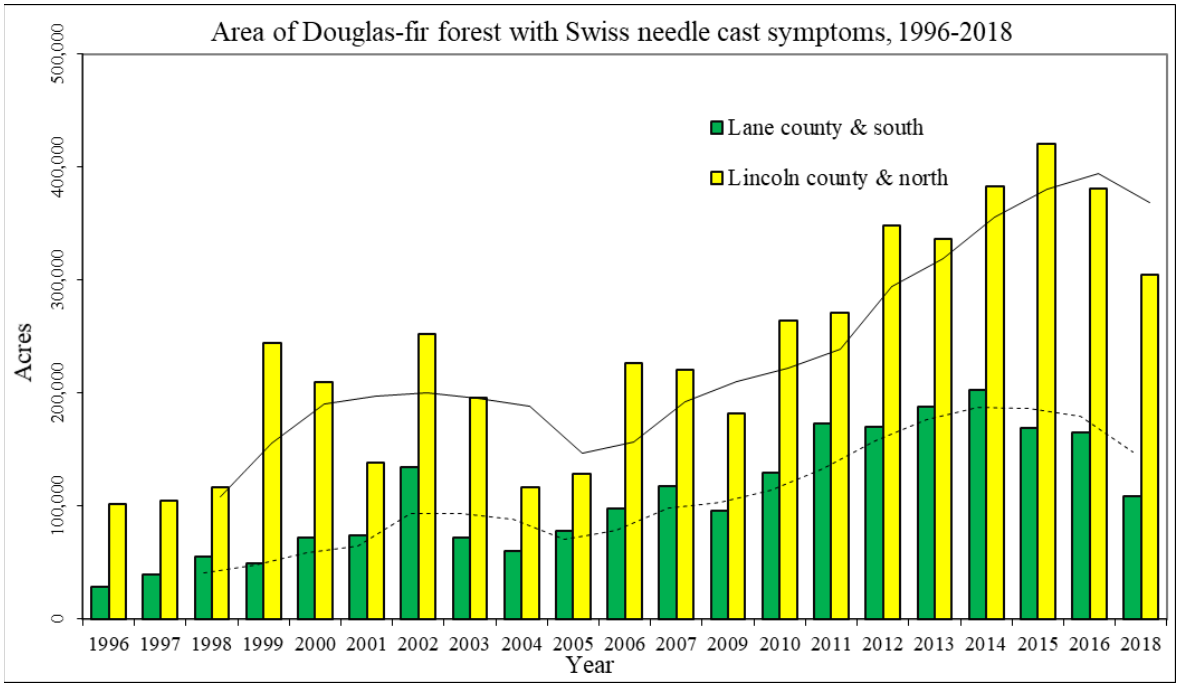

Figure 4. Area of Douglas-fir forest with SNC symptoms detected between April and June, 1996-2018; north and south halves of survey area (2008 area estimated from partial survey consisting of 3 sample blocks). Trend line is 3-year rolling average. Coast Range, Oregon.

Coastal Washington Swiss Needle Cast Aerial and Ground Survey, 2018

Amy Ramsey[1], Dan Omdal[1], Aleksandar Dozic[1], Glenn Kohler[1], Justin Hoff[2] and Marty Kimbrel[3]

[1]Washington Department of Natural Resources, Forest Health Program, Olympia, WA, [2]USDA Forest Service, Forest Health Protection, Sandy, OR, [3]Washington Department of Fish and Wildlife, Olympia, WA

Abstract

In late April and May, an aerial survey, covering 2.7 million acres, was flown to detect and map the distribution of Swiss Needle Cast (SNC) symptoms in coastal Washington (Figure 1). Nearly 79,000 acres of symptomatic Douglas-fir were mapped, which is a 68% decrease from the 248,000 acres mapped in the 2016 aerial survey and a 78% decrease from the 351,000 acres mapped in the 2015 aerial survey. Twenty-nine ground sites across the range of the aerial survey were surveyed for SNC incidence and severity, determined by counting fungal reproductive structures in the stomata of Douglas-fir needles, and Douglas-fir needle retention. An average of 2.3 years of foliage were on the trees across all sites, which is similar to the foliar retention surveyed in past years. The average percentage of occluded stomata on all sites was less than 1% for 2017 (1-year-old) foliage and 16% for 2016 foliage (2-years-old), both a reduction when compared to the data from the 2016 survey.

Figure 1. Aerial photo of Swiss Needle Cast in Douglas-fir. The light green trees are alder and the infected Douglas-fir trees are yellowish-brown.

Introduction

The fungus that causes SNC, *Nothophaeocryptopus gaeumannii* (T.Rohde) Petrak is found throughout the range of its only host, Douglas-fir (Shaw et al. 2011). Swiss Needle Cast causes premature foliage loss and defoliation and can reduce growth of host trees, alter wood properties, and affect stand structure and development (Johnson et al. 2005, Maguire et al. 2011, Weiskittel et al. 2006). The disease is most damaging near the coast due to the fungi-favorable climatic (mild winters and wet springs and summers) and topographic conditions.

An aerial survey for SNC has been conducted in the Oregon Coast Range since 1996, with over 300,000 acres of SNC symptomatic Douglas-fir mapped since 2006 and over 500,000 acres mapped each year since 2012 (Navarro and Norlander 2016).

In 2018 a SNC aerial survey was coupled with a ground survey in Washington. Ground surveys have been conducted in Washington since 1997, with aerial surveys occurring in 1998-2000, 2012, 2015, 2016 and 2018. The objective of the ground surveys is to monitor changes in incidence and severity of the disease over time.

Methods

The aerial survey observation plane flew at 1,500 to 2,000 feet above the terrain, following north-south or east-west lines separated by 3 miles. Observers looked for areas of Douglas-fir forest with obvious yellow-brown foliage, a rather generic symptom that appears to be indicative of moderate to severe SNC disease. Patches of forest with these symptoms were sketched onto computer touch-screens displaying topographic maps or ortho-photos and the position of the aircraft. Each polygon was classified for degree of discoloration as either “S” (severe) or “M” (moderate). Polygons classified as “S” (CODE, SNC-S) had very sparse crowns and brownish foliage, while those classified as “M” (CODE, SNC-M) were predominantly yellow-brown foliage with slightly denser crowns than those classified as “S”.

The 2018 Washington SNC aerial survey was flown on April 26, May 3, 14, 17 and covered 2,675,000 acres. The survey is timed to occur when the crown color symptoms have developed, but before the new foliage has emerged (bud break) in late spring. The survey area extended from the Columbia River in Washington north to the Strait of Juan de Fuca, and from the coastline eastward.

Twenty-nine ground sites were included in the SNC survey. Stand color, landscape position, elevation, aspect and average tree age were recorded for each site. Foliar retention, diameter at breast height and crown color were recorded for ten trees at each site. Foliage from 2017 and 2016 were collected from the upper third of each of the ten trees at each site and taken back to the lab for microscopic examination of *N. gaeumannii* pseudothecia, a reproductive structure of the fungus. Three hundred stomata on each of ten needles from each foliage cohort were examined for pseudothecial occurrence.

Results and Discussion

The aerial surveyors flew and made observations on 2.7 million acres of forest land in coastal Washington and mapped 79,000 of Douglas-fir with obvious symptoms of SNC (Figure 2). This is a 68% decrease from the 248,000 acres mapped during the 2016 SNC aerial survey (Figure 3, Table 1). The survey boundaries were similar to those in the 2012, 2015 and 2016 surveys.

	Severe SNC Symptoms		Moderate SNC Symptoms		Total Acres Mapped	
Year of Survey	% of total acres mapped	Severe SNC Acres	% of total acres mapped	Moderate SNC Acres	% with SNC symptoms	Total SNC Acres
2018	< 1%	6,000	3%	73,000	3%	79,000
2016	< 1%	14,000	10%	234,000	10%	248,000
2015	1%	19,000	13%	332,000	14%	351,000
2012	< 1%	6,000	8%	222,000	9%	228,000

Table 1. Total acres with Swiss Needle Cast symptoms mapped during the aerial survey, by year.

Swiss Needle Cast symptoms were detected on 3% of the total acres surveyed (Table 1). Severely symptomatic stands were generally located near Forks and the Neah Bay area and the most southwest corner of the survey, near Ilwaco. The cause of the decrease in mapped acres from 2016 to 2018 remains uncertain, but it is likely a combination of environmental factors influencing infections patterns and foliar retention, in addition to site and soil characteristics affecting water retention and soil nutrition on sites. Figure 4 shows how the 2018 SNC aerial survey compares to previous years SNC aerial surveys in Washington.

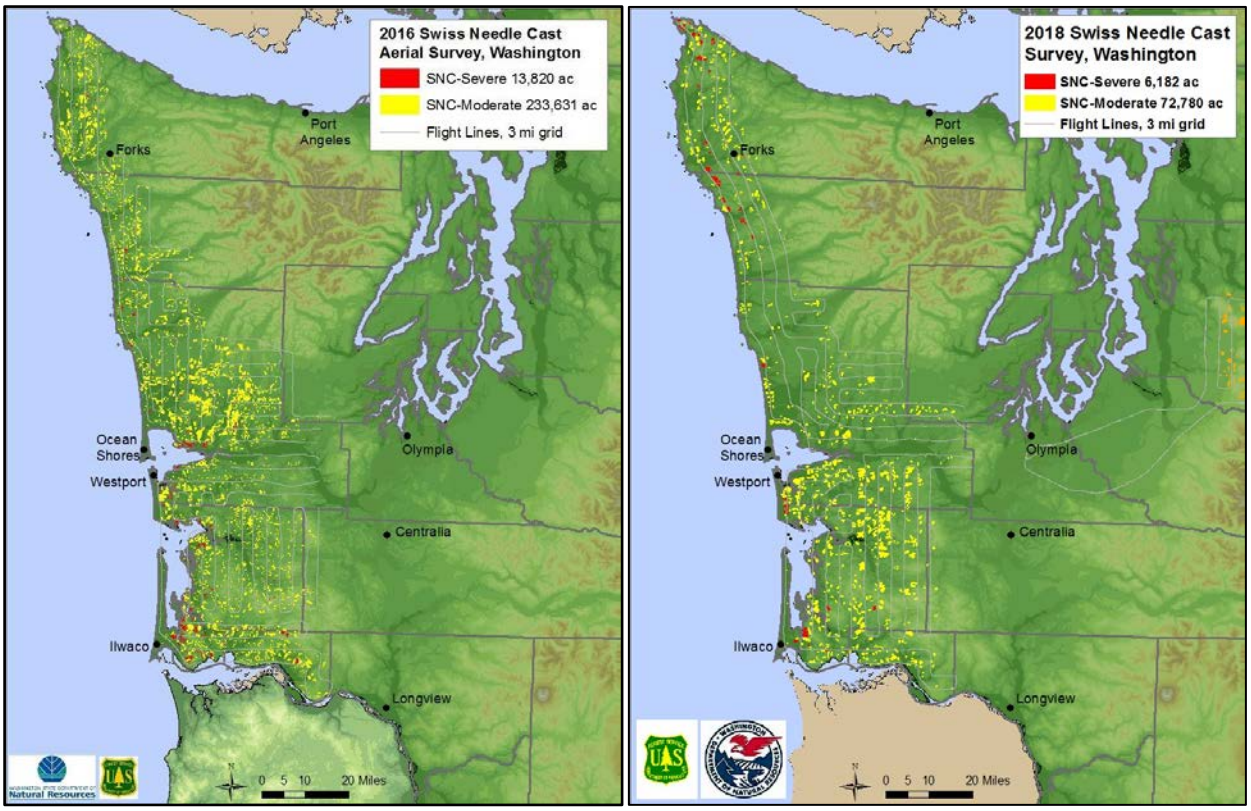

Figure 2 (right). Washington 2018 Swiss needle cast (SNC) aerial survey map. 79,000 acres of affected area mapped.

Figure 3 (left). Washington 2016 SNC aerial survey map. 248,000 acres of affected area mapped.

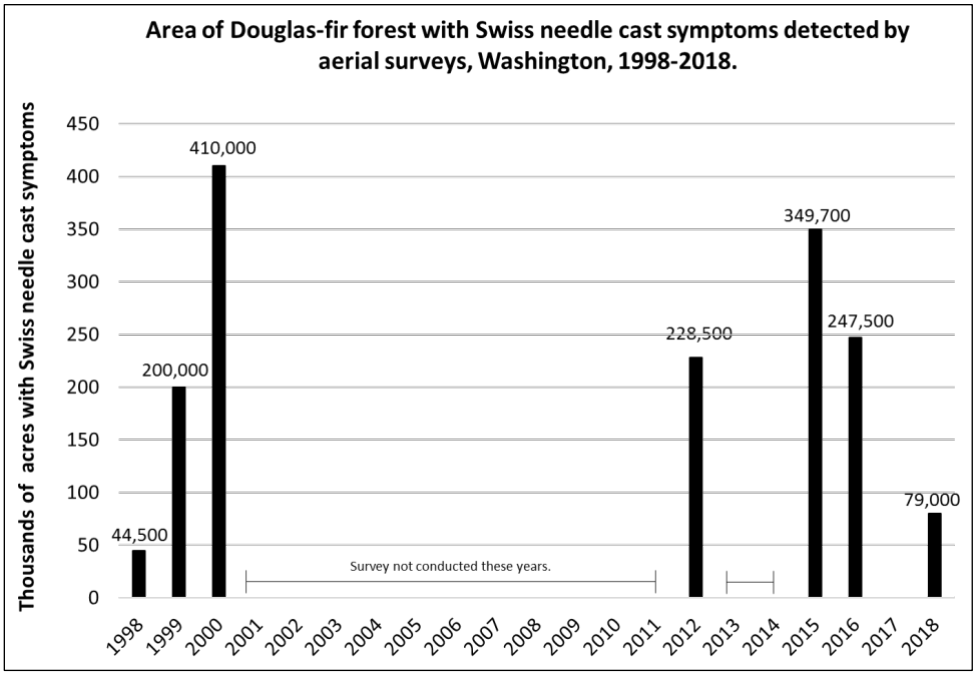

Figure 4. Area of Douglas-fir forest with Swiss needle cast symptoms detected by aerial surveys in Washington, 1998-2018.

The average percentage of occluded stomata across all sites was 1% for 2017 (1-year-old) foliage and 16% for 2016 foliage (2-years-old), with ranges from 0 to 82 percent, depending on the tree, site and needle age. Foliar retention varied across the survey area, ranging from 1.4 to 3.1 years, with an average of 2.3 years across all sixty-three ground survey sites. The amount of disease causing fungus in the foliage (pseudothecia) remains relatively stable across years of survey, as does the amount of foliage retained on sample trees (Figure 5).

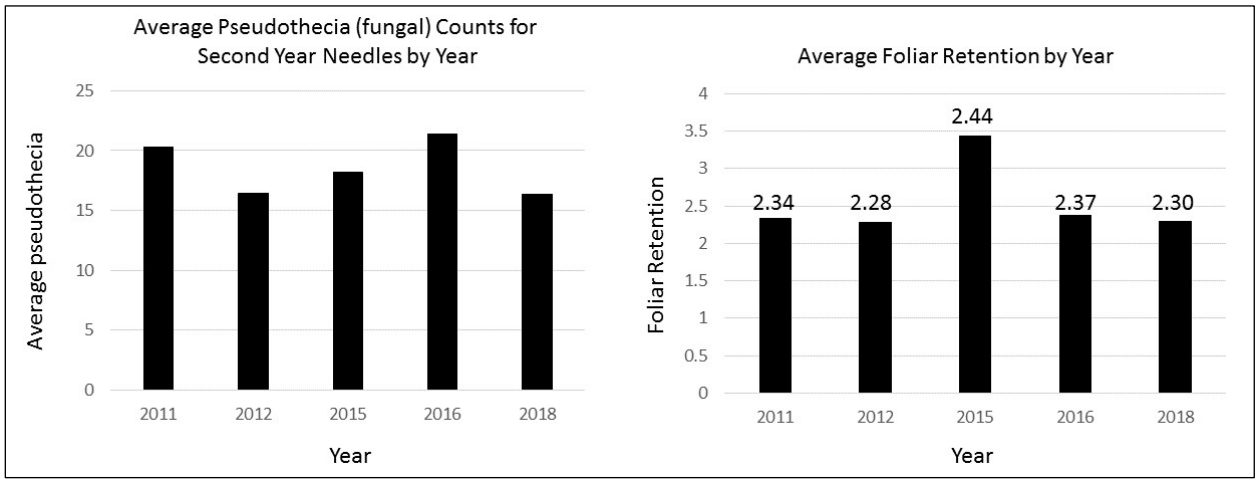

Figure 5. Average pseudothecia counts for second year needle by year (left) and average foliar retention by year (right).

Caution should be advised when interpreting aerial survey data. The SNC survey should be considered a conservative estimate of the acreage affected by SNC because aerial observers can only map areas where disease symptoms have developed enough to be visible from the air. SNC aerial survey can be used to coarsely document trends in damage over time. The ground data indicates that SNC is present in areas that were not mapped during the aerial survey. While the aerial survey can be used as a guide for identifying areas impacted by SNC, on the ground surveys should be conducted in stands of interest before SNC mitigating management decisions are made.

Douglas-fir is the only host of this disease, therefore forest managers can grow non-host species such as red alder, western red cedar, western hemlock and Sitka spruce in efforts to reduce damage from SNC. However, it should be noted that if Douglas-fir has more than three years of foliage on its branches, then damage in the form of growth loss are likely to be minimal to none.

For more information about foliar retention assessments or Swiss Needle Cast in general, this document has some great information.
http://sncc.forestry.oregonstate.edu/sites/default/files/ForestHealthFS.pdf.

For more information and details about the SNC aerial survey, follow this link to a great storyboard about the survey.

https://usfs.maps.arcgis.com/apps/MapJournal/index.html?appid=da5cda5003d24544b9231dbb8edf82fb

Acknowledgements

The survey was conducted by the Washington Department of Natural Resources (WDNR) Forest Health Program and the Washington Department of Fish and Wildlife (WDFW) aviation section. Marty Kimbrel (WDFW) piloted the plane. Funding for the survey was provided by the Washington State Legislature, Washington Department of Natural Resources and the USDA Forest Service, an equal opportunity employer.

Additional Notes

We appreciate any information regarding the accuracy or usefulness of the maps and ground survey data. Please contact Amy Ramsey (amy.ramsey@dnr.wa.gov or 360-902-1309) if you have questions, comments or suggestions.

References

Johnson, G.R., A.T. Grotta, B.L. Gartner and G. Downes. 2005. Impact of the foliar pathogen Swiss needle cast on wood quality of Douglas-fir. Can. J. For. Res. 35: 331–339.

Navarro, S. and D. Norlander. 2016. 2016 Swiss Needle Cast Aerial Survey. Oregon Dept. of Forestry, Office report, Salem, OR.

Maguire, DA, Mainwaring DB, Kanaskie A. 2011. Ten-year growth and mortality in young Douglas-fir stands experiencing a range in Swiss needle cast severity. Can. J. For. Res. 41: 20642076.

Shaw, D.C., G.M. Filip, A. Kanaskie, D.A. Maguire, and W.A. Littke. 2011. Managing an epidemic of Swiss needle cast in the Douglas-fir region of Oregon; the role of the Swiss Needle Cast Cooperative. *J. of For.* 109(2): 109-119.

Weiskittel, A.R., D.A. Maguire, S.M. Garber and A. Kanaskie. 2006. Influence of Swiss needle cast on foliage age-class structure and vertical foliage distribution in Douglas-fir plantations in north coastal Oregon. Can. J. For. Res. 36: 1497–1508.

Foliage retention, elevation, and disease severity (Oh my!) maps of the SNCC research and monitoring plot network

Gabriela Ritóková[1], Dave Shaw[1], Doug Maguire[1], Doug Mainwaring[1], John Browning[2], Mark Gourley[3], Greg Filip[4], Alan Kanaskie[5], Randy Comeleo[6]

[1]SNCC, Forest Engineering, Resource, and Management, Oregon State University, [2]Weyerhaeuser Corporation, [3]Starker Forests, [4]US Forest Service, [5]Oregon Department of Forestry, [6]Environmental Protection Agency

Introduction

The geographic distribution of visual SNC symptoms as represented by the aerial survey (Kanaskie et al. 2015, fig 1) or modeled foliage retention as predicted from climate data (Manter et al. 2005, Latta et al. 2009, Zhao et al. 2011) have proven to be useful tools in predicting the relative risk of sites to SNC infection. Scientists from the EPA have used kriging methods to produce interpolated maps of foliage retention and disease severity based on measured values of each across the range of the SNCC plot network. This report discusses how these new maps compare to other previously-produced maps of SNC symptoms, observed or predicted.

Methods

The SNCC research and monitoring plot network was established between the California border and SW Washington (560 km (338 miles)) and 56 km (35 miles) inland from the Pacific ocean between the fall of 2013 and 2015. Precipitation and temperature vary across the region, with annual precipitation ranging from 1200 - 4800 mm, primarily from October through May, and mean annual temperature ranging from 13 - 18°C. The elevation of plots making up the network ranged from 40 - 800m above sea level.

Field Methods

Foliage samples were collected on each sample plot just prior to budbreak (March-May) in the spring following plot installation in 2014, 2015 and 2016. In each plot, foliage samples were collected from the upper, middle and lower crown positions on the south side of the 5 – 10 largest (by dbh) undamaged trees.

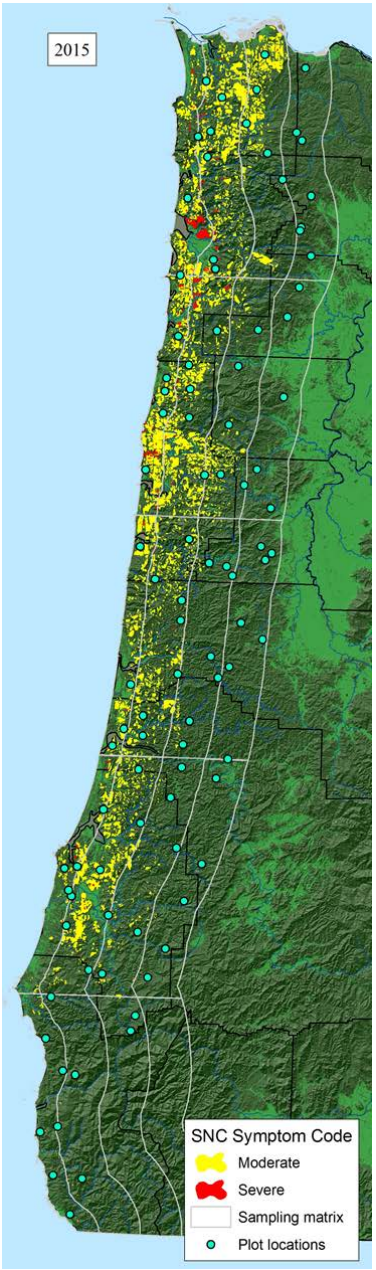

Figure 1. Aerial survey map of SNC distribution in the Oregon Coast Range, 2015. Observed symptoms in Douglas-fir.

Foliage retention was determined onsite by estimating the number of annual cohorts of foliage remaining on a 4-year-old lateral branch (Maguire et al. 2011) to the nearest 10% for each needle cohort. Mid-crown branches were used to estimate foliage retention and to evaluate SNC severity index.

Laboratory Methods

Pseudothecial Occlusion

The degree of fungal colonization was determined visually by estimating the number of *N. gaeumannii* ascocarps (pseudothecia) present on each needle. For each crown position on selected trees, 50 needles were arbitrarily selected from three 2-year-old cohorts (branchlets) of each 4-year lateral branch. The needles were taped to an index card, and each needle was visually inspected with a dissecting microscope to determine proportion of stomates occluded by pseudothecia referred to as SNC incidence. The proportion of pseudothecia emerging from stomata (pseudothecial density) were recorded for the first 10 needles with a positive incidence rate. Pseudothecial density was visually observed and averaged in 3 locations (tip, middle and base) of each of the 10 needles, following methodology described by Manter et al. (2000) and Winton et al. (2002).

The SNC disease severity index was calculated by multiplying the percentage of occluded stomata (pseudothecial density) by proportion of needles with pseudothecia on each index card (incidence) (Manter et al. 2005).

Swiss needle cast foliage retention and severity index continuous surface maps were created by interpolating data from 106 research plots using ordinary kriging. The spatial extent of each surface interpolation was limited to the average distance (17 km) between the nearest five research plots used in interpolation search neighborhoods. Final maps were created by classifying continuous surface maps. All geostatistical analyses were completed using ArcGIS geographic information system (GIS) software (Esri, 1995-2017).

Results and Discussion

The maps of foliage retention and disease severity represent three separate years of sampling (fig 2). Foliage retention on these plots exhibits the same west-east gradient depicted by the symptomatic stands observed by aerial surveillance and as predicted by two different climate models (fig 3). Differences between figure 2a) and figures 3a and 3b represent both the different methodologies used to predict foliage retention as well as the different climatic conditions used for the previous efforts and those occurring during the three year measurement period of the new plot network. The west-east gradient of foliage retention, coupled with the known and displayed (fig 2b) gradient of elevation in the Coast Range explains the general and statistically significant negative relationship between foliage retention and elevation with $p\text{-value}<0.05$ (fig 4).

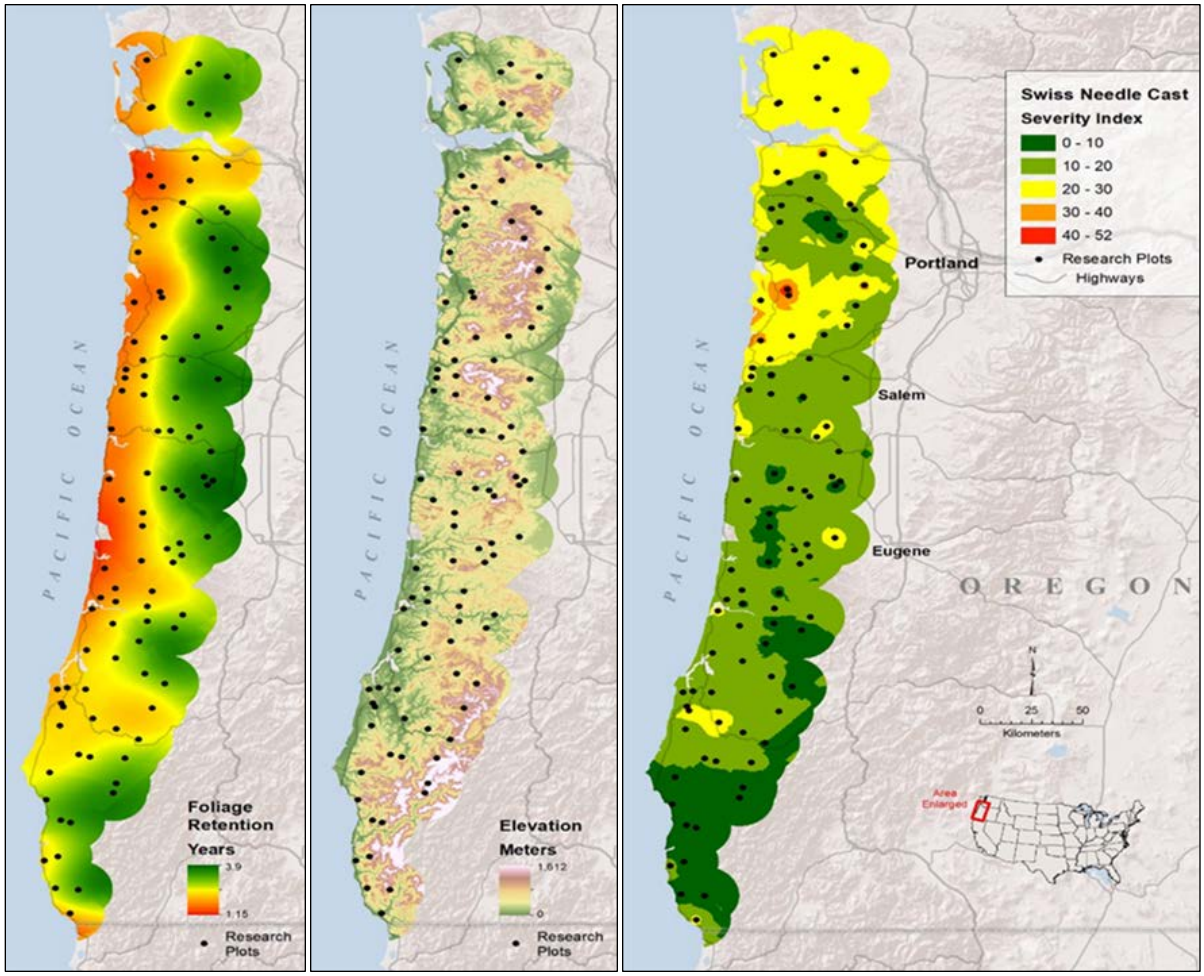

Figure 2 a) Foliage retention distribution; b) Elevation map created using data from the USGS National Elevation Dataset (vertical resolution 1 cm, horizontal resolution 30 m);
c) SNC disease severity index (higher the number, higher level of SNC infection).

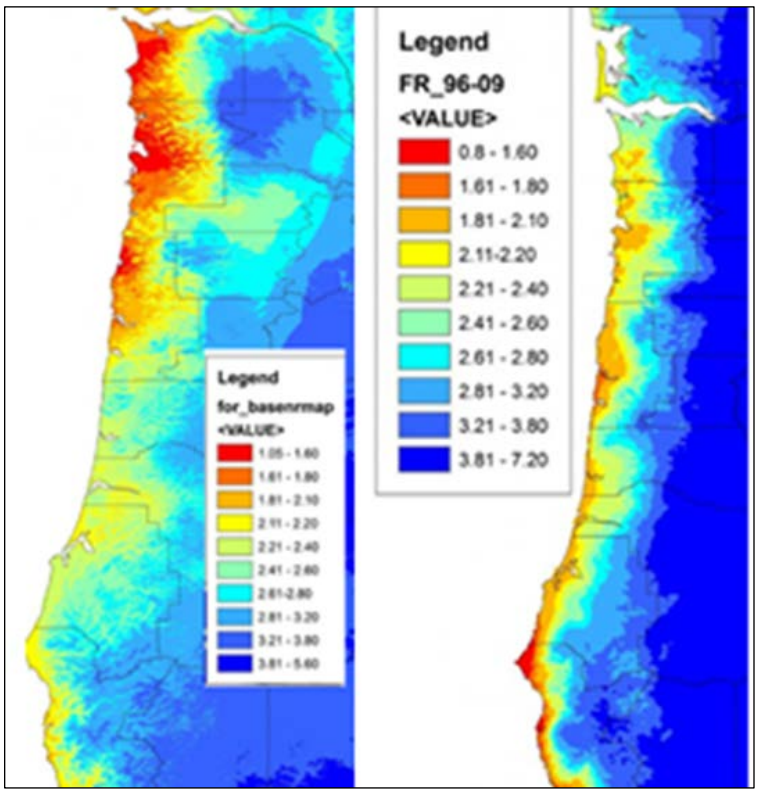

Figure 3. Climate-based predictions of foliage retention based on sampling conducted in 1998-2009 using models constructed by a) Latta et al. 2009; and b) Zhao et al. 2011.

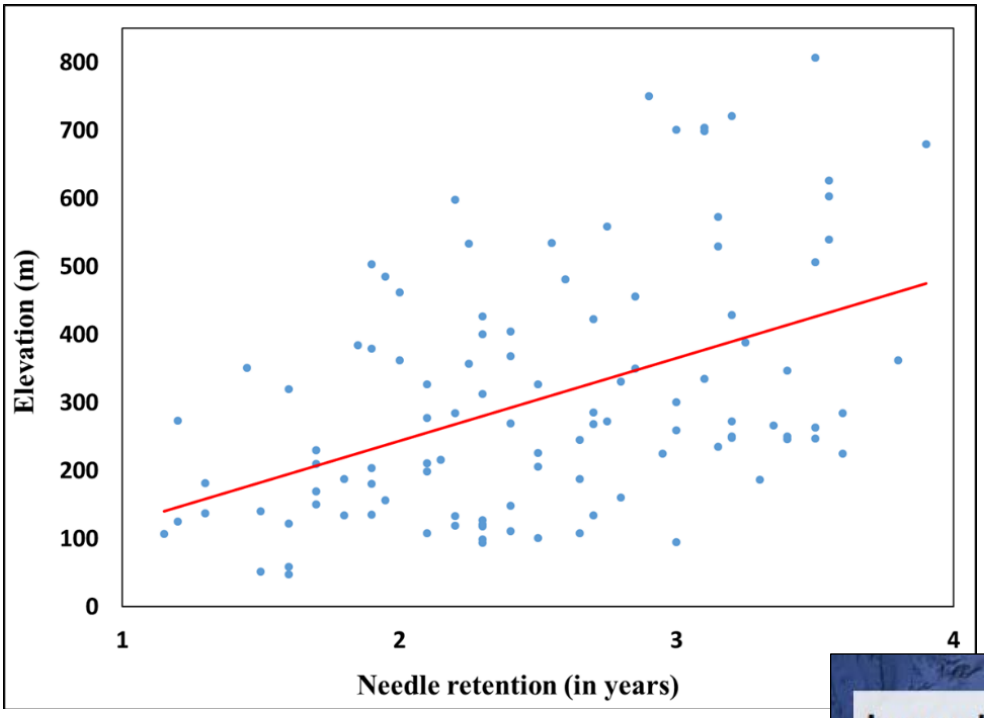

Figure 4. Relationship between foliage retention and elevation.

The disease severity map (fig 2c) exhibits a general north-south gradient, with northernmost stands predicted to have greater two year old stomatal occlusion, and southernmost stands predicted to have lesser occlusion. The fact that this is multi-year data means that some of the differences could relate to year to year differences. Figure 5 shows that the Washington and some NW Oregon plots were sampled in 2013, though the pattern of greater occlusion doesn't exactly follow pattern of sampling. Whether the geographic trend in occlusion is the result of greater occlusion in the north, all else being equal, or greater likelihood of needle cast at lesser levels of occlusion in the south, is unknown. The relatively low levels of occlusion in the southern part of the range could also indicate that foliage retention values in that area are influenced by non-SNC factors related to soil or climate.

The images represented here provide yet another look at the general pattern of SNC risk across the landscape. It reinforces the widely accepted view that the south coast of Oregon has a lower risk of SNC damage, and simultaneously raises questions about what would be found with more sampling in Washington, given both the apparent increase of

Figure 5. SNCC plot network; Sampling by year.

occlusion in the north, coupled with the lower elevation of the Washington coastal forests.

Literature Cited

Latta, G., Temesgen, H., Barrett, T.M. 2009. Mapping and imputing potential productivity of Pacific Northwest forests using climate variables. Canadian Journal of Forest Research. 39: 1197-1207.

Maguire, D.A., D.B. Mainwaring, and A. Kanaskie. 2011. Ten-year growth and mortality in young Douglas-fir stands experiencing a range in Swiss needle cast severity. Canadian Journal of Forest Research 41: 2064-2076.

Manter D.K., Bond B.J., Kavanagh K.L., Rosso P.H., Filip G.M. 2000. Pseudothecia of Swiss needle cast fungus, *Phaeocryptopus gaeumannii*, physically block stomata of Douglas-fir, reducing CO_2. New Phytologist. 2000:481-491.

Manter D.K., Reeser P.W., Stone J.K.. 2005. A climate-based model for predicting geographic variation in Swiss needle cast severity in the Oregon Coast Range. Phytopathology. 95:1256-1265.

Mulvey, L.R., Shaw, D.C., Filip, G., Chastagner, G.A. January 2016. Swiss Needle Cast. Forest Insect & Disease Leaflet 181. U.S. Department of Agriculture, Forest Service.

Ritóková, G., Shaw, D.C., Filip, G., Kanaskie, A., Browning, J., and D. Norlander. 2016. Swiss Needle Cast in Western Oregon Douglas-Fir Plantations: 20-Year Monitoring Results. Forests 7, 155.

Shaw, D.C.; Filip, G.M.; Kanaskie, A. [and others]. 2011. Managing an epidemic of Swiss needle cast in the Douglas-fir region of Oregon: the role of the Swiss Needle Cast Cooperative. Journal of Forestry.109: 109-119.

Shaw, D.C., Woolley, T., and A. Kanaskie. 2014. Vertical foliage retention in Douglas-fir across environmental gradients of the western Oregon coast range influenced by Swiss needle cast. Northwest Science 88: 23-32.

Winton L.M., Stone J.K., Watrud L.S., Hansen E.M.. 2002. Simultaneous one-tube quantification of host and pathogen DNA with real-time polymerase chain reaction. Phytopathology. 92:112-116.

Zhao, J., Mainwaring, D.B., Maguire, D.A., Kanaskie, A. 2011. Reginal and annual trends in Douglas-fir foliage retention: Correlations with climatic variables. Forest Ecology and Management. 262:1872-1886.

Swiss needle cast monitoring in British Columbia

Stefan Zeglen[1] and Harry Kope[2]
British Columbia Ministry of Forests, Lands and Natural Resource Operations and Rural Development, West Coast Region[1] and Forest Practices Branch[2]

Further to our inaugural report in the 2017 SNC Co-op Annual Report, efforts to monitor Swiss Needle Cast (SNC) in British Columbia (BC) have progressed along two complimentary paths. One was the completion of the first annual aerial overview survey (AOS) for SNC in BC and the other was the establishment of a further 23 plots into the coastal SNC monitoring plot network.

In April 2018, we invited Danny Norlander (Oregon Department of Forestry) to conduct the first aerial survey. In BC, we lack comprehensive information about the spatial distribution of SNC since our annual province-wide AOS happens too late (July-August) to catch the best window (April-May, pre-bud flush) for observing symptoms. We concentrated on the Chilliwack District, an area encompassing the upper Fraser Valley east of Vancouver and the area with the highest reported incidence and severity of SNC. Rather than the usual specialized fixed wing aircraft used in the Oregon surveys, we used a helicopter to provide observation from a lower elevation (350-500 m) and better manoeuverability in our narrow coastal valleys. Accompanying Danny were the contract aerial surveyors who usually conduct the coastal AOS. The flight area covered much of the eastern portion of the district but focussed on identified (from ground surveys) high incidence areas north of the Fraser River like around Harrison and Stave Lakes and south of the river in the Chilliwack and Skagit Valleys.

This aerial survey is primarily of plantations (<25 years old) from which good crown symptoms can be distinguished. Over 1100 ha of SNC were mapped and the result will be converted to BC severity classes and included in the provincial AOS database. For comparison, this year over 167,000 ha of SNC was mapped in Oregon. Given the success of the survey, we propose to repeat the exercise next year and perhaps expand the area surveyed to the Sunshine Coast and the southern half of Vancouver Island. This would cover the majority of the area determined to be currently experiencing varying levels of infection by SNC.

We expanded our SNC monitoring plot network from 13 to 36 plots by adding plots in the Coastal Western Hemlock very dry maritime ecological subzone (CWHxm). This expanded area places plots on southeastern Vancouver Island and the mainland Sunshine Coast (see map). Our plots were installed using the same protocol as the SNC co-op network. We have collected the same sorts of tree and site data including stomatal occlusion counts and molecular ecology work on the pathogen (through our UBC collaborators) and foliar and soils analysis (using our Ministry analytical lab). On 12 sites we also collect environmental data including air and soil temperatures, relative humidity, solar irradiance and leaf wetness. We are trying to

determine what site or seasonal factors affect the severity of SNC in our coastal plantations. In 2019 we will be adding some plots in the CWHvm, a wetter subzone that is less suitable for Douglas-fir.

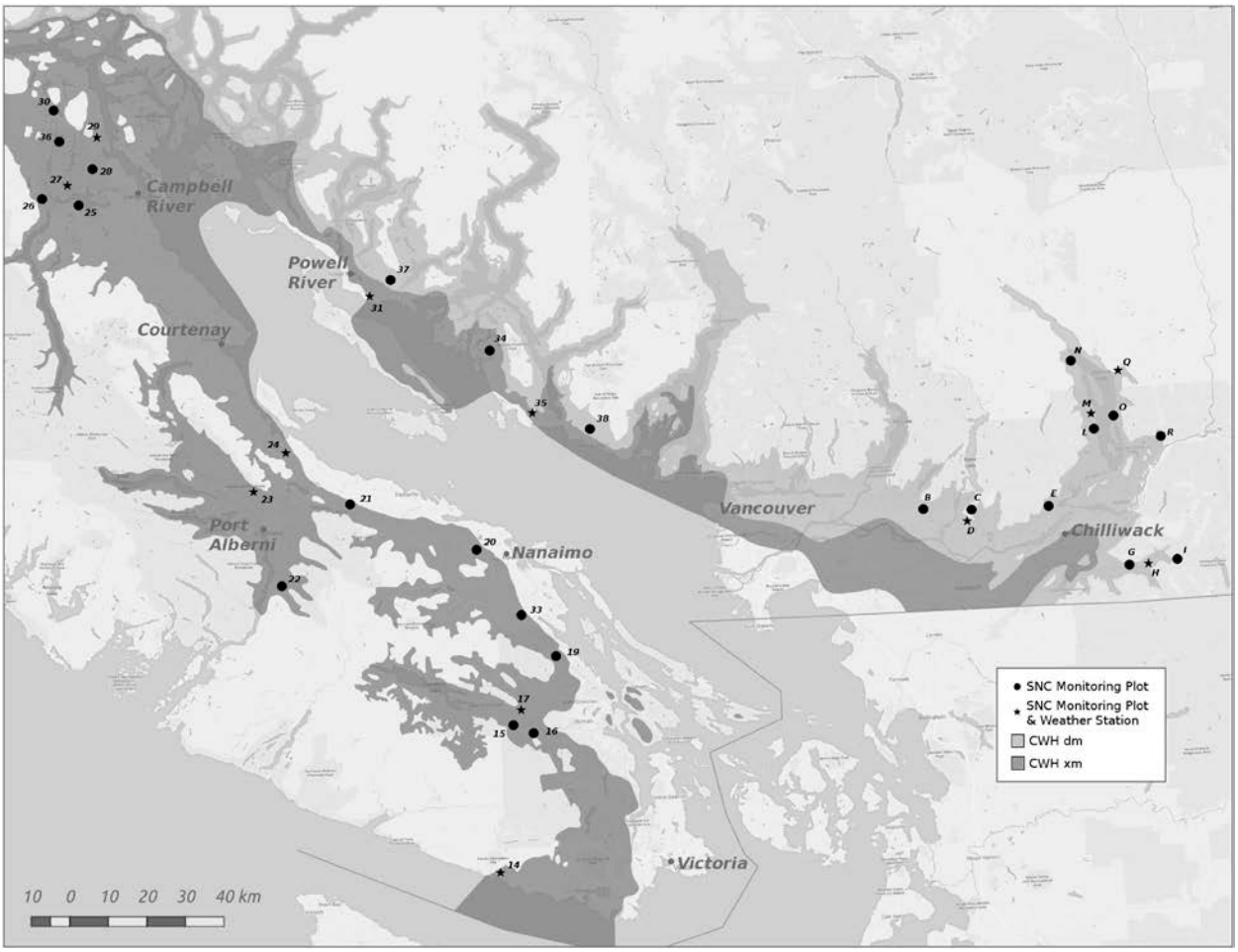

Preliminary results from the first remeasurement of the SNCC research and monitoring plot network

Doug Mainwaring[1], Doug Maguire[1], Gabriela Ritokova[2], Dave Shaw[2]
Center for Intensive Planted-Forest Silviculture[1], Swiss Needle Cast Cooperative[2],
Oregon State University

Abstract

The first five year remeasurement of the SNCC research and monitoring plot network is underway, with tree data from 14 of 30 plots having already been collected. Though these 14 plots represent an unbalanced sample of the range in foliage retention estimated for the first year's group of plots, plot-level analysis of volume growth does find a significant positive effect of foliage retention when site index is not included in the regression equation. The implied negative effect of SNC infection from this model is greater than has been estimated for previous growth periods from data of the SNCC Growth Impact Study plots. Inclusion of site index in the regression equation renders foliage retention an insignificant variable ($p=0.16$), underscoring the importance of using the full set of remeasurement data for a conclusive analysis.

Introduction

The first plots of the SNCC research and monitoring plot network were installed in 2013, with 30 established the first year and an additional 76 established in the following two years. The objectives of this plot network are to have a set of intensively managed stands throughout the Oregon and SW Washington Coast Range from which to monitor the effects of SNC on the growth of Douglas-fir, to monitor the development of infection levels and disease expression, and to have a plot infrastructure available for other studies pursuing a better understanding of Swiss needle cast.

During the 10 year lifespan of the SNC's Growth impact study plots (GIS), estimates of plot-level growth loss were calculated from fitting a regression equation predicting cubic volume growth from Douglas-fir basal area, basal area in other trees, site index, and foliage retention. Inclusion of foliage retention in the equation enabled estimation of the marginal effect of retained foliage on cubic volume growth. Estimates during the four growth periods of that earlier effort produced relatively similar estimates of cubic volume growth loss (fig 1).

The plots are scheduled for remeasure every five years, and tree diameter and heights of 14 of the first 30 plots have thus far been remeasured this off-season. With mid-crown estimates of foliage retention made in the spring of 2014, plot-level estimates of cubic volume growth loss can be inferred from a similar statistical model as described above, the incomplete sample notwithstanding.

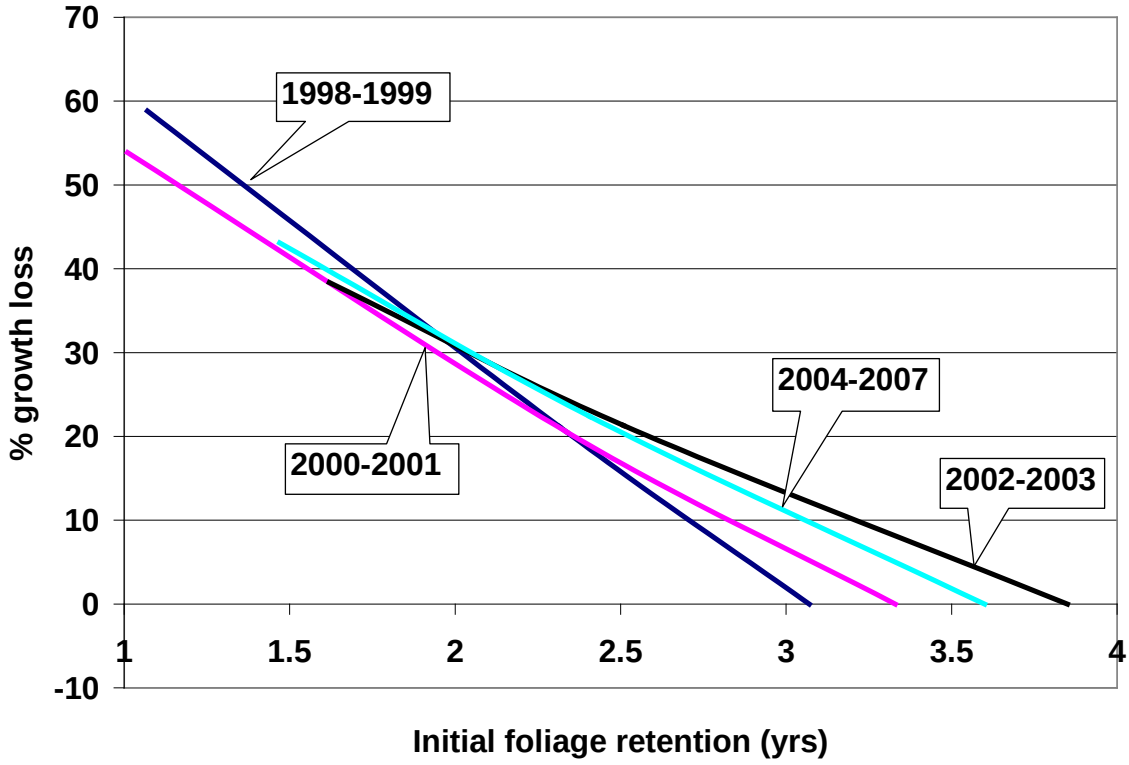

Figure 1. Implied relative growth losses for the four GIS growth periods. Ranges of foliage retention represent those measured at the start of each growth period.

The objectives of this report are: 1) to quantify the most recent 5-yr growth responses relative to initial SNC severity; and 2) to compare this response to those estimated retrospectively for 1996 and on permanent plots for 1998-99, 2000-2001, and 2002-2003.

Methods

Thirty plots were established and measured in the fall of 2013. All trees >5 cm dbh were measured for dbh to the nearest 0.1 cm. A subset of 40 undamaged Douglas-fir (10 largest by dbh, 4 smallest by dbh, and others distributed across the diameter distribution) were measured for height and height to lowest live branch.

In the spring of 2014, the ten largest undamaged trees (by dbh) was climbed for foliage sampling. The sample taken within the mid-crown was used to estimate the tree-level average. The plot-level average used for the analysis was the average of all plot trees for which foliage retention was estimated.

In the fall of 2018, remeasurement of the first set of plots began. All live trees were measured for dbh, and all previously measured height trees were remeasured for height and height to the lowest live branch. Any height trees that were damaged or had died in the last five

years were replaced with new height trees. The largest 10 trees (by dbh) were cored for breast height age, from which site index was estimated.

Statistical analysis

In the growth analyses, all variation in initial needle retention was assumed totally controlled by SNC. Individual mid-crown tree values were averaged for the 5-10 sample trees on each plot to arrive at a plot average. A simple growth model was fitted to the data from the 14 plots remeasured in the fall of 2018, using initial foliage retention as the index of SNC severity:

$$\ln[PAI] = b_0 + b_1X_1 + b_2X_2 + \ldots + b_kX_k + b_{k+1}\ln(FOLRET) \quad [1]$$

where

PAI=plot-level periodic annual increment for cubic volume of surviving Douglas-fir

X_i=plot-level predictor variables

FOLRET is mid-crown foliage retention in the spring of 2014.

Results and Discussion

The fourteen plots for which growth data was available at the time of the analysis constituted approximately half of the first period's plots. Importantly, uninfected plots were more heavily represented in the sample (fig 2), thus minimizing the power of the regression analysis to assess the marginal effect of foliage retention.

For the 14 plots remeasured in the fall of 2018, approximately 93% of the variation in cubic volume PAI was explained by the following model:

$$\ln[PAI] = b_0 + b_1 \cdot \ln(BA_{DF}) - b_2 \cdot \ln(BA_{OC})\ b_3 \cdot \ln(BA_{OH}) + b_4 \cdot \ln(SI) + b_5 \cdot \ln(FOLRET) \quad [2]$$

where

PAI = plot-level periodic annual cubic volume growth of Douglas-fir for 2004-2007(m^3/ha)

BA_{DF} = initial Douglas-fir basal area (m^2/ha in Fall/2013)

BA_{OC} = initial plot basal area of all conifers other than Douglas-fir (m^2/ha in Fall/2013)

BA_{OH}= initial plot basal area of hardwoods (m^2/ha in Fall/2013)

SI = 50-yr site index based on 2018 heights (Bruce 1981)

FOLRET = initial (2004) average foliage retention for plot (yrs)

Parameter estimates and standard errors are provided in table 1. Foliage retention was not a significant factor (p=0.16).

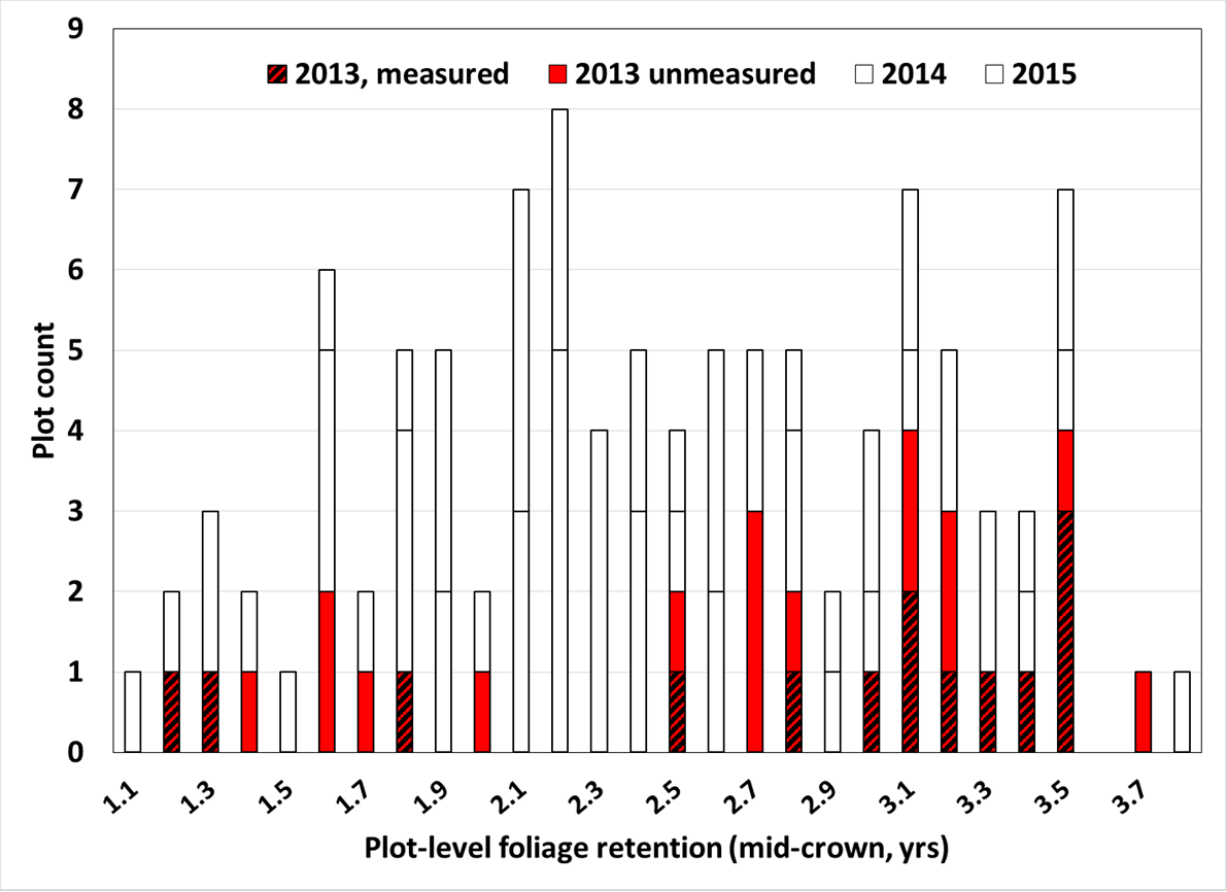

Figure 2: Initial foliage retention of all measured plots, with 2013 cohort in red. Black hatching indicates which plots are represented in this preliminary analysis.

	Full model		Reduced model	
	Parameter estimate	Standard error	Parameter estimate	Standard error
b_0	-9.4299	3.12993	0.29591	0.37609
b_1	0.37022	0.14683	0.75506	0.13372
b_2	-0.02152	0.01585	0.00173	0.0203
b_3	-0.04431	0.0145	-0.05665	0.1961
b_4	2.22261	0.7084	NA	NA
b_5	0.42228	0.27813	1.12469	0.23302

Table 1: Parameter estimates and standard errors for the full and reduced model represented by equation [2].

The negative effect of SNC on height increment (Maguire et al. 2002) can be expected to result in diminished height increment and subsequently, in a site index underestimate that doesn't accurately reflect the site productivity of uninfected Douglas-fir trees. Accordingly, a reduced form of equation [2] (without SI) was fit, producing a result that explained approximately 82% of the variation in cubic volume growth, and with a significant effect of foliage retention (table 1).

The implied negative effect of foliage retention on Douglas-fir cubic volume growth with both the full and reduced models is shown in figure 3. It should be emphasized that use of the incomplete (and unbalanced) dataset means that neither should be considered a final result.

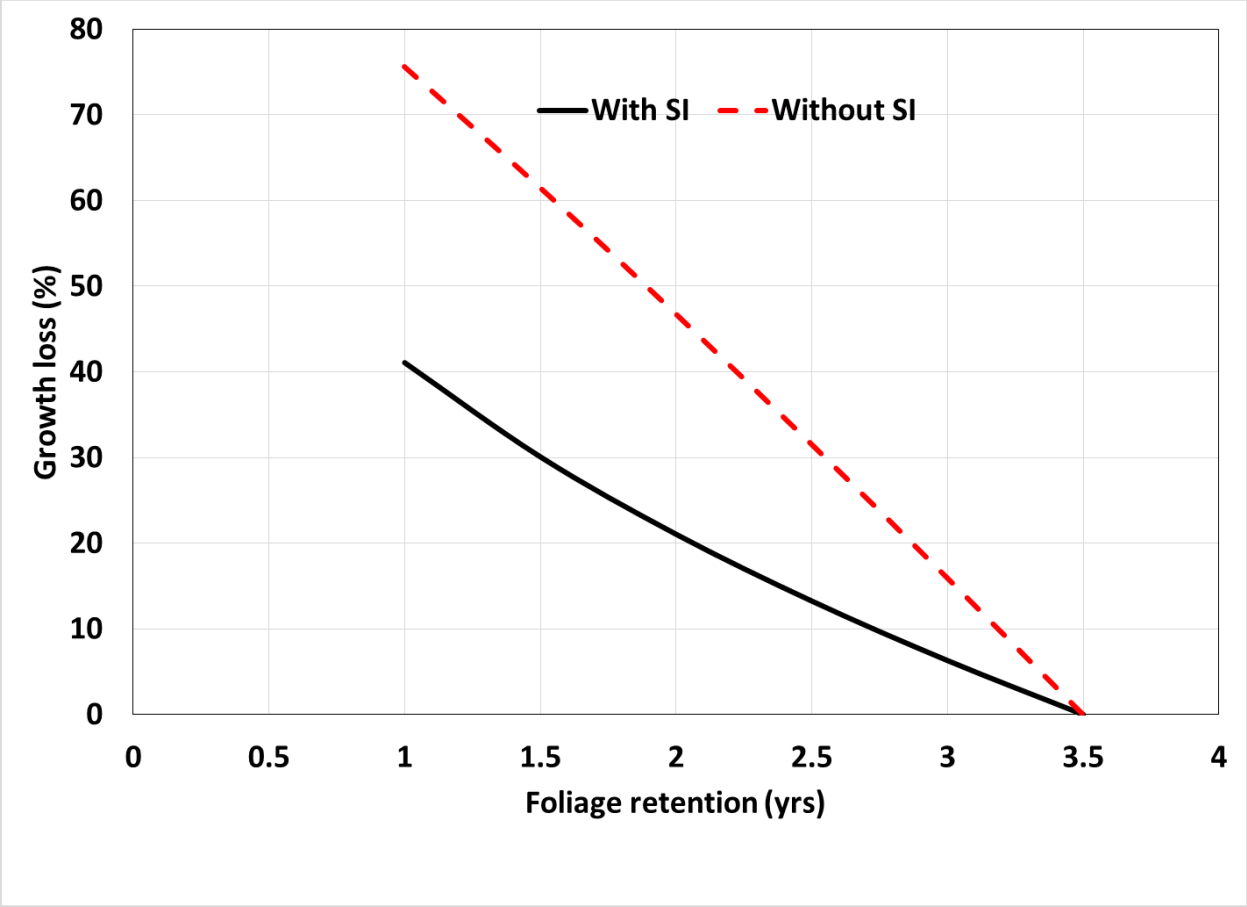

Figure 3: Implied growth loss (%) from full (with SI) and reduced (without SI) models for 14 plots measured in the preliminary phase of the remeasurement of year 1 plots. Implied value with SI is statistically insignificant (p=0.16).

The value (or not) of including site index in the analysis is worth exploring. The original analyses used for the Growth Impact plots generally used site index, thus complicating the analysis of SNC growth impacts due to the likely underestimation of site index from existing height-age pairs. Because of the age of the stands making up that dataset, the year of initiation of SNC impact and the length of time that plots had been subjected to significant SNC pressure was unknown, making it difficult adjust dominant heights by the expected negative effect on height increment. In the case of the new plot network, plots are young enough to have spent their entire lives under SNC pressure. As a result, it may be appropriate to apply ORGANON height increment modifiers to the measured dominant heights on infected plots as a means of estimating an average annual percentage loss of height increment. It will give a higher value of estimated site index for an infected plot, and potentially a more realistic estimate of growth loss due to SNC.

Literature Cited

Bruce, D. 1981. Consistent height-growth and growth-rate estimates for remeasured plots. For. Sci. 27:711-725.

Maguire, D.A., Kanaskie, A., Voelker, W., Johnson, R., and G. Johnson. 2002. Growth of young Douglas-fir plantations across a gradient in Swiss needle cast severity. West J. Appl. For. 17: 86-95.

Quantitative analysis of the spread of Swiss needle cast in the Oregon Coast range

Andrew Russo
MF candidate, Forest Engineering, Resource, and Management, Oregon State University

Introduction

Swiss needle cast (SNC) is a disease of Douglas-fir (*Pseudotsuga menziesii*) caused by the fungal pathogen *Nothophaeocryptopus gaeumannii*, an ascomycete fungus that is a host specific obligate parasite. The infection cycle begins in May or June, when ascospores are released from mature fruiting bodies and are dispersed by wind and water splashes. These spores land on the surface of newly emerging needles, where they germinate and grow across the surface until they can reach a stoma to grow into. From there the fungus grows in the needle, eventually creating a black fruiting body known as a pseudothecium that emerges sometime between October and February, clogs the stoma as it emerges (Temel et al. 2005).

Despite initially being regarded as nothing more than a minor pathogen in its natural range, in 1984 severe growth reductions caused by SNC resulted in the first written reports of disease-related impacts on the landscape, and retrospective studies have shown evidence of localized growth reductions sporadically since at least 1950 (Black et al. 2010). Outside of the Pacific Northwest, *N. gaeumannii* has been found in introduced plantations of Douglas-fir in climate conditions similar to coastal areas that have been impacted in its native range.

Though the multitude of factors that may cause relatively low intensity of *N. gaeumannii* infection to progress to severe level of SNC are not fully understood, it is well understood that SNC is most prevalent and most damaging close to the coast. The most severe pockets of disease have also been associated with a variety of linked climate and topographic variables, including spring leaf wetness from precipitation and fog, mild temperatures in the winter and spring, and low-elevation valleys.

In Oregon, aerial surveys have been used to detect the extent of SNC severity across the Coast Range, looking for the distinctive chlorotic, yellow–brown discoloration that infected trees exhibit in April to early-June. These surveys have detected regular, though not continuous, increases in the extent of diseased areas since they began in 1996. In 2015, approximately 590,000 acres of forested areas in Oregon and 350,000 acres in Washington had visible symptoms of the disease, and 4 million acres of forest in western Oregon were considered to be at risk of being impacted (Ritóková et al. 2016, Shaw et al. 2011). Despite these surveys, since

SNC was first mapped in the Oregon Coast Range, the question of whether the disease has been progressing east or merely intensifying within the same zone has been up for debate.

Twenty-year aerial survey data collection was used for the analysis. The first objective of the study was to determine if over time the weight of symptomatic stands had remained stationary or shifted eastwards over time. Second objective was to determine if there was an eastwards shift in response to increases in the total infected acreage.

Methods

The study was performed using the data from the SNC aerial surveys performed by the Oregon department of Forestry (ODF), and contains data collected annually from 1996 until 2016 except 2008 when the surveys were incomplete. The surveys were performed by an observation plane flown at 1,500 to 2,000 feet above the terrain, following north-south lines separated by 2 miles (Navarro, Norlander. 2016). Observers looked for areas of Douglas-fir forest with obvious yellowing to yellow-brown foliage. Patches of forest with these symptoms were sketched onto computer touch-screens displaying topographic maps or ortho-photos and the position of the aircraft. The survey area extended from the Columbia River in Oregon south to the California border, and from the coastline eastward until obvious symptoms were no longer visible.

Using ArcGIS and the datasets provided by ODF, the acreage and centerpoint for each symptomatic patch was found. This distance from the coastline from each centerpoint was measured. For each year, the distance from the coast that contained 50, 75, 95 and 99.9% of the total infected acreage was found and compared to year to year variations. The 50^{th}, 75^{th} and 95^{th} percentile distances were intended to outline the main weight of the infected acreage, while the 99.9^{th} percentile was intended to roughly estimate the eastern edge of all symptomatic stands.

Results

While the main weight of symptomatic acres expanded eastwards for the first 2 years of the study, over the next 18 years almost no net change occurred, even while the total symptomatic acreage rose from 187,167 acres in 1998 to 546,243 acres in 2016 (Figure 1A). The four studied percentiles averaged a net shift of only 0.0189 miles per year, and none shifted by more than 0.0294 miles per year.

A similar pattern occurred when the years were arranged by total infected acreage. Beyond 200,000 symptomatic acres the trendlines were nearly flat again, with the four percentile categories averaging a shift of only 0.156 miles for every additional 100,000 symptomatic acres,

and none shifting by more than 0.42 miles for every additional 100,000 symptomatic acres (figure 1B).

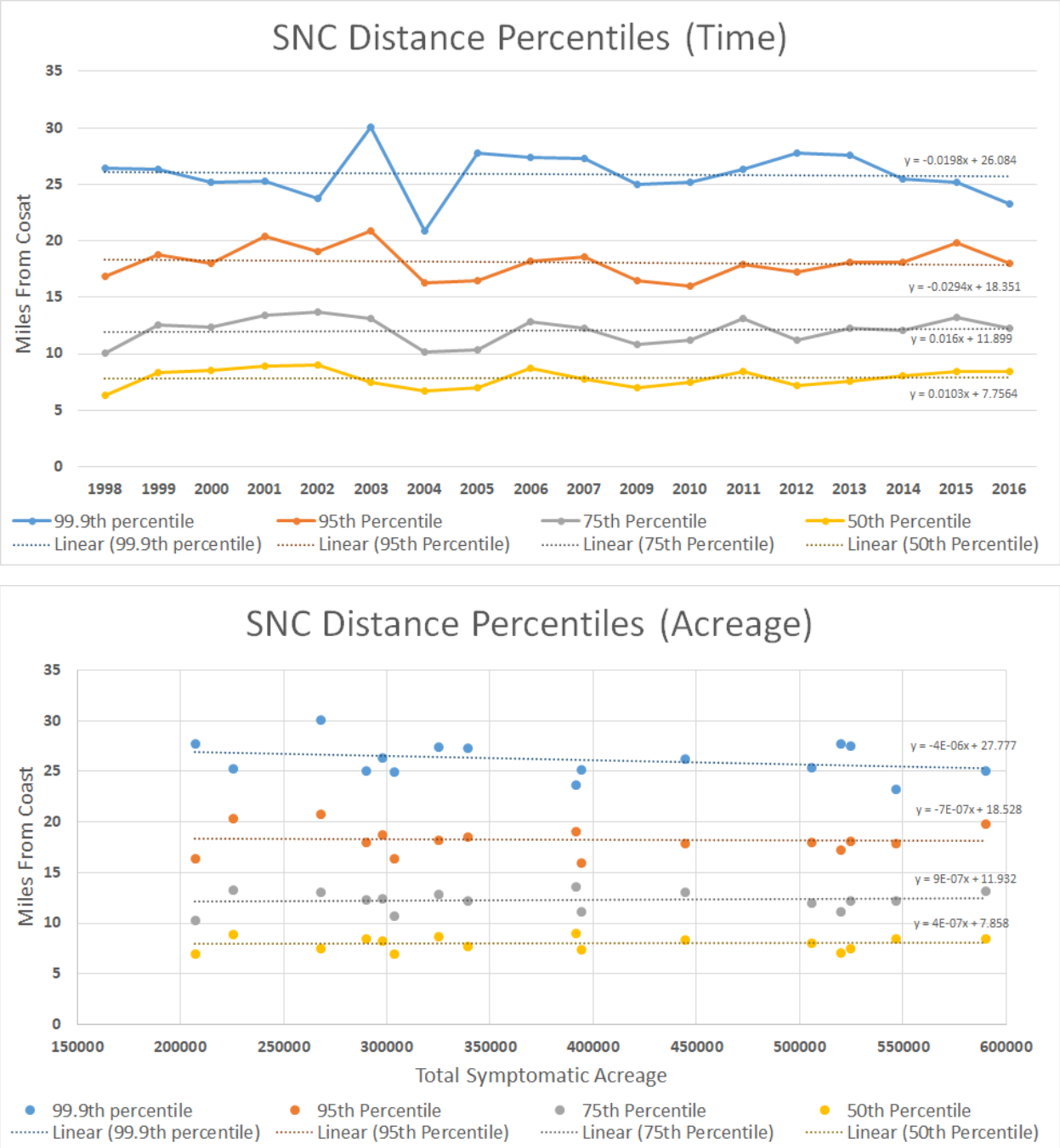

Figure 1. A: The distance from the coast that contains 50, 75, 95 and 99.5 percent of all SNC symptomatic acreage from 1998 to 2006 arranged by year. B: The distance from the coast containing the

same percentages arranged by total symptomatic acreage for years that contained over 200,000 symptomatic acres.

Discussion

The results of this analysis show that while the general distribution of SNC symptomatic stands did progress eastwards over the first 2 years of the study period, after this point the total weight of infected acreage remained almost completely stationary. This trend remained consistent after arrangement by total symptomatic acreage, with an initial eastward expansion as total acreage increased, before leveling out above 200,000 total acres. While this is a general trend, and cannot be used to make specific predictions in specific areas, it shows that unless ecological trends change in the future, Douglas-fir stands on the eastern slopes of the Oregon coast range should remain relatively free of the disease, though certain areas with ideal conditions for the pathogen might see some local increases.

Instead of linearly progressing eastwards, the next area where SNC may become a management issue is the western cascades, where initial ODF aerial surveys have showing an increasing number of symptomatic stands.

Literature Cited

Black A.B., Shaw D.C., and Stone, J.K. 2010. Impacts of Swiss needle cast on overstory Douglas-fir forests of the western Oregon Coast Range. Forest Ecology and Management 259:1673–1680

Temel F., Johnson G.R., Adams W.T. 2005. Early genetic testing of coastal Douglas-fir for Swiss needle cast tolerance. Canadian Journal of Forest Research 35:521-529

Shaw D. C., Filip G. M., Kanaskie A., Maguire D.A., and Littke W.A. 2011. Managing an Epidemic of Swiss Needle Cast in the Douglas-Fir Region of Oregon: The Role of the Swiss Needle Cast Cooperative. Journal of Forestry.

Ritóková G., Shaw D.C., Filip G., Kanaskie A., Browning J., and Norlander D. 2016. Swiss Needle Cast in Western Oregon Douglas-Fir Plantations: 20-Year Monitoring Results. Forests 7,155

Rosso, P. H. and E. M. Hansen. 2003. Predicting Swiss Needle Cast Disease Distribution and Severity in Young Douglas-Fir Plantations in Coastal Oregon. Epidemiology 93: 790-798

A summary of associations between Swiss needle cast disease severity and multiple site-level factors

Yung-Hsiang (Sky) Lan
Forest and Ecosystem Sciences, Oregon State University

Epidemiology of *Nothophaeocryptopus gaeumannii* is generally well known in young plantation trees, but the relationship between disease expression, foliage nutrition and some climate variables is unclear, the dynamics of Swiss needle cast (SNC) in older trees is poorly understood. In this study, associations between foliar nutrients and climate factors and the SNC severity index were analyzed using data from the Swiss Needle Cast Cooperative (SNCC) research and monitoring plot network data. In addition, comparisons of SNC severity and disease incidence on both old and young trees were conducted by sampling 21 old trees and 21 young trees across 7 sites in western Oregon.

The SNCC plot network was established between 2013 and 2015, across western Oregon and SW Washington State. Five to ten Douglas-fir trees with the largest dbh were selected for sampling. Foliage samples were collected from the upper, middle and lower crown thirds of each selected tree. SNC severity was evaluated on 2-year old needles by multiplying the ratio of occluded stomates and disease incidence, with the incidence defined as percentage of needles with pseudothecia among the 50 randomly chosen needles. A linear mixed model was adapted for statistical analyses of disease severity and foliar nutrients and climate factors.

Manuscripts with details of the following three studies are currently under review and will be available by the end of 2019. Dissertation chapters are available upon request.

Preliminary analysis of foliar nutrients

Plot network data was also utilized to assess the associations between disease severity, needle retention, carbon, and 9 foliage nutrients (N, Na, K, P, Ca, Mg, Mn, Al, and S).

The highest association between SNC severity and needle retention was observed in the mid crown. SNC severity showed significant positive trends with C, N, Na, K, and S, no relationship with Ca, Mg, or Al, and slightly negative trends that were not significant for P and Mn. Although some nutrients were associated with increasing SNC severity, more research is required to determine the cause-effect.

Preliminary analysis of climate factors

Plot network data was also utilized to assess the associations between disease severity and long term climate factors obtained from PRISM (http://prism.oregonstate.edu/explorer/). We used the long-term averaged climate data and have found criticism in this approach because disease severity might be more closely related to past two or three years of weather at each site. However, given that we used long-term averaged data, the following climate variables were tested : i) monthly precipitation and ii) annual precipitation, iii) minimum temperature, iv) maximum temperature, v) mean temperature, vi) mean dew point temperature, and vii) maximum vapor pressure deficit (VPD). Figure 1 shows the results of the climate variables. The estimated fitted slope represents the association between SNC disease severity index and monthly climate variables. Notice that the scales are different for each variables based on their fitted models.

We also examined the influence of latitude and longitude on these climate variables and SNC severity. Minimum temperature and dew point temperature were the factors most significantly associated with SNC severity. Oct.-Apr. mean temperature, Oct.-Apr. maximum temperature, and Nov.-Apr. maximum VPD were also positively or negatively associated with SNC severity depends on the variables. Monthly precipitation was not associated with mean SNC severity during the summer months possibly because it does not vary enough within the sample area. We know leaf wetness is important for leaf colonization. Dew point temperature for all months was positively associated with SNC severity, suggesting that dew point temperature may be more influential in epidemiology of *N. gaeumannii* than previously thought. The general idea of warmer winters being associated with SNC severity was supported, but perhaps should be expanded to warm mid-fall through mid-spring. Latitude had a strong positive relationship with SNC severity and climate variables, while longitude did not. The Tillamook latitudinal region appears to be more tightly linked to climate variables that other regions because the climate relationships had a steeper slope.

Mature vs young trees comparison

While there is considerable evidence of SNC in coastal Douglas-fir plantations, the severity of SNC in mature and old-growth forests is poorly understood. We compared the SNC severity, disease incidence, needle retention, and foliar nitrogen in tree crowns of mature and old-growth forests and nearby young forests at three locations in the Oregon Coast Range and four locations in the western Cascade Mountains of Oregon. At Cascade Head, Klickitat Mountain, Woods Creek, Moose Mountain, Falls Creek, Soapgrass Mountain and Toad Creek, three old trees and three young trees were sampled at each site. Foliage samples were collected from the upper, middle and lower crown. SNC severity, disease incidence, needle retention and

foliar nitrogen were measured using the SNCC lab protocol. MANOVA was used for statistical analysis. Needle wetness sensors were deployed at five sites.

Disease severity on 2-year old needles was greater in younger forests than older forests at all sites. Retention of the four-year needle cohorts were greater in older than younger trees. Pseudothecia incidence was highest on 2-year-old needles in young trees and on 3-, 4- and 5-year-old needles in mature trees. Foliar nitrogen concentration differed among years, canopy positions, and sites, but was not different between mature and young trees. Leaf wetness differences were not consistent between young and old tree crowns. Leaf wetness and foliar N were hypothesized to play a controlling role in SNC severity difference between mature and young trees, but while we know these factors are important, they did not explain why disease severity was different. We can only speculate why there are differences between mature and younger trees.

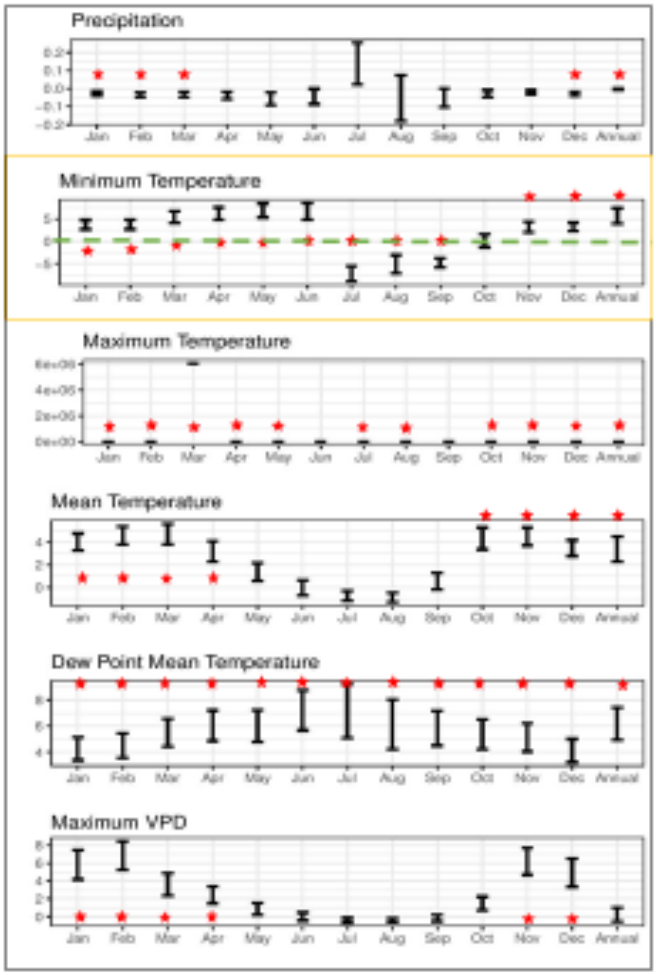

Figure 1. Fitted model slopes between SNC disease severity index and climate variables on SNCC study plots in coastal western Oregon and southwest Washington in 2013-2015.

Modeling the severity and impact of Swiss needle cast in Douglas-fir from soil and climate variables in coastal Western Oregon and Southwest Washington.

Jeff Hatten[1*], Dave Frey[2], Yung-Hsiang Lan[3], Gabriela Ritóková[1], and Dave Shaw[1]
[1] Oregon State University, Forest Engineering Resources and Management, [2] Cornell University, [3] Oregon State University, Forest Ecosystems and Society

Introduction

The severity of Swiss Needle Cast (SNC) has been shown to vary as a function of climate, soils, and foliar characteristics. Generally, the disease is more severe with proximity to the coast and along the gradient of climate and soil characteristics. Distance from the coast was associated with gradients in both soils and climate. Generally, temperatures are cooler and precipitation rates higher near the coast (when controlling for elevation). Additionally, soil and foliar N content are higher and Ca contents lower near the coast, and these elements are inversely related along this gradient.

Seasonal temperature, especially winter temperature, may be related to the rapid development of the fungus within the needle resulting in a higher abundance of N. gaeumannii on needles (Lee et al., 2017; Manter et al., 2005; Rosso and Hansen, 2003; Zhao et al., 2012, 2011). Additionally, spore germination and initial colonization on needles can be affected by factors that impact leaf-wetness which include late spring and summer temperature and precipitation during this critical growth period (May-August). In the most extensive study of SNC in Oregon and Washington, Lan et al., (in review) found that minimum temperature, dew point temperature were the most significant factors related to SNC disease severity followed by Oct-Apr mean temperature, Oct-Apr maximum temperature, and Nov-Apr maximum VPD.

Furthermore, the role of N and Ca are hypothesized to play an essential role in SNC disease development (El-Hajj et al., 2004; Mulvey et al., 2013; Perakis et al., 2006). However, Mulvey et al. (2013) found no increase in disease severity associated with standard amounts of fertilization with N, Ca, P, and custom blends of fertilizers in the Oregon Coast Range, even though there were increases detected in foliage nutrient concentrations.

The interaction of climate and soils and their subsequent impacts on foliage chemistry is a challenging swarm of factors to untangle. Solution to this issue will allow for better prediction of where SNC will be most severe and where management activities could overcome the disease. To this end, we utilized soil and foliage chemistry in conjunction with climate variables across a 106 plot network established by the Swiss Needle Cast Cooperative to study the impacts of SNC on coastal Douglas-fir in Oregon and Washington. Utilizing a multi-

variate modeling procedure, we endeavored to create a model that would predict SNC severity and needle retention. Furthermore, we expect also to have the ability to examine the controls on this system in order to inform future experiments examining the biology and ecology of the SNC disease.

Methods

Soil and Foliar Sampling

Soils and foliage were sampled from the SNC monitoring plots currently being established by the Swiss Needle Cast Cooperative (SNCC). From each 0.08ha plot soils were collected from O-horizons, 0-10, 10-20, and 20-30cm. Soils were collected from 5 different locations within each SNCC monitoring plot, one was about plot center and the other four were 4.5m from the corners toward plot center (this was approximately 2/3 the distance from the plot center towards the corners). O-horizons were sampled at the plot center by removing material from a known area using a cutting template 1m north of plot center. All material within the template was collected except live vascular plants and mineral soil. Depths of the O horizon were recorded along 4 sides of the template in order to calculate bulk density. Mineral soils were collected at 0-10, 10-20, and 20-30cm using a push probe form an area devoid of O-horizon. Mineral soils from each depth were composited across the 5 locations from each plot (i.e. one sample per plot per depth). One-year old needles were collected from three branch tips of one branch from 5th whorl of the south side of the tree. Since 10 trees are being sampled in each plot we collected 25-30 needles from each tree and composited this material prior to drying. Approximately 1 g of material was collected (200-250 needles). Foliage, O-horizon, and mineral soil samples were stored in a refrigerator (<4 °C) for less than 4 weeks prior to being oven dried at 40 °C until a constant weight achieved. Mineral soil samples were weighed, sieved to 2mm and the fine fraction weighed to determine coarse content.

Soil and Foliar Chemical Analyses

Mineral soil pH was determined in deionized water using the 2:1 method (Thomas, 1996). C and N were determined on dried and ground O-horizon, mineral soil (<2mm), and foliar material using dry combustion on a Thermo FlashEA 1112. Mineral soils were extracted using 50mL of 1M NH_4Cl to 5g of soil (<2mm) shaken for one hour and centrifuged prior to ICP analysis to extract the exchangeable pools of cations. O-horizons and foliar samples were digested using 30% H_2O_2 and a 1:10 nitric-hydrochloric (HNO_3-HCL) acid digestion of organic matter in conjunction with external heating (EPA method 3050; Benton and Wolf, 1997). Digests and extracts were analyzed for Ca, K, Na, Mg, B, Al, Cu, Fe, Mn, Mo, P, S, and Zn on an inductively coupled plasma atomic emission spectrometry (ICP-AES) using a Thermo Scientific ICP-OES 61E.

Ortho-phosphate was extracted for 3 minutes using a Bray 1 solution (0.03 M NH_4F and 0.025 N HCl) at a ratio of 7:1 (solution to soil) and filtered using a VWR 494 quantitative filter paper (Olsen and Sommers, 1982). The filtrate was analyzed for total extractable P using the previously described ICP-AES.

Climate Data

Climate data were retrieved from PRISM Data Explorer, using coordinates as location parameters (PRISM, 2017). We obtained monthly and annual 30-year normal (1981-2010) climate data for mean temperature, precipitation, and dew point for interpolated grid cells with a resolution of 800 m. Monthly data were used to calculate seasonal climate parameters using subsets of months that a previous study found to be related to SNC pathology on our sites. We defined three seasonal variables including average winter temperature (October-April), total growing season precipitation (May-September), and average growing season dew point (May-September). Additionally, as continentality may influence SNC pathology (Zhao et al., 2011), we calculated a continentality index defined as the difference between the mean 30-year normal temperatures of the warmest month and the coldest month.

Foliar, Soil, Stand, and SNC Data

In addition to climate data, we also used concentrations of multiple nutrients from foliage samples collected from the middle canopy as candidate predictors during model selection. Total estimated mineral soil nutrient contents (0-30 cm) and pH averaged over depths of 0-10 cm, 10-20 cm, and 20-30 cm were also considered during model selection. Soil nutrient contents were calculated using average bulk density values by depth across all sites reported in Hynicka (2014), as volumetric soil samples were not collected. Additionally, we included the ratios of N, P, and Ca contents at 0-10 cm to nutrient contents at 20-30 cm in the model selection procedure. These ratios may indicate how tightly a nutrient is cycling in the system, and N, P, and Ca are the nutrients most likely to be limiting in coastal forests of the Pacific Northwest.

We also included three forest stand structural metrics in our analysis, including basal area (m^2/ha), trees per hectare, and average height to crown base (m). These metrics were only calculated for Douglas-fir. Response variables included needle retention and SNC severity index in the middle canopy.

Statistical Analysis

Three of the 106 total sites were excluded prior to analyses, due to incomplete nutrient data. We used the glmnet package (Friedman et al., 2010) in R version 3.4.4 (R Core Team, 2018) to perform variable selection. Generalized linear models were fit assuming Gaussian distributions using penalized maximum likelihood via LASSO regularization. Both tuning

parameter and variable selection were performed using 5-fold cross validation via the cv.glmnet function. We selected models using cross validation as recommended by Hastie et al., 2009, where the most parsimonious model with a mean square error no larger than one standard deviation greater than the model with the lowest mean square error was chosen. Both predictor and response variables were standardized to unit variance using the default settings in the glmnet package. We then used predictors with non-zero coefficients selected from LASSO regularization in multiple linear regressions, where predictor variables were standardized and centered. Coefficients and adjusted R-squares for final models were obtained from linear regression models. We note that standard errors are likely overly optimistic, as variable selection was performed prior to fitting multiple linear regression models.

Predictor variable selection and regression model development for needle retention and SNC severity index were performed using multiple combinations of potential predictors: 1.) foliar nutrients, stand characteristics, and 30-year normal climate data; 2.) soil nutrients, stand characteristics, and 30-year normal climate data; 3). foliar nutrients, soil nutrients, stand characteristics, and 30-year normal climate data; and 4). soil nutrients and 30-year normal climate data. In all cases, we elected a priori to restrict model sizes to a maximum of ten predictors (plus intercept) to prevent overfitting.

All models were examined for violations of the assumptions of multiple linear regression. Logit transformations were performed on severity indices prior to feature selection as severity index is the product of two continuous proportions. However, residual plots indicated that these models violated model assumptions. Severity indices were subsequently square root transformed, and the resulting models reasonably met the assumptions of multiple linear regression. Additionally, variable selection was performed with standardized, but otherwise untransformed predictor variables, but in limited cases where violations of model assumptions were evident from residual vs. predictor plots, predictors were transformed to meet model assumptions in multiple linear regressions.

Sensitivity Analyses and Model Validation:

Diagnostic plots indicated a high leverage point in SNC severity models that warranted further investigation. This point corresponded to a plot where Douglas-fir basal area was more than 5.5 standard deviations greater than the mean. We performed sensitivity analyses on all models where basal area was selected following the same procedure as described above with this plot removed to determine if the plot's drastically different stand characteristics influenced model selection and parameter estimation.

We also performed model validation using a bootstrapping procedure where LASSO regularization was implemented by iteratively executing the 5-fold cross validation procedure described above on 1000 bootstrapped replicates, each selected randomly with replacement. Due to uncertainty in both model sizes and the individual predictors selected in the initial model selection procedure, we assessed the consistency of both predictors selected and model sizes. We calculated the proportion of times a best model of a given size was selected and the proportion of times a given variable was selected for all 1000 models. We also identified models that were selected with the greatest frequency in the bootstrapping procedure and compared their performance on the original dataset using AICc.

Results

Models produced from foliage, soil, climate, and stand characteristics explained better than 60% of the variance in needle retention (Table 1). The model produced from foliage chemical characteristics did a slightly better job than the model produced from soil characteristics. Foliage and soil N and Na, growing season precipitation, continentality, height to crown base, and basal area were in all models of needle retention. Standardized coefficients indicate that either foliage or soil and climate variables had strong control on needle retention.

Models produced from foliage, soil, climate, and stand characteristics explained between 39 and 47% of the variance in SNC severity (Table 1). As with needle retention, the model produced from foliage chemical characteristics did a slightly better job than the model produced from soil characteristics. Foliage and soil N, Na, and Mn, growing season dewpoint, and basal area were in all models of SNC severity.

The best models produced combined both foliage and soil variables with climate and stand characteristics. Over 50% of the variability in severity and nearly 70% of the variability in needle retention was explained by these models. Foliage N, Na, and Mn were in both the needle retention and SNC severity models. While the same variable was not chosen, both models selected a climate variable that related to growing season atmospheric moisture (dewpoint and precipitation).

Our Prediction of SNC behavior (i.e. foliar retention, and severity index) from soil and foliar chemical characteristics was moderately to fairly successful with this effort, resulting in models that could predict around half or more of the variability (Adjusted R2 ranged from 0.39 to 0.69; Tables 1-2). In all cases both climate and soil or foliar characteristics were needed to produce the best models. Growing season moisture (precipitation and dewpoint) was frequently found to be significant predictors of SNC behavior as has been found by other researchers. Foliar

and soil N, Na, and Mn were found to have significant controls on SNC behavior, as has been found in previous pilot-scale research.

Conclusion

Foliage or soil N was in all models produced from this work supporting the preliminary findings of Waring et al. There appears to be – something going on here related to fungal biology

Foliage and soil Na were both in all the models. Na typically decreases with distance from coast due to the deposition of salt spray. We did not assess distance from coast in this model building work in order to uncover environmental and chemical characteristics related to mechanisms that control SNC severity and needle retention. However, foliage and soil Na would actually measure the direct influence of the coast on these sites and may be autocorrelated with a factor not measured in this study.

Soil and Foliage Mn was in nearly all the models suggesting that it has some control over SNC severity and needle retention as has been found in other coniferous pathogen systems.

Growing season dewpoint or precipitation were in all the models, which supports the finding that moisture is important for fungal development and spread.

We consistently found that SNC severity index was important for predicting needle retention supporting our use of the variable as a predictor of disease in Douglas-fir.

What was not important was as interesting as what we found significantly related with SNC severity and needle retention. Soil pH, foliage and soil Ca and K, distribution of nutrients in soil (indicator of nutrient limiting factors), MAP, stand density, and winter temp never came out as significant in any model. More analysis is needed to determine why these factors were not important.

One caveat to this study. The scale of data may have impacted our results. It is possible that soil and climate variables are autocorrelated, but the soil variables were collected directly from the plots while PRISM climate variables were modeled from weather stations sometimes long-distances from the sites. This may have resulted in soil variables being better predictors of the plot-specific response. This might explain the contradictory results this study found relative to other studies that examined climate variables such as winter temperature (which would could have been explained by continentality).

References

El-Hajj, Z., Kavanagh, K., Rose, C., Kanaan-Atallah, Z., 2004. Nitrogen and carbon dynamics of a foliar biotrophic fungal parasite in fertilized Douglas-fir. New Phytol. 163, 139–147. doi:10.1111/j.1469-8137.2004.01102.x

Lee, E.H., Beedlow, P.A., Waschmann, R.S., Tingey, D.T., Cline, S., Bollman, M., Wickham, C., Carlile, C., 2017. Regional patterns of increasing Swiss needle cast impacts on Douglas-fir growth with warming temperatures. Ecol. Evol. 1–30. doi:10.1002/ece3.3573

Manter, D.K., Reeser, P.W., Stone, J.K., 2005. A climate-based model for predicting geographic variation in swiss needle cast severity in the Oregon coast range. Phytopathology 95, 1256–1265. doi:10.1094/PHYTO-95-1256

Mulvey, R.L., Shaw, D.C., Maguire, D.A., 2013. Fertilization impacts on Swiss needle cast disease severity in western Oregon. For. Ecol. Manage. 287, 147–158. doi:10.1016/j.foreco.2012.08.050

Perakis, S.S., Maguire, D.A., Bullen, T.D., Cromack, K., Waring, R.H., Boyle, J.R., 2006. Coupled nitrogen and calcium cycles in forests of the Oregon Coast Range. Ecosystems 9, 63–74. doi:10.1007/s10021-004-0039-5

Rosso, P.H., Hansen, E.M., 2003. Predicting swiss needle cast disease distribution and severity in young douglas-fir plantations in coastal Oregon. Phytopathology 93, 790–798. doi:10.1094/PHYTO.2003.93.7.790

Zhao, J., Maguire, D.A., Mainwaring, D.B., Kanaskie, A., 2012. Climatic influences on needle cohort survival mediated by Swiss needle cast in coastal Douglas-fir. Trees - Struct. Funct. 26, 1361–1371. doi:10.1007/s00468-012-0711-x

Zhao, J., Mainwaring, D.B., Maguire, D.A., Kanaskie, A., 2011. Regional and annual trends in Douglas-fir foliage retention: Correlations with climatic variables. For. Ecol. Manage. 262, 1872–1886. doi:10.1016/j.foreco.2011.08.008

SNC transect plots in the Oregon Cascade foothills

Gabriela Ritóková[1], Dave Shaw[1], Doug Mainwaring[1], Doug Maguire[1], Bill Marshall[2]
[1]SNCC, Forest Engineering, Resource, and Management, Oregon State University, [2]Cascade Timber Consulting

Background

In addition to the SNCC research and monitoring plot network, 47 disease monitoring sites were established in the Oregon Cascades foothills in 2017. The sites were located in young Douglas-fir plantations on SNCC member lands: Weyerhaeuser, Cascade Timber Consulting, Oregon Department of Forestry, and a private landowner, Melcher Logging and Timber Harvesting Inc. (fig. 1).

The aim of the survey was to evaluate SNC conditions annually for five years with the intention of repeating the height and diameter measurement in 5 years to determine volume growth of each tree.

In the winter of 2019 we anticipate installing two weather stations; for collecting leaf wetness data in three crown positions, as well as air temperature, relative humidity and solar irradiance. This will help us determine which seasonal factors or site affect SNC severity within the study area.

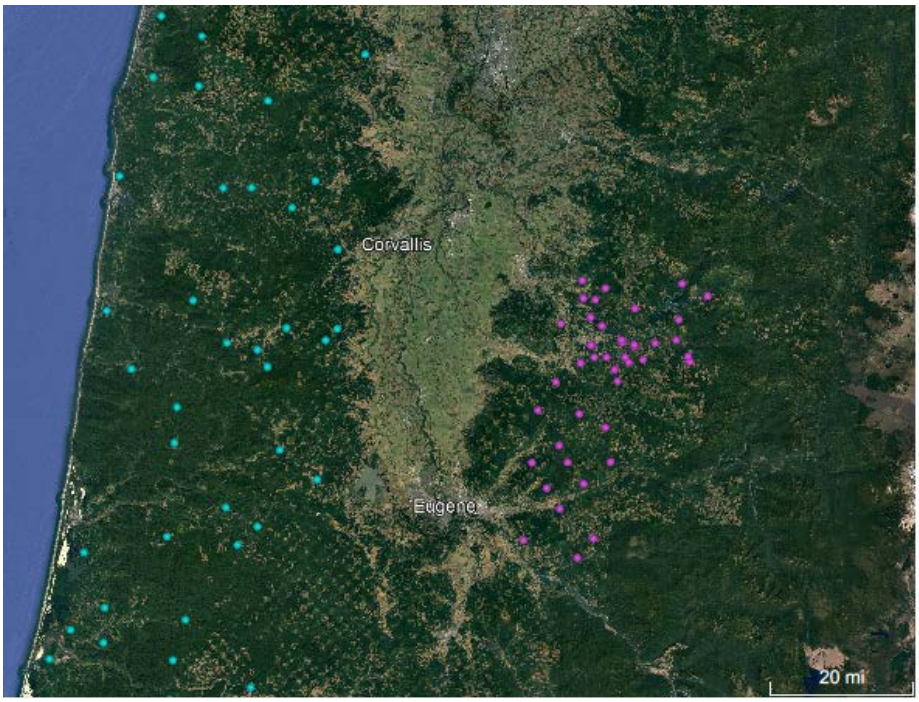

Figure 1. Transect plot locations in the Oregon Cascade foothills (pink dots) in relation to the coastal permanent plots (blue dots)

Methodology

A subset of the original stands was monitored in 2018 due to the difficulties of observing foliage retention in the larger (and older) trees. The initial study proposal and field methodology did not involve tree climbing, a lack of which limits foliage sampling opportunities in older trees. As a result, during the resampling period in May and June 2018, we sampled 370 trees in 37 transects. The age of sampled Douglas-fir ranged from 10 – 20 years. At every 20 m of the 100 meter transect the same two dominant or codominant Douglas-fir trees that had been evaluated in 2017 were reevaluated for foliar retention and disease severity, though the height and diameter were not remeasured. In addition, the four-year-old mid-crown secondary lateral branches were collected from the south side of each sample tree to determine SNC disease severity and foliage retention (in years). Plot establishment methodology was described in the 2017 SNCC annual report.

SNC disease severity was observed in the field and severity classes were described and based on the % of occluded stomates on second year needles. A zero rating indicates no pseudothecial presence, while a rating of one was considered lightly occluded of stomates up to ~20%. A rating of two is assigned to needles with occlusion of stomates between 21 and 50%. Lastly, severe occlusion with >50% stomates plugged with pseudothecia was represented by a rating of three (fig.2).

The lateral branches were also used to estimate the average number of annual needle compliments present. This was done by estimating the proportion of attached needles present within each cohort of the lateral's primary axis. The foliage retention estimate protocol was adopted from the field methods described by Kanaskie and Maguire (2002).

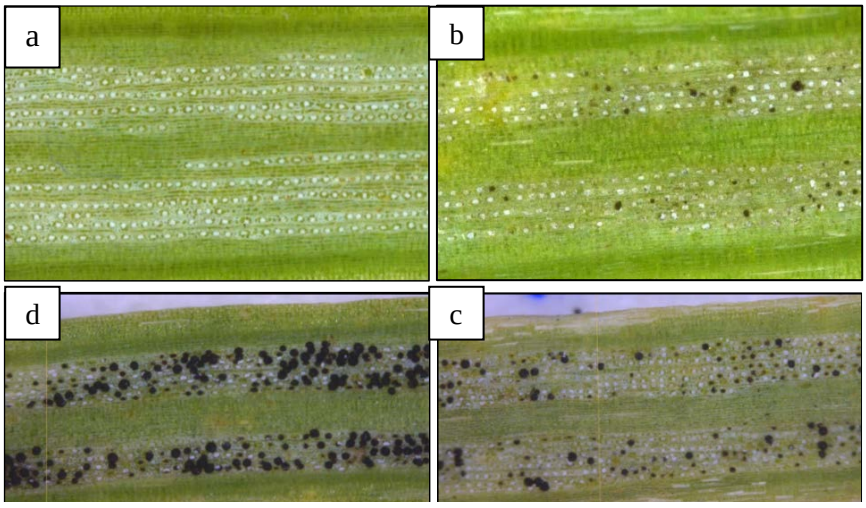

Figure 2. Severity ratings: a) none – 0; b) light – 1; c) moderate – 2; d) severe – 3.

2018 Results

Characterization of relative disease severity in these sites was based on Hansen et al. (2000). Although the pathogen was present in some sites classified as healthy, disease symptoms were minimal. This was observed especially in 2018, when disease severity was more intense and second year needles had a greater number of occluded stomates than in 2017. Nevertheless, foliage retention was higher and foliage color observed was healthier, darker green. In comparison with 2017, the foliage retention of sampled stands in 2018 was slightly greater, ranging between 2.25 and 3.75 (fig.3).

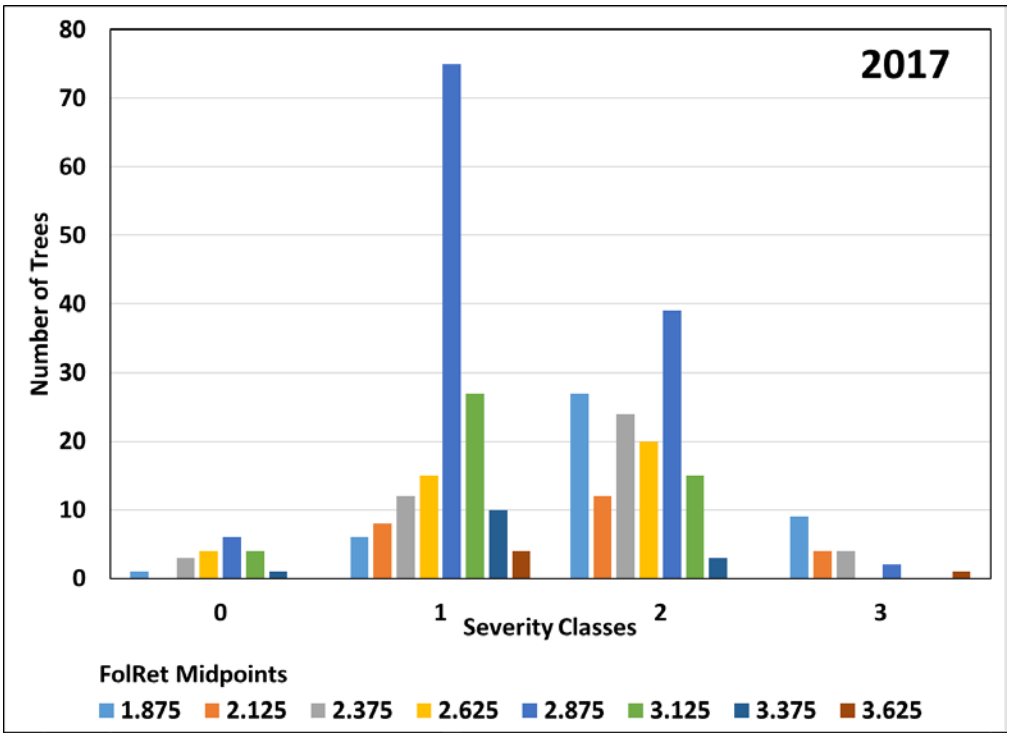

Figure 4. Tree-level distribution of severity classes in 2017.

According to Maguire et al. (2011), foliage retention is an imperfect index for the effect SNC has on the growth of trees. There are plots that have low foliage retention that exhibit good growth while others with the same low FR exhibit poor growth. There is a wide variation in the amount of growth loss for a given level of foliage retention. One possible reason is that at a given level of foliage retention, needles can have many occluded stomates or not, and foliage retention has only a loose correlation with occlusion (fig 4 and 5). Still, foliage retention remains the best index of tree growth. It is an easy way to estimate growth loss because foliage retention in different areas of the crown is relatively easy to see, unlike pseudothecial occlusion.

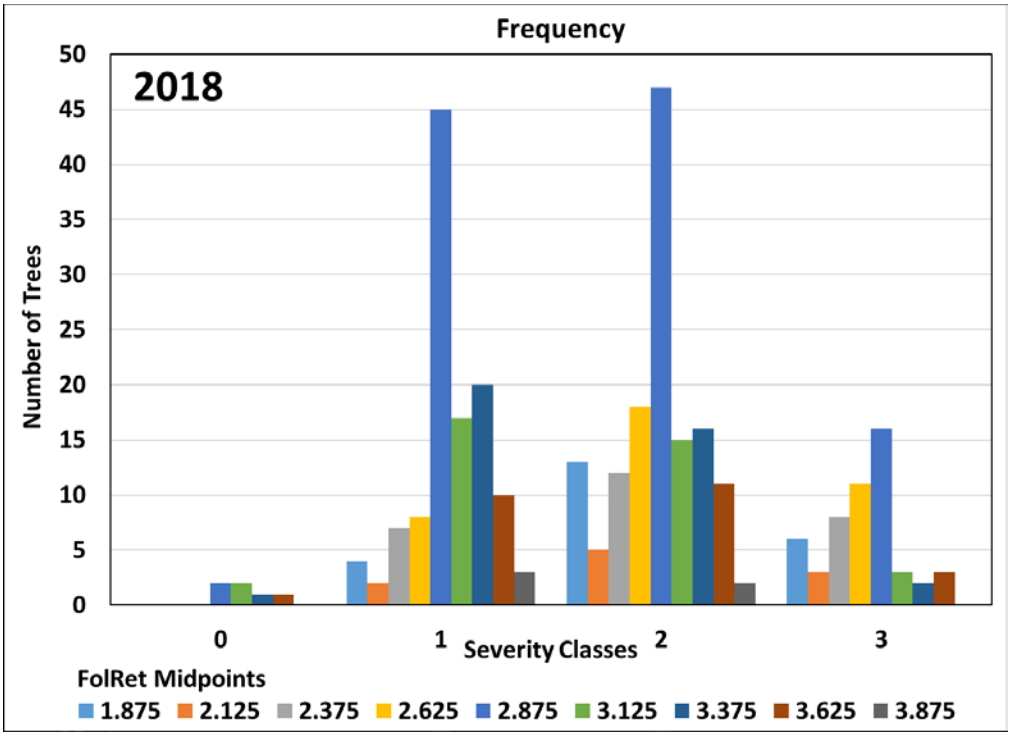

Figure 5. Tree-level distribution of severity classes in 2018.

Maguire et al. (2011) observed that the effect of foliage retention varies by year but is generally stable. These observations and analysis were based on the Growth Impact Plot network and Mainwaring et al. (2018) in the SNCC annual report show the effect of foliage retention on growth loss (page 26, figure 1).

Data collected in 2018 exhibited some differences from that collected from the same plots in 2017: 1) In 2018 severity increased with severity classes 2 and 3 higher than in 2017 (fig 6); 2) In both years, stands sampled above 1,700 feet (~520m) did not exhibit foliage retentions below an average of 2.8 years (fig 7); 3) From 2017 to 2018 severity ratings increased. In general severity decreased with an increase in elevation (fig 8). Trees on these plots exhibited a negative relationship between pseudothecial occlusion and foliage retention, suggesting that some of the explanation for differences in foliage retention can be explained by SNC.

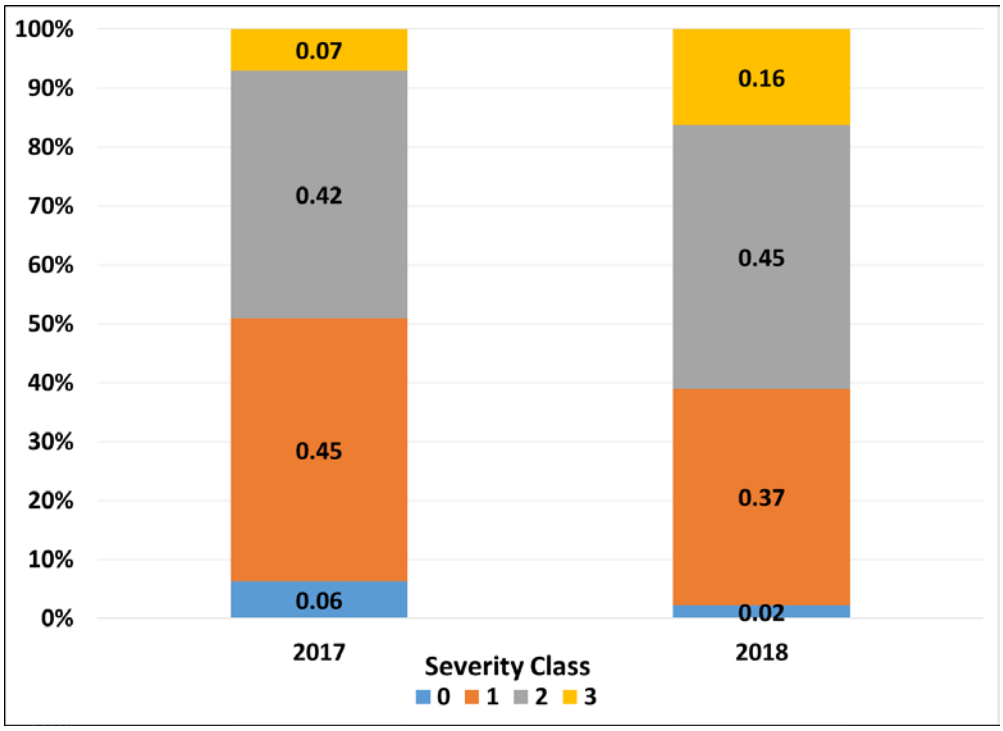

Figure 6. Relative distribution of severity classes by plot.

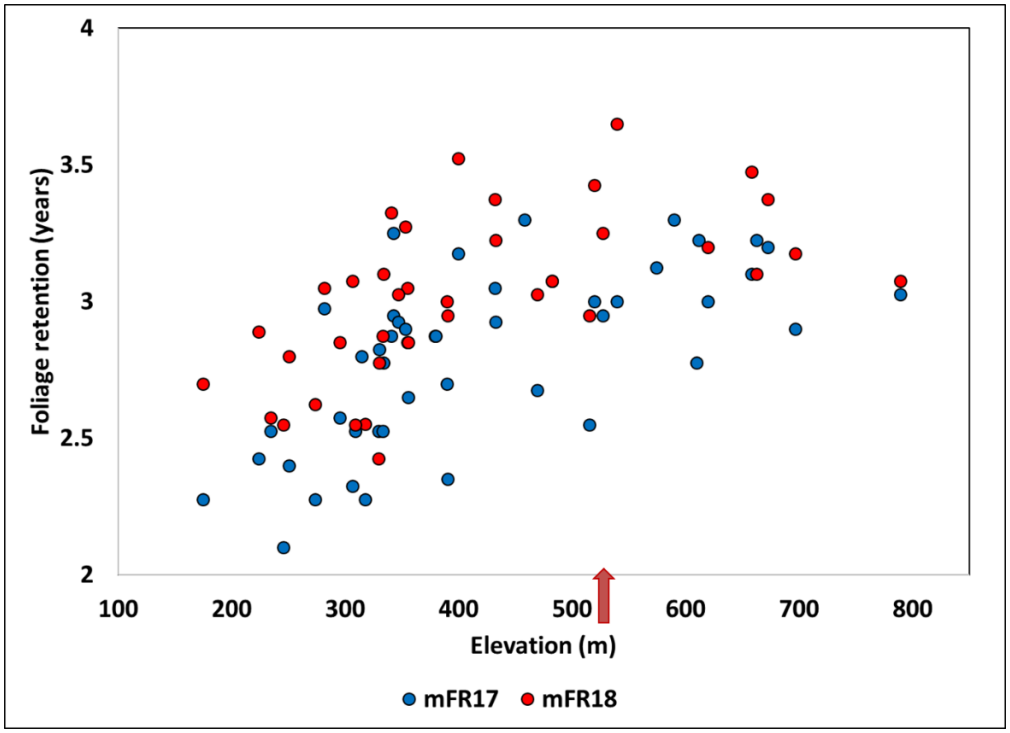

Figure 7. Plot-level foliage retention by elevation and year.

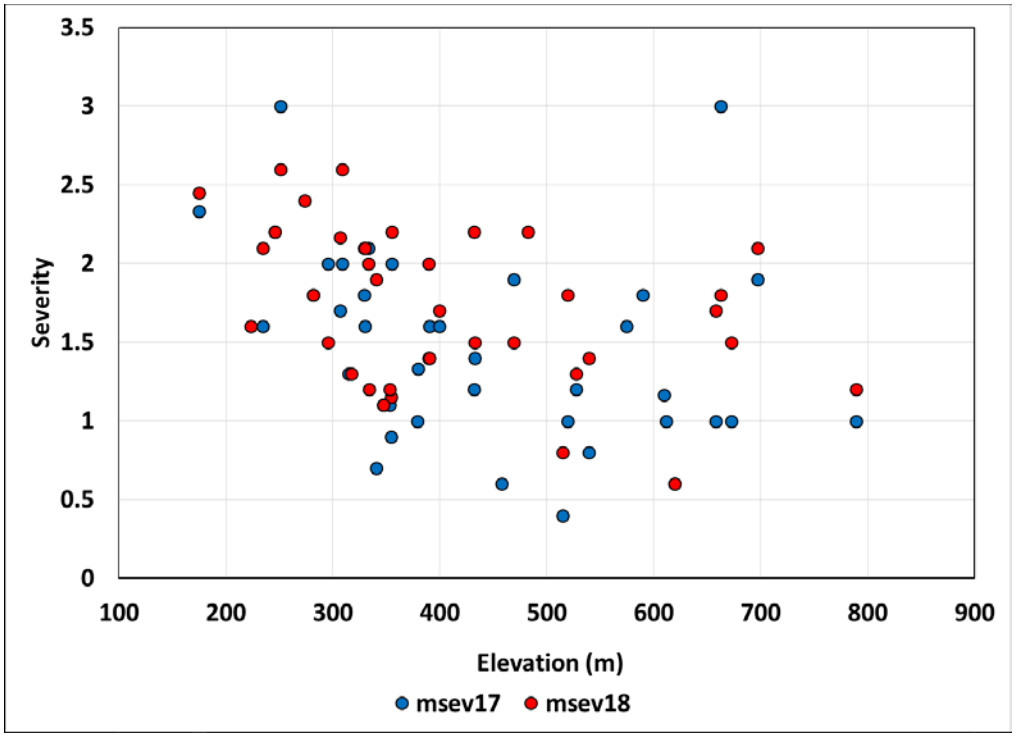

Figure 8. Plot-level severity by foliage retention and year.

Literature Cited

Maguire, D.A., D.B. Mainwaring, and A. Kanaskie. 2011. Ten-year growth and mortality in young Douglas-fir stands experiencing a range in Swiss needle cast severity. Canadian Journal of Forest Research 41: 2064-2076.

Ritóková, G., Shaw, D.C., Filip, G., Kanaskie, A., Browning, J., and D. Norlander. 2016. Swiss Needle Cast in Western Oregon Douglas-Fir Plantations: 20-Year Monitoring Results. Forests 7, 155.

List of Refereed Publications

Disease Distribution, Severity and Epidemiology

Agne, MC, Beedlow PA, Shaw DC, Woodruff DR, Lee EH, Cline S, Comeleo RL. 2018. Interactions of predominant insects and diseases with climate change in Douglas-fir forests of western Oregon and Washington, U.S.A.. Forest Ecology and Management. 409:317-332.

Hansen, E. M., Stone, J. K., Capitano, B. R., Rosso, P., Sutton, W., Winton, L., Kanaskie, A. and M. G. McWilliams. 2000. Incidence and impact of Swiss needle cast in forest plantations of Douglas-fir in coastal Oregon. Plant Disease. 84: 773-779.

Manter, D. K., Reeser, P. W., and J. K. Stone. 2005. A climate-based model for predicting geographic variation in Swiss needle cast severity in the Oregon coast range. Phytopathology. 95: 1256-1265.

Ritóková, G, Shaw DC, Filip GM, Kanaskie A, Browning J, Norlander D. 2016. Swiss Needle Cast in Western Oregon Douglas-Fir Plantations: 20-Year Monitoring Results. Forests. 7(155)

Rosso, P. H. and E. M. Hansen. 2003. Predicting Swiss needle cast disease distribution and severity in young Douglas-fir plantations in coastal Oregon. Phytopathology. 93: 790-798.

Stone, J. K., Hood, I. A., Watt, M. S. and J. L. Kerrigan. 2007. Distribution of Swiss needle cast in New Zealand in relation to winter temperature. Australasian Plant Pathology. 36: 445-454.

Stone, J. K., Capitano, B. R. and J. L. Kerrigan. 2008. The histopathology of *Phaeocryptopus gaeumannii* on Douglas-fir needles. Mycologia. 100: 431-444.

Stone, J. K., Coop, L. B. and D. K. Manter. 2008. Predicting the effects of climate change on Swiss needle cast disease severity in Pacific Northwest forests. Canadian Journal of Plant Pathology. 30: 169-176.

Watt, M. S., Stone, J. K., Hood, I. A. and D. J. Palmer. 2010. Predicting the severity of Swiss needle cast on Douglas-fir under current and future climate in New Zealand. Forest Ecology and Management (*in press*).

Forest Protection Issues

Kelsey, R. G. and D. K. Manter. 2004. Effect of Swiss needle cast on Douglas-fir stem ethanol and monoterpene concentrations, oleoresin flow, and host selection by the Douglas-fir beetle. Forest Ecology and Management. 190: 241-253.

Shaw, D. C., Filip, G. M., Kanaskie, A., Maguire, D. A. and W. Littke. 2011. Managing an epidemic of Swiss needle cast in the Douglas-fir region of Oregon: The Swiss Needle Cast Cooperative. Journal of Forestry (*in press*).

Genetic Resistance/Tolerance in Douglas-fir

Kastner, W., Dutton, S. and D. Roche. 2001. Effects of Swiss needle cast on three Douglas-fir seed sources on a low-elevation site in the northern Oregon Coast Range: Results after five growing seasons. Western Journal of Applied Forestry. 16 (1): 31-34.

Jayawickrama, K.J.S., D. Shaw, and T.Z. Ye. 2012. Genetic Selection in Coastal Douglas-fir for tolerance to Swiss Needle Cast Disease. Proceedings of the fourth international workshop on the genetics of host-parasite interactions in forestry: Disease and insect resistance in forest trees. Gen. Tech. Rep. PSW-GTR-240. Albany, CA: Pacific Southwest Research Station, Forest Service, U.S. Department of Agriculture. 372 p.

Johnson, G. R. 2002. Genetic variation in tolerance of Douglas-fir to Swiss needle cast as assessed by symptom expression. Silvae Genetica. 51: 80-86.

Temel, F., Johnson, G. R. and J. K. Stone. 2004. The relationship between Swiss needle cast symptom severity and level of *Phaeocryptopus gaeumannii* colonization in coastal Douglas-fir (*Pseudotsuga menziesii var. menziesii*). Forest Pathology. 34: 383-394.

Temel, F., Johnson, G. R. and W. T. Adams. 2005. Early genetic testing of coastal Douglas-fir for Swiss needle cast tolerance. Canadian Journal of Forest Research. 35: 521-529.

Wilhelmi, N.P., Shaw D.C., Harrington C.A., St. Clair J.B., Ganio L.M. 2017. Climate of seed source affects susceptibility of coastal Douglas-fir to foliage diseases. Ecosphere. 8(12):e02011.

Genetics of *Nothophaeocryptopus gaeumannii*

Winton, L. M., Hansen, E. M. and J. K. Stone. 2006. Population structure suggests reproductively isolated lineages of *Phaeocryptopus gaeumannii*. Mycologia. 98 (5): 781-791.

Winton. L. M., Stone, J. K. and E. M. Hansen. 2007. The systematic position of *Phaeocryptopus gaeumannnii*. Mycologia. 99: 240-252.

Mensuration and growth effects

Lee, E.H., Beedlow P.A., Waschmann R.S., Tingey D.T., Cline S., Bollman M., Wickham C., Carlile C. 2017. Regional patterns of increasing Swiss needle cast impacts on Douglas-fir growth with warming temperatures. Ecology and Evolution. 7(24):11167–11196.

Maguire D. A., Kanaskie, A., Voelker, W., Johnson, R. and G. Johnson. 2002. Growth of young Douglas-fir plantations across a gradient in Swiss needle cast severity. Western Journal of Applied Forestry. 17: 86-95.

Maguire, D. A. and A. Kanaskie. 2002. The ratio of live crown length to sapwood area as a measure of crown sparseness. Forest Science. 48: 93-100.

Maguire, D. A., Mainwaring, D. B. and Kanaskie A. 2011. Ten-year growth and mortality in young Douglas-fir stands experiencing a range in Swiss needle cast severity. Can. J. For. Res. 41: 2064-2076.

Weiskittel, A. R., Garber, S. M., Johnson, G. P., Maguire, D. A. and R.A. Monserud. 2007. Annualized diameter and height growth equations for Pacific Northwest plantation-grown Douglas-fir, western hemlock, and red alder. Forest Ecology and Management. 250: 266-278.

Weiskittel, A. R., Maguire, D. A., Garber, S. M. and A. Kanaskie. 2006. Influence of Swiss needle cast on foliage age class structure and vertical distribution in Douglas-fir plantations of north coastal Oregon. Canadian Journal of Forest Research. 36: 1497-1508.

Weiskittel, A. R., Maguire, D. A. and R. A. Monserud. 2007. Modeling crown structural responses to competing vegetation control, thinning, fertilization, and Swiss needle cast in coastal Douglas-fir of the Pacific Northwest, USA. Forest Ecology and Management. 245: 96-109.

Weiskittel, A. R., Maguire, D. A. and R. A. Monserud. 2007. Response of branch growth and mortality to silvicultural treatments in coastal Douglas-fir plantations: Implications for predicting tree growth. Forest Ecology and Management. 251: 182-194.

Weiskittel, A. R. and D. A. Maguire. 2007. Response of Douglas-fir leaf area index and litterfall dynamics to Swiss needle cast in north coastal Oregon, USA. Annals of Forest Science. 64: 121-132.

Weiskittel, A. R. and D. A. Maguire. 2006. Branch surface area and its vertical distribution in coastal Douglas-fir. Trees. 20: 657-667.

Weiskittel, A. R., Temesgen, H., Wilson, D. S. and D. A. Maguire. 2008. Sources of within and between-stand variability in specific leaf area of three ecologically distinct conifer species. Annals of Forest Science. 65: 103-112.

Zhao, J., Maguire, D. A., Mainwaring, D. B., Kanaskie, A. 2012. Climatic influences on needle cohort survival mediated by Swiss needle cast in coastal Douglas-fir. Trees 26: 1361-1371

Zhao, J., Mainwaring, D. B., Maguire, D. A., Kanaskie, A. 2011. Regional and annual trends in Douglas-fir foliage retention: Correlations with climatic variables. For. Ecol. And Management 262: 1872-1886

Zhao, J, Maguire DA, Mainwaring DB, Kanaskie A. 2015. The effect of within-stand variation in Swiss needle cast intensity on Douglas-fir stand dynamics. Forest Ecology and Management. 347:75-82.

Zhao, J., Maguire, D. A., Mainwaring, D. B., Wehage, J., Kanaskie, A. 2013. Thinning Mixed Species Stands of Douglas-Fir and Western Hemlcok in the Presence of Swiss Needle Cast: Guidelines Based on Relative Basal Area Growth of Individual Trees. For. Sci. 60 (1): 191-199.

Nutrition and soil interactions

Waring, R. H., Boyle, J., Cromack, K. Jr., Maguire, D. and A. Kanaskie. 2000. Researchers offer new insights into Swiss needle cast. Western Forester. 45 (6): 10-11.

El-Hajj, Z., Kavanagh, K., Rose, C., and Z. Kanaan-Atallah. 2004. Nitrogen and carbon dynamics of a foliar biotrophic fungal parasite in fertilized Douglas-fir. New Phytologist. 163: 139-147.

Mulvey, R.L., Shaw, D.C., Maguire, D.A. 2013. Fertilization impacts on Swiss needle cast disease severity in Western Oregon. Forest Ecology and Management 287: 147-158.

Perakis, S. S., Maguire, D. A., Bullen, T. D., Cromack, K., Waring, R. H. and J. R. Boyle. 2005. Coupled nitrogen and calcium cycles in forests of the Oregon Coast Range. Ecosystems. 8: 1-12.

Pathology and physiological host effects

Bennett, P., Stone, J. 2016. Assessments of Population Structure, Diversity, and Phylogeography of the Swiss Needle Cast Fungus (*Phaeocryptopus gaeumannii*) in the U.S. Pacific Northwest. Forests: 7, 14.

Black, B. A., Shaw, D. C. and J. K. Stone. 2010. Impacts of Swiss needle cast on overstory Douglas-fir forests of western Oregon Coast Range. Forest Ecology and Management. 259: 1673-1680.

Lee, H.E., Beedlow, P.A., Waschamnn, R.S., Burdick, C.A., Shaw, D.C. 2013. Tree-ring analysis of the fungal disease Swiss needle cast in western Oregon coastal forests. Can Journal of For. 43(8):677-690.

Manter, D. K., Bond, B. J., Kavanagh, K. L., Rosso, P. H. and G. M. Filip. 2000. Pseudothecia of Swiss needle cast fungus, *Phaeocryptopus gaeumannii*, physically block stomata of Douglas-fir, reducing CO_2 assimilation. New Phytologist. 148 (3): 481-491.

Manter, D. K. 2002. Energy dissipation and photoinhibition in Douglas-fir needles with a fungal-mediated reduction in photosynthetic rates. Phytopathology. 150: 674-679.

Manter, D. K., Bond, B. J., Kavanagh, K. L., Stone, J. K. and G. M. Filip. 2003. Modeling the impacts of the foliar pathogen, *Phaeocryptopus gaeumannii*, on Douglas-fir physiology: net canopy carbon assimilation, needle abscission and growth. Ecological Modeling. 164: 211-226.

Manter, D. K. and Kavanagh, K. L. 2003. Stomatal regulation in Douglas-fir following a fungal-mediated chronic reduction in leaf area. Trees. 17: 485-491.

Manter, D. K., Kelsey, R. G., and J. K. Stone. 2001. Quantification of *Phaeocryptopus gaeumannii* colonization in Douglas-fir needles by ergosterol analysis. Forest Pathology. 31: 229-240.

Manter, D. K., Winton, L. M., Filip, G. M. and J. K. Stone. 2003. Assessment of Swiss needle cast disease: temporal and spatial investigations of fungal colonization and symptom severity. Phytopathology. 151: 344-351.

Saffell, B.J., Meinzer, R.C., Voelker, S.L., Shaw, D.C., Brooks, R.J., Lachenbruch, B, McKay, J. 2014. Tree-ring stable isotopes record the impact of a foliar fungal pathogen on CO_2 assimilation and growth in Douglas-fir. Plant, Cell & Environment. doi: 10.1111/pce.12256

Winton, L. M., Manter, D. K., Stone, J. K. and E. M. Hansen. 2003. Comparison of biochemical, molecular and visual methods to quantify *Phaeocryptopus gaeumannii* in Douglas-fir foliage. Phytopathology. 93: 121-126.

Winton, L. M., Stone, J. K., Watrud, L. S. and E. M. Hansen. 2002. Simultaneous one-tube quantification of host and pathogen DNA with real-time polymerase chain reaction. Phytopathology. 92: 112-116.

Winton, L. M., Stone, J. K. and E. M. Hansen. 2007. Polymorphic microsatellite markers for the Douglas-fir pathogen *Phaeocryptopus gaeumannii*, causal agent of Swiss needle cast disease. Molecular Ecology. 7: 1125-1128.

Silviculture and Control

Filip, G., Kanaskie, A., Kavanagh, K., Johnson, G., Johnson, R. and D. Maguire. 2000. Research Contribution 30, Forest Research Laboratory, College of Forestry, Oregon State University, Corvallis, Oregon.

Mainwaring, D. B., Maguire, D. A., Kanaskie, A. and J. Brandt. 2005. Growth responses to commercial thinning in Douglas-fir stands with varying intensity of Swiss needle cast. Canadian Journal of Forest Research. 35: 2394-2402.

Stone, J. K., Reeser, P. W. and A. Kanaskie. 2007. Fungicidal suppression of Swiss needle cast and pathogen reinvasion in a 20-year-old Douglas-fir stand. Western Journal of Applied Forestry. 22: 248-252.

Wood Quality

Johnson, G. R., Gartner, B. L., Maguire, D. and A. Kanaskie. 2003. Influence of Bravo fungicide applications on wood density and moisture content of Swiss needle cast affected Douglas-fir trees. Forest Ecology and Management. 186: 339-348.

Grotta, A. T., Leichti, R. J., Gartner, B. L. and G. R. Johnson. 2004. Effect of growth ring orientation and placement of earlywood and latewood on MOE and MOR of very-small clear Douglas-fir beams. Wood and Fiber Science. 37: 207-212.

Johnson, G. R., Grotta, A. T., Gartner, B. L. and G. Downes. 2005. Impact of the foliar pathogen Swiss needle cast on wood quality of Douglas-fir. Canadian Journal of Forest Research. 35: 331-339.

Phytopathology • XXXX • XXX:X-X • https://doi.org/10.1094/PHYTO-06-18-0195-R

Population Biology

e-Xtra*

The Genetic Structure of Populations of the Douglas-Fir Swiss Needle Cast Fungus *Nothophaeocryptopus gaeumannii* in New Zealand

P. I. Bennett,[1,†] I. A. Hood,[2] and J. K. Stone[1]

[1]Department of Botany and Plant Pathology, Oregon State University, Corvallis 97331; and [2]Scion Forest Protection, Private Bag 3020, Rotorua 3046, NZ.

Accepted for publication 16 August 2018.

ABSTRACT

Swiss needle cast is a foliar disease of Douglas-fir (*Pseudotsuga menziesii*) that results in premature foliage loss and reduced growth. The causal fungus, *Nothophaeocryptopus gaeumannii,* was first detected in New Zealand in 1959 and spread throughout the North and South Islands over the following decades. The contemporary genetic structure of the *N. gaeumannii* population in New Zealand was assessed by analyzing 468 multilocus SSR genotypes (MLGs) from 2,085 *N. gaeumannii* isolates collected from 32 sites in the North and South Islands. Overall diversity was lower than that reported from native *N. gaeumannii* populations in the northwestern United States, which was expected given that *N. gaeumannii* is introduced in New Zealand. Linkage disequilibrium was significantly higher than expected under random mating, suggesting that population structure is clonal. Populations of *N. gaeumannii* in the North and South Islands were weakly differentiated, and the isolates collected from sites within the islands were moderately differentiated. This suggests that gene flow has occurred between the *N. gaeumannii* populations in the North and South Islands, and between the local *N. gaeumannii* populations within each island. Eighteen isolates of *N. gaeumannii* Lineage 2, which has previously been reported only from western Oregon, were recovered from two sites in the North Island and four sites in the South Island. The most likely explanation for the contemporary distribution of *N. gaeumannii* in New Zealand is that it was introduced on infected live seedlings through the forestry or ornamental nursery trade, as the fungus is neither seed borne nor saprobic, and the observed population structure is not consistent with a stochastic intercontinental dispersal event.

The foliar disease Swiss needle cast (SNC) is specific to Douglas-fir (*Pseudotsuga menziesii* (Mirb.) Franco), and results from cumulative occlusion of needle stomata by the ascocarps of *Nothophaeocryptopus gaeumannii* (T. Rohde) Videira, C. Nakash., U. Braun & Crous (Manter et al. 2000; Stone et al. 2008a). The disease was first described from a Douglas-fir plantation in Switzerland in 1925 and became established throughout central Europe and the U.K. in the following decades (Boyce 1940; Liese 1939; Peace 1962; Rohde 1936; Wilson and Waldie 1928). However, there is ample evidence to suggest that the fungus is endemic in the native range of its host in western North America (Boyce 1940; Hood 1982; Meinecke 1939). The pathogen has since accompanied its host worldwide as exotic Douglas-fir plantings have been established for timber production. The presence of this fungus has been confirmed in Douglas-fir plantations in the northeastern United States (McCormick 1939; Morton and Patton 1970), Australia (Marks 1975), New Zealand (Hood et al. 1990; Hood and Kershaw 1975), Turkey (Temel et al. 2003), Chile (Osorio 2007), and Spain (Castaño et al. 2014). A severe outbreak of SNC that started in mid-1980s continues to intensify in the low-elevation forests along western slopes of the Coast Ranges in Oregon and Washington where both host and pathogen are native (Hansen et al. 2000; Ritóková et al. 2016; Stone et al. 2008b).

†Corresponding author: Patrick Bennett; E-mail: bennetpa@oregonstate.edu

Funding: Major funding, laboratory, technical, and logistic support provided by Scion Research, Ltd. is gratefully acknowledged. Additional funding was provided from the New Zealand Ministry of Business, Innovation and Employment Strategic Science Investment Fund.

*The *e-Xtra* logo stands for "electronic extra" and indicates that three supplementary figures are published online.

Douglas-fir has been cultivated as a commercial timber species in New Zealand since the early 20th century, but accounts for only a small fraction of the total forest land area and timber production (Ministry for Primary Industries 2016). The origins of Douglas-fir seed imported into New Zealand before 1926 are unknown, but plantations were established thereafter from seed sources in the Coast Ranges of Oregon, Washington, and British Columbia, with the majority of seed stock coming from southern Washington (Weston 1957). The first reported presence of *N. gaeumannii* in New Zealand was in 1959 in the North Island near Taupo, where it was initially restricted to an area with a radius of approximately 130 km (Hood and Kershaw 1975). However, symptoms of SNC, such as chlorosis and needle loss, were not reported in the region until 1962 (Hood and Kershaw 1975). Over the following 10 years, the fungus was found in most of the Douglas-fir plantations in the North Island and was detected for the first time in the South Island in 1969 (Hood and Kershaw 1975). By 1974, the fungus had been found throughout the Douglas-fir growing region in the northern part of the South Island, and sporadically at sites farther south (Hood and Kershaw 1975). It has been suggested that the spread of the disease to the South Island may have been due to the movement of infected seedlings from the North Island (Hood and Kershaw 1973). In total, it took approximately 30 years for *N. gaeumannii* to become established in all but a few of the most remote Douglas-fir plantations in New Zealand (Hood et al. 1990).

A comparison of the genetic structures of *N. gaeumannii* populations in New Zealand, Europe, and the United States revealed that the populations in western Oregon, where SNC symptoms had become increasingly more severe in many natural Douglas-fir stands and timber plantations, consisted of two reproductively isolated lineages (Winton et al. 2006). Lineage 1 was found to be widespread, occurring throughout the native range of Douglas-fir (except for the extreme southern coast of Oregon)

and wherever its host was grown abroad as an exotic, including Europe and New Zealand (Winton et al. 2006). Lineage 2 was found to be much less common, occurring in pure (i.e., nonadmixed) populations along the southern Oregon coast, and in admixed populations with lineage 1 in the central and northwestern Oregon Coast Range (Bennett and Stone 2016; Winton et al. 2006). Lineage 2 was not detected in collections from Washington, the eastern United States, Europe, or New Zealand (Winton et al. 2006). At the time of this discovery, it was suggested that Lineage 2 may be responsible for the recent emergence of SNC in western Oregon, as it was found in high abundance in severely diseased stands near the coast and was often not detected in healthier stands further east (Winton et al. 2006).

The aims of this study were to (i) examine the effects of the introduction and spread of *N. gaeumannii* in New Zealand on the genetic structure of its populations, and (ii) determine whether *N. gaeumannii* Lineage 2 is present in New Zealand. There is evidence to suggest that this fungus is capable of homothallic reproduction, i.e., fertile asci arise from self-fertilization (asexual conidial reproduction is not known in *N. gaeumannii*) (Bennett and Stone 2016; Winton et al. 2006). Thus, we hypothesized that the introduction of *N. gaeumannii* to New Zealand would have resulted in a founder event, and successive generations of self-fertilization along with genetic drift would result in a genetic bottleneck. We also considered several hypotheses about the expected spatial genetic structure of the *N. gaeumannii* population in New Zealand, and considered two possible scenarios that might explain the current extent of colonization: (i) *N. gaeumannii* spread from an initial site of introduction in the North Island to its current distribution by the anthropogenic movement of infected Douglas-fir seedlings (or foliage) or long-distance aerial spore dispersal, or (ii) *N. gaeumannii* spread from the site of initial introduction via local ascospore dispersal and colonized the South Island gradually as described in Hood and Kershaw (1973). The first scenario would likely result in a relatively homogeneous distribution of *N. gaeumannii* genotypes and an abundance of shared multilocus genotypes (MLGs) between islands and sites. We might also expect the first scenario to result in a lack of isolation by distance, where genetic dissimilarity between sites is not related to geographic distance between sites. On the other hand, the second scenario should result in a more heterogeneous spatial distribution of MLGs and an abundance of regionally specific genotypes resulting from selection or genetic drift. The second scenario would be expected to result in isolation by distance.

MATERIALS AND METHODS

Field sampling, isolations, and culturing. The isolates included in these analyses were collected from Douglas-fir plantations in New Zealand in 2005 and 2007 (Stone et al. 2007; Watt et al. 2010). Foliage was sampled from 13 sites in the North Island and 19 in the South Island (Fig. 1). Samples were collected from secondary branches in the upper crowns of 10 Douglas-fir trees of the coastal variety (*P. menziesii* var. *menziesii*) at each site. Twenty needles were selected from each tree for single-ascospore isolations. Double-sided adhesive tape was used to affix 2-year-old needles bearing pseudothecia to the lids of Petri dishes. These plates were then incubated at room temperature for approximately 24 to 48 h, during which time the ascospores discharged onto the agar surface below. Between 20 and 50 individual ascospores were isolated from each foliage sample, transferred onto 2% malt agar, and incubated for a minimum of 2 to 6 months to allow adequate growth for DNA extraction.

Molecular techniques. DNA was extracted with the procedure described in Winton et al. (2006). Briefly, mycelium was scraped from the agar surface and macerated by shaking in a mini-beadbeater with glass beads and CTAB (cetyltrimethylammonium bromide) extraction buffer (Winton et al. 2006). The samples were then incubated at 65°C for 2 h and precipitated in 24:1 chloroform/isoamyl alcohol (Winton et al. 2006). A QIAAmp Spin Column (Qiagen, Hilden, Germany) was then used to purify the DNA and reduce PCR inhibitors (Winton et al. 2006). Ten microsatellite loci were amplified in three multiplexed PCR reactions with fluorescently-labeled reverse primers (Bennett and Stone 2016; Winton et al. 2007). Genotyping was performed via capillary electrophoresis at the Oregon State University Center for Genome Research and Biocomputing (CGRB) with the parameters described in Winton et al. (2007) and Bennett and Stone (2016). Allele scoring was performed as described in Bennett and Stone (2016). A positive control isolate was included to ensure consistency between each independent PCR amplification and genotyping run. One of the loci, Pgdi5, did not amplify consistently for all isolates and was omitted from subsequent analyses.

Data analysis. The map of sampling sites in New Zealand was created in R version 3.4.1 (R Core Team 2017) with the R packages ggplot2 (Wickham 2016), ggrepel (Slowikowski 2017), and ggsn (Baquero 2017). The multilocus SSR genotypes for the N. gaeumannii isolates collected in New Zealand were formatted with GenAlEx 6.503 (Peakall and Smouse 2012, 2006), and imported into R version 3.4.1 (R Core Team 2017) for use with the R packages poppr version 2.5.0 (Kamvar et al. 2015a, 2014), adegenet 2.0.1 (Jombart, 2008), and ade4 1.7-8 (Dray and Dufour 2007). Analyses were performed with a population hierarchy that included levels for lineage, island, and site. Implementation and interpretation of poppr graphics, as well as source code for modifying poppr output, was adapted from http://grunwaldlab.github.io/Population_Genetics_in_R/ (Kamvar and Grünwald et al. 2016).

Genotypic and gene diversity estimates were calculated with the R package *poppr* (Kamvar et al. 2015a, 2014), including Shannon-Weiner diversity (H) (Shannon 2001) and Nei's unbiased gene diversity (H_e) (Nei 1978). Genotypic richness was estimated as the number of expected multilocus genotypes (eMLG) in a minimum shared sample size of 10 isolates (Kamvar and Grünwald et al. 2016). Repeated MLGs occurring across the subpopulations within each level of the population hierarchy were identified with the function mlg.crosspop from the R package *poppr* (Kamvar et al. 2014). Because analyses of genotypic diversity are sensitive to differences in sample size between groups (Grünwald et al. 2003), H was estimated from 1,000 iterations of a bootstrap analysis with rarefaction, as implemented in *poppr* (Kamvar et al. 2015a, 2014). Random subsamples of the data were selected such that the number of samples in each group was equal to the sample size of the group with the smallest number of samples, with a minimum rarefaction sample size of 10 (Kamvar et al. 2015a, 2014). This allowed for the direct comparison of diversity estimates among lineages, islands, and sites. Rarefaction genotypic richness curves were constructed using the *vegan* package in R (Oksanen et al. 2017), and a genotype accumulation curve was produced with the R package *poppr* (Kamvar et al. 2015a, 2014).

The effect of the reproductive mode of the fungus on the genetic structure of the New Zealand population was examined by estimating linkage disequilibrium. The standardized multilocus index of association, $\bar{r}_d$ (Agapow and Burt 2001), was calculated with the R package *poppr* (Kamvar et al. 2015a, 2014). Analyses were performed with the full dataset, on a clone-censored dataset (to eliminate the influence of repeated MLGs), and on the lineage 1 isolates separately (to eliminate the influence of reproductively-isolated subpopulations). The linkage disequilibrium estimate was not calculated for the clone-corrected Lineage 2 isolates due to inadequate sample size. The observed values of $\bar{r}_d$ were plotted in relation to a simulated population in linkage equilibrium. The probability of obtaining the observed value of $\bar{r}_d$, or more extreme, under the null hypothesis of no linkage among loci (H_0: $\bar{r}_d = 0$) was calculated with 999 permutations of the data.

Genetic structure due to differentiation among subpopulations was evaluated with a hierarchical analysis of molecular variance

(AMOVA) (Excoffier et al. 1992) in the R package *poppr* (Kamvar et al. 2015a, 2014), and utilized the *ade4* implementation (Dray and Dufour 2007). This method partitioned the genetic variance within and among populations and subpopulations across all levels of the population hierarchy, which was clone-censored with respect to hierarchical level. Fixation indices (ϕ statistics) were interpreted as measures of subpopulation differentiation (Excoffier et al. 1992). The probability of obtaining the observed ϕ, or more extreme, under the null hypothesis of no differentiation between subpopulations (H_0: $\phi = 0$) was obtained from 1,000 iterations of a permutation test implemented with the R package *ade4* (Dray and Dufour 2007).

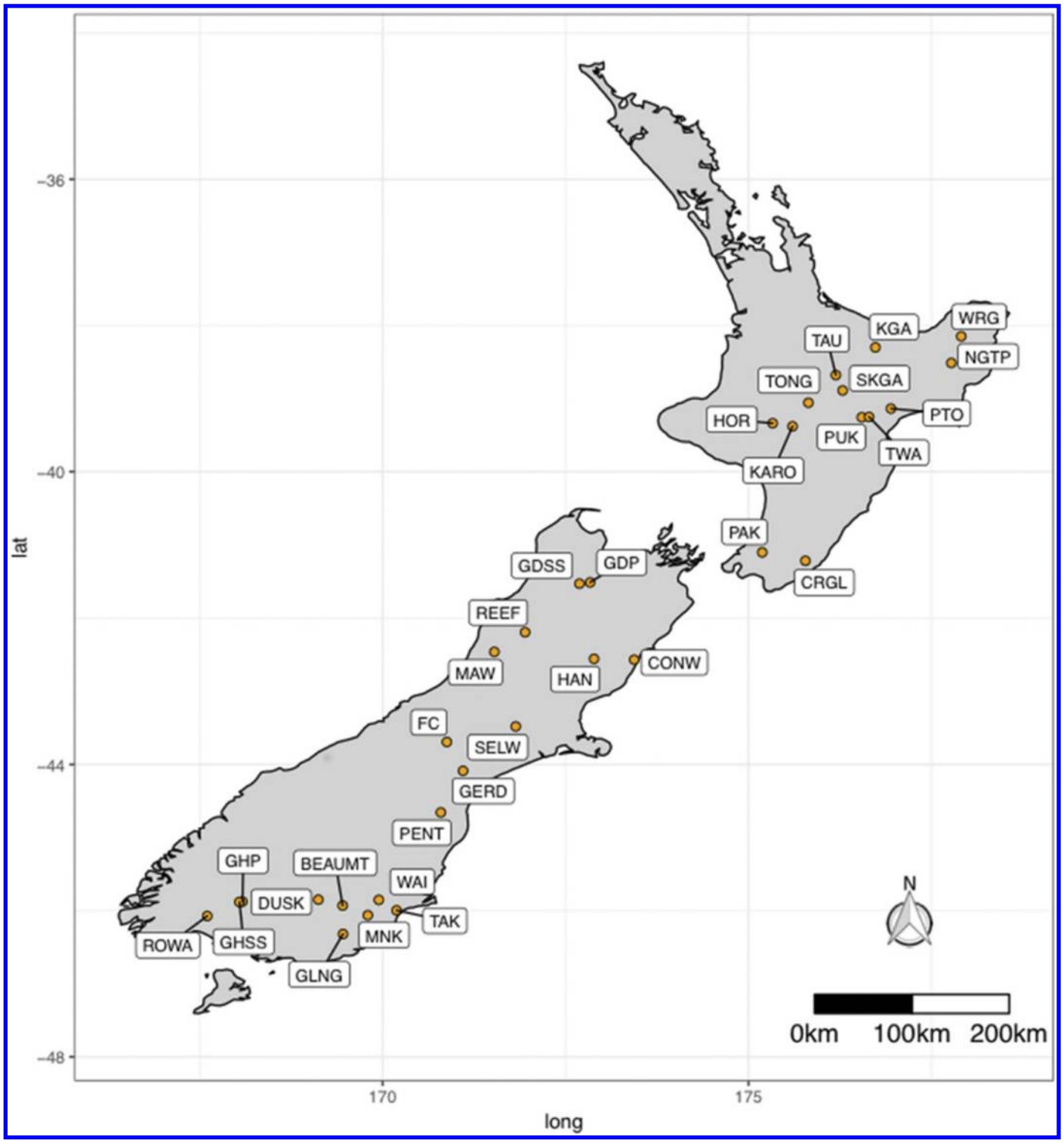

Fig. 1. Locations of 32 sampling sites from which foliage was collected for isolation of *Nothophaeocryptopus gaeumannii* in New Zealand. Sites were Craigie Lea (CRGL), Horopito (HOR), Karioi (KAR), Kaingaroa (KGA), Ngatapa (NGTP), Pakuratahi (PAK), Putorino (PTO), Puketitiri (PUK), South Kaingaroa (SKGA), Tauhara (TAU), Tongariro (TONG), Te Waka (TWA), and Wairangi (WRG) on the North Island and Beaumont (BEAUMT), Conway Hills (CONW), Dusky (DUSK), Forest Creek (FC), Golden Downs (Progeny) (GD-P), Golden Downs (Seed Source) (GD-SS), Geraldine (GERD), Gowan Hills (Progeny) (GH-P), Gowan Hills (Seed Source) (GH-SS), Glenelg (GLNG), Hanmer (HAN), Mawhera (MAW), Manuka Awa (MNK), Pentland Hills (PENT), Reefton (REEF), Rowallen (ROWA), Selwyn (SELW), Takitoa (TAK), and Waipori (WAI) on the South Island.

Subpopulation differentiation between islands and sites within islands was further explored with discriminant analysis of principal components (DAPC), a multivariate analysis of genetic clustering among isolates (Jombart et al. 2010). The function xvaldapc from the R package *adegenet* (Jombart 2008) was utilized with a dataset that was clone-censored with respect to the hierarchical level of interest. For the DAPC analyses presented here, the number of principal components corresponding to the lowest mean squared error was selected via cross-validation, with a training set consisting of 90% of the data (Jombart and Collins 2015).

Similarities among the MLGs were visualized as a UPGMA dendrogram constructed with 10,000 replicates of a bootstrap analysis of Nei's genetic distance (Nei 1978, 1972). This analysis was performed with the aboot function in the R package *poppr* (Kamvar et al. 2015a, 2014), and the dendrogram was visualized with the R package *ggtree* version 1.12.0 (Yu et al. 2017).

Mantel's test (Mantel 1967) was performed with the R package *ade4* (Dray and Dufour 2007). This test utilizes a regression approach to test for a statistical correlation between a matrix containing pairwise Euclidean geographic distances among the 32 sample sites and a matrix containing pairwise values for Roger's genetic distance (Rogers 1972) among the sites. The genetic distance among sites was calculated with the R package *adegenet* (Jombart 2008). A randomization test with 10,000 permutations was employed to test the null hypothesis of no correlation between genetic distance and geographic distance (H_0: $r = 0$).

RESULTS

Genetic diversity. Of the 2,085 total isolates analyzed for this study, 468 unique MLGs were detected. The genotype accumulation curve showed that 90% of the MLGs could be distinguished on the basis of eight SSR loci (Supplementary Fig. S1). A total of 2,067 of the isolates were associated to lineage 1, while 18 isolates were associated to Lineage 2 (Table 1). The Lineage 2 isolates were collected from Forest Creek (FC), Golden Downs (GD-P, GD-SS), Kaingaroa (KGA), South Kaingaroa (SKGA), and Mawhera (MAW). Even with a large sample size, we did not capture all of

TABLE 1. Sample sizes and diversity estimates for the *Nothophaeocryptopus gaeumannii* isolates collected from 32 sites in the North and South Islands of New Zealand

Population level	$N_{isolates}$[a]	MLG[b]	eMLG[c]	SE[d]	H*[e]	H_e[f]
Lineage						
L1	2,067	464	14.4	1.68	2.56	0.65
L2	18	4	4	0	1.24	0.43
Total lineage	2,085	468	14.4	1.67	2.57	0.66
North Island						
Craigie Lea (CRGL)	47	25	7.70	1.21	1.93	0.55
Horopito (HOR)	25	15	7.59	1.11	1.92	0.46
Karioi (KAR)	168	64	8.51	1.08	2.08	0.64
Kaingaroa (KGA)	176	56	7.10	1.36	1.78	0.48
Ngatapa (NGTP)	49	21	7.36	1.19	1.89	0.53
Pakuratahi (PAK)	46	21	7.57	1.16	1.94	0.41
Putorino (PTO)	18	10	6.52	1.02	1.68	0.31
Puketitiri (PUK)	60	33	8.30	1.13	2.02	0.52
South Kaingaroa (SKGA)	46	27	8.76	0.94	2.13	0.60
Tauhara (TAU)	177	112	9.49	0.70	2.23	0.65
Tongariro (TONG)	24	15	7.62	1.10	1.93	0.44
Te Waka (TWA)	64	31	7.79	1.21	1.96	0.37
Wairangi (WRG)	53	35	8.59	1.07	2.08	0.54
Total North Island	953	335**	–	–	–	0.64
South Island						
Beaumont (BEAUMT)	154	48	8.10	1.14	2.02	0.53
Conway Hills (CONW)	12	7	6.00	0.67	1.50	0.44
Dusky (DUSK)	29	12	5.66	1.21	1.54	0.25
Forest Creek (FC)	25	10	6.08	1.05	1.65	0.23
Golden Downs (Progeny) (GD-P)	127	28	5.37	1.35	1.36	0.23
Golden Downs (Seed Source) (GD-SS)	71	26	7.37	1.22	1.88	0.54
Geraldine (GERD)	15	7	6.02	0.72	1.69	0.34
Gowan Hills (Progeny) (GH-P)	170	49	7.64	1.23	1.93	0.68
Gowan Hills (Seed Source) (GH-SS)	91	21	6.03	1.28	1.60	0.62
Glenelg (GLNG)	22	10	6.83	0.96	1.82	0.39
Hanmer (HAN)	138	39	7.16	1.31	1.82	0.59
Mawhera (MAW)	10	2	2.00	0.00	0.50	0.20
Manuka Awa (MNK)	48	12	4.99	1.22	1.30	0.30
Pentland Hills (PENT)	12	9	7.82	0.65	1.98	0.31
Reefton (REEF)	18	7	5.65	0.80	1.61	0.50
Rowallen (ROWA)	38	14	6.94	1.09	1.82	0.48
Selwyn (SELW)	12	11	9.32	0.47	2.21	0.41
Takitoa (TAK)	17	11	7.24	1.01	1.85	0.47
Waipori (WAI)	123	30	5.89	1.35	1.55	0.44
Total South Island	1,132	193**	–	–	–	0.64
Total	2,085	468**	8.73	1.06	2.12	0.66

[a] $N_{isolates}$ = number of *N. gaeumannii* isolates.
[b] MLG = number of multilocus genotypes.
[c] eMLG = expected number of multilocus genotypes in rarefied sample equal to the number of samples in the group with the smallest number of samples (N = 10 isolates for pooled sites).
[d] SE = standard error of eMLG estimate.
[e] H = Shannon- Weiner diversity index (Shannon 2001).
[f] H_e = Nei's unbiased gene diversity (expected heterozygosity) (Nei 1978). *indicates estimated genotypic diversity from 1,000 bootstrap replicates with rarefaction sample sizes equal to the number of samples in the group with the smallest number of samples (N = 10 isolates for pooled sites). – = data not calculated. ** indicates total MLG not equal to the sum of population totals due to shared MLGs.

the expected genetic variation in lineage 1 (Supplementary Fig. S2). However, the four MLGs from the 18 Lineage 2 isolates were sufficient to represent the expected genetic variation within Lineage 2. Lineage 2 had lower genetic diversity than lineage 1 after accounting for differences in sample size via rarefaction (Table 1).

Overall, genotypic diversity and richness were higher for the North Island populations, but gene diversity did not differ considerably between the *N. gaeumannii* populations in the North and South islands (Table 1). Isolates sampled from Tauhara (TAU), near Taupo in the central part of the North Island, had the highest genotypic diversity of all sites in New Zealand, the highest genotypic richness, and the second highest gene diversity (Table 1). The lowest diversity was observed for the *N. gaeumannii* isolates collected at the South Island site Mawhera (Table 1).

Population structure and differentiation. The observed value of the multilocus index of association ($\bar{r}_d$; Agapow and Burt 2001), an estimate of linkage disequilibrium, for the total New Zealand population (N = 2,085 isolates) was significantly larger than expected for the simulated population in which there was no linkage among loci ($\bar{r}_d = 0.307$, $P = 0.001$) (Supplementary Fig. S3). This indicates that alleles do not pair randomly in MLGs, and thus the population is not panmictic. This linkage disequilibrium was also detected, though to a lesser extent, when the repeated MLGs (i.e., clones) were removed from the data (N = 468 isolates) ($\bar{r}_d$ = 0.130, P = 0.001). Linkage disequilibrium was slightly less when the analysis was performed with only the unique lineage 1 MLGs (n = 464 isolates) ($\bar{r}_d$ = 0.126, P = 0.001).

The partitioning of molecular variance within and among the levels of a clone-corrected population hierarchy indicated that most of the genetic variation was within sites (Table 2). Strong genetic differentiation was detected between the two *N. gaeumannii* lineages (Table 2). Moderate genetic differentiation was detected between sample sites within the islands, but there little genetic differentiation between the North and South Island populations (Table 2).

Many isolates had a high probability of being assigned to the North Island cluster, even if they had been collected in the South Island, and vice versa. The bar plot produced from the DAPC with clusters representing the North and South Islands showed a high degree of admixture, as the bars representing each genotype had high probabilities of membership in both clusters (Fig. 2A). The DAPC scatterplot depicting the relationships among isolates collected from each of the sites in New Zealand showed considerable overlap among sites, with few isolates lying outside of the central cluster of points (Fig. 2B). The isolates that appeared to be the most highly differentiated in this plot are the *N. gaeumannii* Lineage 2 genotypes from South Kaingaroa (North Island), Mawhera (South Island), and Golden Downs (South Island) (Fig. 2B).

The isolates corresponding to lineages 1 and 2 clustered into distinct groups in the UPGMA dendrogram based on Nei's genetic distance. These clusters were separated at the basal node with strong bootstrap support (Fig. 3).

Spatial distributions of multilocus genotypes. A total of 104 MLGs occurred at more than one site. Sixty of those 104 MLGs were recovered from both islands (Table 1, Fig. 4). The most common genotype (MLG 261) was shared among 291 individuals (Fig. 4), and was present at 17 sites across the North and South Islands. There were 104 unique (private) alleles in the South Island subpopulation, and 71 private alleles the North Island subpopulation. There was no isolation by distance detected, as no significant correlation was found between the geographic and genetic distance matrices (r = −0.013, P = 0.562). The 18 Lineage 2 isolates comprised only four distinct MLGs (Table 1, Fig. 5). One Lineage 2 MLG was collected from two sites in the North Island: Kaingaroa (KGA) and South Kaingaroa (SKGA), while the other three Lineage 2 MLGs were present at four sites in the South Island: Golden Downs (GD-SS and GD-P), Mawhera (MAW), and Forest Creek (FC) (Fig. 5). The most common Lineage 2 genotype (MLG 11) occurred at both Mawhera and Forest Creek (Fig. 5), and the second Lineage 2 genotype that occurred at Mawhera (MLG 10) was also present at a Golden Downs site (GD-P).

TABLE 2. Hierarchical analysis of molecular variance (AMOVA) performed with clone-corrected dataset including unique SSR multilocus genotypes from 468 *Nothophaeocryptopus gaeumannii* isolates collected from 32 sites in the North and South Islands of New Zealand

Hierarchical level	Variance (%)	ϕ	P[a]
ϕ_{LT} (between lineages)	33.546	0.335	<0.001
ϕ_{IL} (between islands within lineages)	0.245	0.004	0.222
ϕ_{SI} (between sites within islands)	8.264	0.125	<0.001
ϕ_{SS} (within sites)	57.945	0.421	<0.001

[a] P value was obtained for the ϕ statistic with 1,000 permutations of the data.

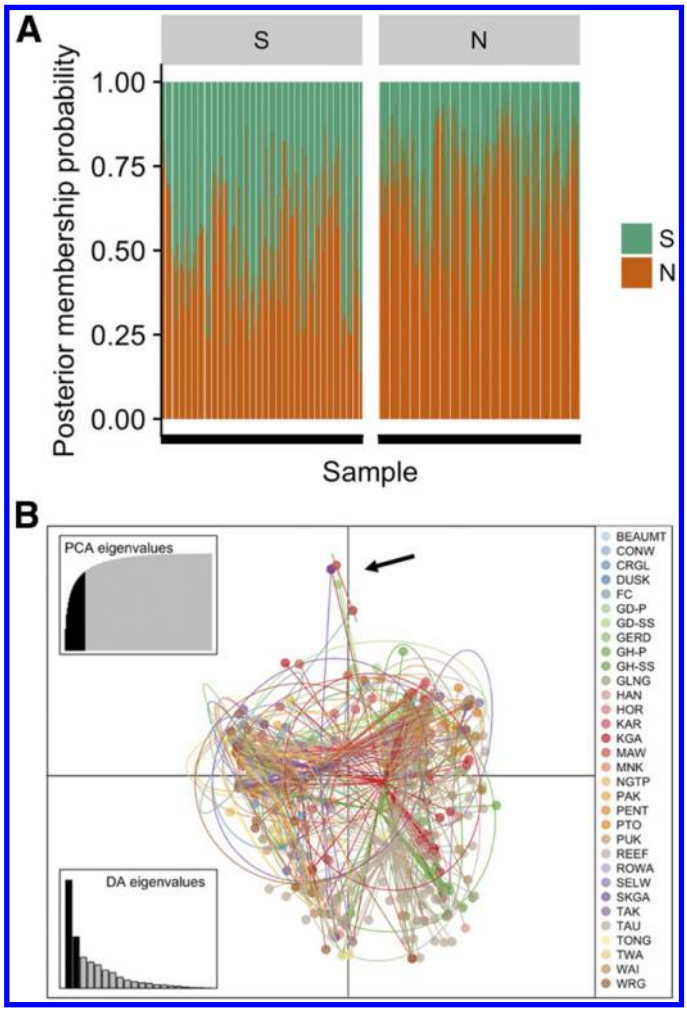

Fig. 2. A, Bar plot from discriminant analysis of principal components (DAPC) showing posterior membership probabilities of 468 *Nothophaeocryptopus gaeumannii* multilocus genotypes (MLGs) in clusters representing the North (N) and South (S) Islands of New Zealand. Each bar represents one MLG, and the colored portion of each bar represents the probability of membership of that MLG in the North and/or South Island clusters. **B,** DAPC scatterplot showing clustering among MLGs from 32 sites. Each color represents a cluster (here, a site), and each point represents an MLG. Overlapping points represent identical MLGs. Inertia ellipses are drawn around 2/3 of the isolates in each cluster. The inset at top left indicates the proportion of principal components retained, while the graph at lower left indicates the number of discriminant functions retained. The legend at right shows the site name abbreviations corresponding to each cluster (Table 1, Fig. 1). The arrow in B points to the divergent genotypes (Lineage 2) from Mawhera (MAW), South Kaingaroa (SKGA), and Golden Downs (GD).

DISCUSSION

Populations of *N. gaeumannii* in New Zealand exhibit characteristics that are typical of an introduced pathogen. Estimates of both Shannon diversity and Nei's gene diversity were lower for the total New Zealand population compared with the U.S. population (4.59 versus 6.09 and 0.655 versus 0.820 for H and H_e, respectively) (Bennett and Stone 2016). This, along with the high linkage disequilibrium observed, may indicate a genetic bottleneck whereby a small group of individuals was introduced in one or more discrete events, and a founder effect due to subsequent genetic drift in the introduced population. Isolates from Tauhara (TAU), a site in the central North Island near Taupo where *N. gaeumannii* was first reported in 1959, had the highest genotypic diversity and richness (Table 1). This is consistent with the central North Island being the locus of initial introduction of *N. gaeumannii*, as suggested by Hood and Kershaw (1975). However, isolates recovered from this site consisted of lineage 1 genotypes exclusively. Isolates of Lineage 2 were recovered nearby at Kaingaroa, but their MLGs were not similar to the Lineage 2 isolates collected from the South Island sites Mawhera, Forest Creek, and Golden Downs (Fig. 5). The presence of distinct Lineage 2 MLGs in the North and South Islands could be the result of independent introductions from western North America, as these isolates exhibited combinations of alleles in MLGs that, until now, have only been detected in western Oregon (Bennett and Stone 2016; Winton et al. 2006). This strongly suggests that the New Zealand *N. gaeumannii* population originated from a source in the coastal Douglas-fir forests of western North America.

One potential limitation of the sampling design for this study is that there was unequal sampling among the levels of the population hierarchy. Although foliage was collected from 10 trees at each site, the number of isolates collected from each of the trees was not uniform. This was due to variation in infection levels, as well as sample loss due to culture contamination. Another factor that contributed to unequal sample sizes was that not all sites were sampled in both years. Those that were sampled in only 2005 or 2007 generally had fewer isolates. We attempted to account for unequal sample sizes by using rarefaction when calculating genetic diversity and richness.

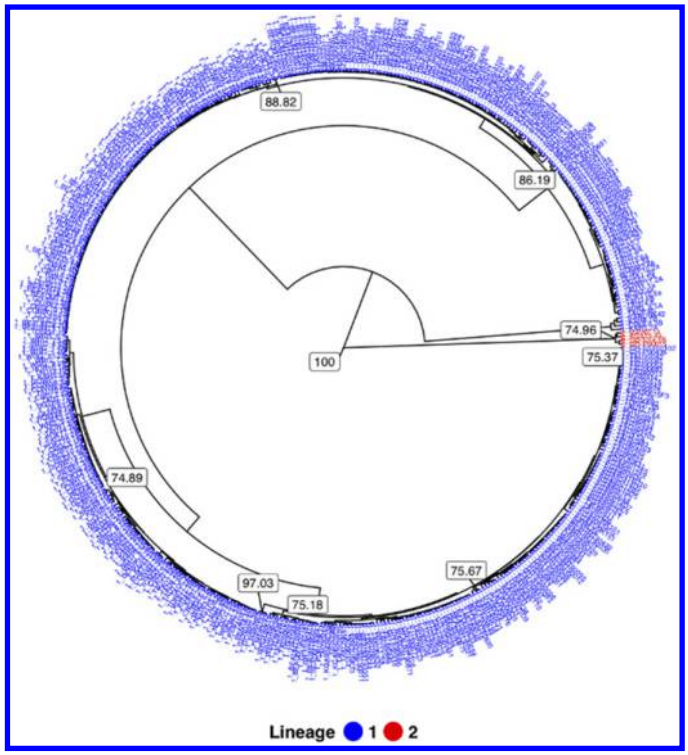

Fig. 3. UPGMA dendrogram from a bootstrap analysis of Nei's genetic distance (Nei 1972, 1978) showing divergence among *Nothophaeocryptopus gaeumannii* multilocus genotypes (MLGs) corresponding to two lineages from New Zealand (clone-censored, N = 468). Node labels represent bootstrap statistics (≥70%) from 10,000 replicate trees.

The reproductive biology of *N. gaeumannii* appears to have had a strong influence on the contemporary structure of the introduced New Zealand population. Estimates of the multilocus index of association suggested that alleles in this population do not associate randomly in multilocus genotypes, as would be expected in a random-mating population (Agapow and Burt 2001). For a haploid fungus, self-fertilization and asexual reproduction both can result in clonal population structures (Taylor et al. 1999; Winton et al. 2006). The clonal population structure we observed might be expected to result from asexual reproduction via mitospores (conidia), except that conidial reproduction has not been observed in *N. gaeumannii*, despite considerable scrutiny (Stone et al. 2008a). Rather, the explanation for this population structure appears to be that *N. gaeumannii* is homothallic, resulting in progeny that are genetically identical to the parent. An alternative explanation is that *N. gaeumannii* is outcrossing, but recombination between individuals with similar or identical MLGs does not lead to significant change in genetic diversity.

Significant linkage disequilibrium was also detected, albeit to a lesser degree, when repeated MLGs were removed, suggesting that the population structure of *N. gaeumannii* is strongly influenced by its reproductive mode. High linkage disequilibrium due to the presence of clones is often interpreted as evidence of an "epidemic" population structure in pathogenic microbes, whereby natural selection results in an abundance of certain genotypes that have superior fitness (often due to greater virulence or aggressiveness) relative to the rest of the population (Smith et al. 1993). In addition to the observation that a few genotypes were particularly abundant in this invasive population, the high linkage disequilibrium due to large numbers of clones could be an indication of such an epidemic population structure in New Zealand. However, the relative aggressiveness of the overrepresented genotypes has not been examined experimentally, and disease severity does not appear to coincide with the distribution of Lineage 2 or the overrepresented genotypes (discussed below). The apparent linkage disequilibrium was also due, at least in part, to the presence of reproductively-isolated subpopulations (i.e., lineages 1 and 2). When the two lineages were analyzed separately, $\bar{r}_d$ for the lineage 1 subpopulation was reduced. However, after removing duplicate MLGs from the dataset, linkage disequilibrium for the lineage 1 subpopulation was still much higher than would be expected with random mating. High linkage disequilibrium in the absence of repeated MLGs and reproductively isolated subpopulations may have resulted from a bottleneck due to the introduction of a small founding population in which allele frequencies were subsequently altered by genetic drift (Hartl and Clark 2007).

The AMOVA and bootstrap analyses revealed that the lineages were strongly differentiated, as they accounted for a large proportion of the between-population variation, and were separated at a basal node into distinct clusters on the UPGMA dendrogram with strong statistical support. These results are consistent with the findings of Winton et al. (2006), who provided evidence that the two *N. gaeumannii* lineages are reproductively isolated in endemic populations in the northwestern United States. In addition to a thorough examination of morphological, biochemical, and ecological traits that might differ between the two lineages, nucleotide sequence data from multiple genes (or full genomes) should be analyzed to determine whether sufficient evidence exists to recognize them as separate species.

Given that the Douglas-fir production regions in the North and South Islands are very patchy and do not form a contiguous distribution, we expected that spread via aerial ascospore

dispersal would result in some genetic differentiation between the islands, and between sites within the islands, due to dispersal limitations. However, only a very small proportion of the overall genetic variation occurred between islands (Table 2), and there was little genetic differentiation between them (Table 2, Fig. 2A). The lack of genetic differentiation between the North and South Islands is further supported by the fact that there were 60 shared MLGs between them (Fig. 4). Despite the apparent lack of differentiation, there were private alleles that were unique in the North and South Islands. This could be due to independent introduction events or genetic divergence due to mutation, selection, or drift.

A moderate, but significant, degree of genetic differentiation was identified among the isolates collected from sites within the islands, but there was little differentiation among genotypes from the 32 sites (Fig. 2B). Several Lineage 2 genotypes fell outside of the central cluster of points in the DAPC scatter plot suggesting that some of the genetic variation among sites was due to the presence of Lineage 2 (Fig. 2B). Still, the majority of the genetic variation was partitioned to the within-site component, suggesting that gene flow has occurred between them (Table 2).

There were 104 MLGs that occurred at more than one site, and the most common MLG was shared by 271 individuals (Fig. 4) across 17 sites. This MLG was present at both Wairangi (North Island) and Gowan Hills (South Island), which are nearly 1,000 km apart (Fig. 1). However, our ability to distinguish genotypes could have been enhanced if additional loci had been included. Despite the large

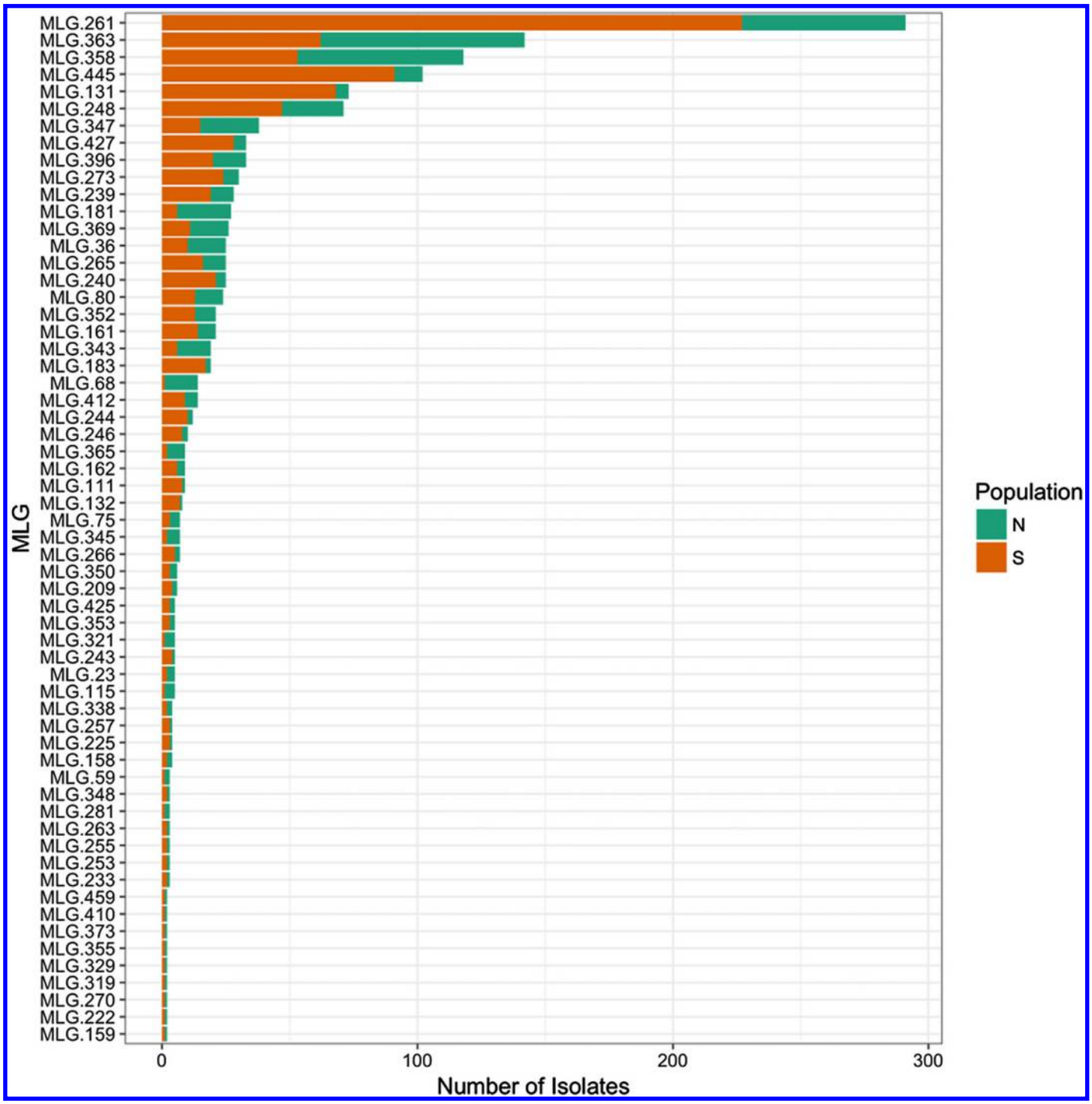

Fig. 4. Abundances of the 60 *Nothophaeocryptopus gaeumannii* simple sequence repeat multilocus genotypes (MLGs) shared between the North (N) and South (S) Islands of New Zealand. Each bar represents a unique MLG, with the shaded portions of each bar corresponding to the number of isolates with that MLG on each island.

number of samples and the fact that the genotype accumulation curve suggested that we should have been able to resolve 90% of the MLGs with only eight loci, the rarefaction curve indicated that we were not able to capture all of the expected genetic variation within lineage 1. This also suggests that had we continued to genotype more lineage 1 isolates, we would have continued to discover new genotypes.

There was no isolation by distance in the New Zealand *N. gaeumannii* populations, as no correlation between the genetic distances and geographic distances among sites was detected. The distribution of lineage 1 MLGs across New Zealand was relatively homogeneous, with few genetic barriers or dispersal limitations. Hood and Kershaw (1975) and Hood et al. (1990) documented the gradual spread of *N. gaeumannii* from a single introduction locus near Taupo to the rest of the North Island, and subsequently throughout the South Island, over a period of approximately 30 years. A gradual spread and colonization via the aerial dispersal of ascospores over short distances would be expected to result in some genetic differentiation between the islands, or between sites within each island. The effects of random dispersal, local adaptation, mutation, natural selection, and genetic drift would presumably lead to genetic variation across sites over time. Unless long-distance ascospore dispersal occurs regularly, the gradual expansion from a single source would also be expected to result in an isolation by distance phenomenon whereby genetic dissimilarity increases with the geographic distance between sites. A similar line of reasoning was used to test hypotheses about the introduction and spread of the sudden oak death pathogen, *Phytophthora ramorum*, in Oregon. Kamvar et al. (2015b) described the spread of *P. ramorum* populations from two points of introduction. Those authors suggested that it was the accumulation of mutations during the spread of these clonal populations that resulted in isolation by distance, and that this pattern would not be expected to occur if the spread had occurred via long distance dispersal (Kamvar et al. 2015b). Since we did not observe isolation by distance associated with the introduction and spread of *N. gaeumannii* in New Zealand, we can infer that either mutation rates are low, or that migration rates between sites are high. An alternative explanation for the lack of differentiation between islands, and between sites within islands, is a "stepping-stone" hypothesis in which connectivity between distant patches of a host plant may be attained by ascospore dispersal over shorter distances (Linde et al. 2002). The colonization of isolated Douglas-fir plantations via human-mediated dispersal by movement of infected plant material, or long-distance aerial ascospore dispersal among sites within and between islands could also have resulted in the observed lack of differentiation between sites. The aerial dispersal of ascospores over 1,000 km would be exceedingly rare (Brown and Hovmøller 2002; Rivas et al. 2004). The observed distribution of MLGs also could have resulted from the establishment of Douglas-fir plantations in the North and South Islands with infected seedlings from a single source population such as a nursery.

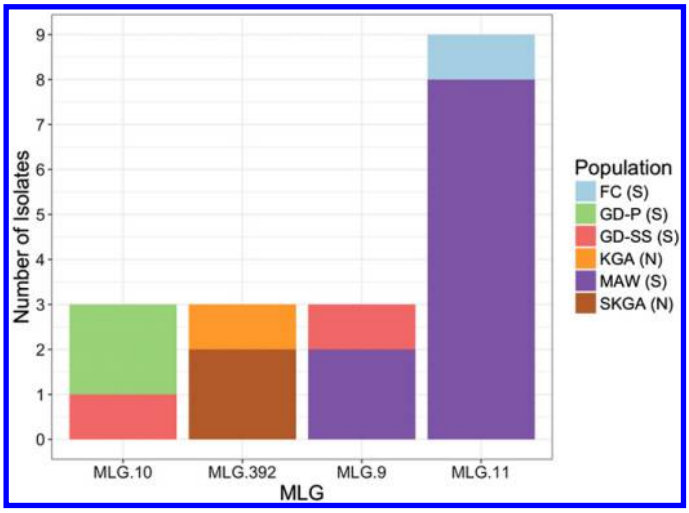

Fig. 5. Bar plot showing the abundances of four *Nothophaeocryptopus gaeumannii* Lineage 2 simple sequence repeat multilocus genotypes (MLGs) at six sites in the North (N) and South (S) Islands of New Zealand. Each bar represents a unique Lineage 2 MLG, with the colored portions of the bars corresponding to the number of isolates with that MLG at each of the sites listed in the legend: Forest Creek (FC), Golden Downs (Progeny) (GD-P), Golden Downs (Seed Source) (GD-SS), Kaingaroa (KGA), Mawhera (MAW), and South Kaingaroa (SKGA); (S) = South Island and (N) = North Island.

Given that there has apparently been gene flow between the Douglas-fir plantations in the North and South Islands, the fact that there were Lineage 2 MLGs that were relatively abundant in the South Island but were not detected in the North Island suggests that there may have been a separate introduction to the South Island from a source in western North America. However, it is possible that either the observed distribution of Lineage 2 genotypes resulted from a single introduction near Taupo and our sampling did not recover Lineage 2 MLGs that were present, or that Lineage 2 genotypes initially present in the North Island spread to the South Island but subsequently went extinct in the North Island. The latter, however, is a much less parsimonious explanation. Nevertheless, the four MLGs we detected from 18 Lineage 2 isolates seemed to account for all of the expected genotypic richness in Lineage 2. It is also possible that differentiation of local populations where Lineage 2 was abundant in the South Island, i.e., at Golden Downs and Mawhera, has occurred via natural selection, or is due to processes such as genetic drift, which is particularly influential in small populations such as these (Hartl and Clark 2007).

One major question that remains largely unanswered is whether the genetic variation in *N. gaeumannii* is related to SNC severity. Winton et al. (2006) suggested that Lineage 2 may have contributed to the emergence of SNC in the native range of Douglas-fir, as they found that a higher Lineage 2 to lineage 1 ratio was associated with lower canopy density and increased foliage discoloration in some stands in coastal northwestern Oregon. The distribution of Lineage 2 in the northwestern Coast Ranges in Oregon and Washington generally corresponds to the region where SNC is most severe (Bennett and Stone 2016; Winton et al. 2006). This suggests that there is some variation in aggressiveness between strains of this fungus (Winton et al. 2006). However, a difference in aggressiveness between the two lineages has not been definitively demonstrated. In New Zealand, the geographic distribution of Lineage 2 was very limited and was not restricted to sites with severe disease (data not shown). Much of the variation in SNC severity among sites occurred where *N. gaeumannii* Lineage 2 was absent. The fact that disease severity seemed to vary across sites in New Zealand despite the fact that the lineage 1 genotypes were relatively uniformly distributed in both the North and South Islands suggests that there is no clear association between specific genotypes or lineages and disease. The observed spatial variation in SNC severity in New Zealand is much more likely to be a function of climate, as areas with warmer winter temperatures and more precipitation in spring and early summer generally have more severe SNC symptoms (Stone et al. 2007; Watt et al. 2010).

The records of the introduction of Douglas-fir into New Zealand for use as a plantation forestry species imply that plantations were established using seed obtained from western North America, rather than planting stock, and were locally propagated thereafter (Hood and Kershaw 1975; Weston 1957). However, *N. gaeumannii* was most likely introduced on infected live seedlings through the forestry or ornamental nursery trade because *N. gaeumannii* can only be vectored on live or recently abscised foliage. It is highly unlikely that *N. gaeumannii* migrated to New Zealand naturally via passive ascospore dispersal, given that major dispersal barriers and vast distances exist between New Zealand and the nearest known *N. gaeumannii* populations in Europe and North America. The SNC fungus was present in Europe long before it was detected in New

Zealand, but Lineage 2 has only been found in coastal northwestern North America and New Zealand, which strongly suggests North America as the source.

ACKNOWLEDGMENTS

We thank J. Britt, J. F. Gardner, R. J. Hood, and W. Sutton for field and laboratory assistance; Z. Kamvar and J. Tabima for assistance in the implementation and interpretation of analyses performed with the R packages *poppr* and *adegenet*; J. Chang, N. Grünwald, and two anonymous reviewers whose comments helped improve this manuscript; and the many forest landowners in New Zealand who generously provided access to their lands.

LITERATURE CITED

Agapow, P., and Burt, A. 2001. Indices of multilocus linkage disequilibrium. Mol. Ecol. Notes 1:101-102.

Baquero, O. S. 2017. ggsn: North symbols and scale bars for maps created with 'ggplot2' or 'ggmap'. R package version 0.4.0. https://cran.r-project.org/web/packages/ggsn/index.html

Bennett, P., and Stone, J. 2016. Assessments of population structure, diversity, and phylogeography of the Swiss needle cast fungus (*Phaeocryptopus gaeumannii*) in the U.S. Pacific Northwest. Forests 7:14.

Boyce, J. S. 1940. A needle-cast of Douglas fir associated with *Adelopus gaumanni*. Phytopathology 30:649-659.

Brown, J. K. M., and Hovmøller, M. S. 2002. Aerial dispersal of pathogens on the global and continental scales and its impact on plant disease. Science 297:537-541.

Castaño, C., Colinas, C., Gómez, M., and Oliva, J. 2014. Outbreak of Swiss needle cast caused by the fungus *Phaeocryptopus gaeumannii* on Douglas-fir in Spain. New Dis. Rep. 29:19.

Dray, S., and Dufour, A.-B. 2007. The ade4 package: Implementing the duality diagram for ecologists. J. Stat. Softw. 22:1-20.

Excoffier, L., Smouse, P. E., and Quattro, J. M. 1992. Analysis of molecular variance inferred from metric distances among DNA haplotypes: Application to human mitochondrial DNA restriction data. Genet. Soc. Am. 131: 479-491.

Grünwald, N. J., Goodwin, S. B., Milgroom, M. G., and Fry, W. E. 2003. Analysis of genotypic diversity data for populations of microorganisms. Phytopathology 93:738-746.

Hansen, E. M., Stone, J. K., Capitano, B. R., Rosso, P., Sutton, W., Winton, L., Kanaskie, A., and McWilliams, M. G. 2000. Incidence and impact of Swiss needle cast in forest plantations of Douglas-fir in coastal Oregon. Plant Dis. 84:773-778.

Hartl, D. L., and Clark, A. G. 2007. Principles of Population Genetics, 4th ed. Sinauer Associates, Sunderland, MA.

Hood, I. A., and Kershaw, D. J. 1973. Distribution and life history of *Phaeocryptopus gaeumannii* on Douglas Fir in New Zealand (Forest Pathology Report No. 37 (unpublished)). New Zealand Forest Service, Forest Research Institute.

Hood, I. A., and Kershaw, D. J. 1975. Distribution and infection period of *Phaeocryptopus gaeumannii* in New Zealand. N. Z. J. For. Sci. 5: 201-208.

Hood, I. A. 1982. *Phaeocryptopus gaeumannii* on *Pseudotsuga menziesii* in Southern British Columbia. N.Z. J. For. Sci. 12:415-424.

Hood, I. A., Sandberg, C. J., Barr, C. W., Holloway, W. A., and Bradbury, P. M. 1990. Changes in needle retention associated with the spread and establishment of *Phaeocryptopus gaeumannii* in planted Douglas fir. Eur. J. For. Pathol. 20:418-429.

Jombart, T. 2008. adegenet: An R package for the multivariate analysis of genetic markers. Bioinformatics 24:1403-1405.

Jombart, T., and Collins, C. 2015. A tutorial for discriminant analysis of principal components (DAPC) using adegenet 2.0.0. Imperial College London, MRC Centre for Outbreak Analysis and Modelling, London.

Jombart, T., Devillard, S., and Balloux, F. 2010. Discriminant analysis of principal components: A new method for the analysis of genetically structured populations. BMC Genet. 11:94.

Kamvar, Z. N., and Grünwald, N. 2016. grunwaldlab/Population_Genetics_in_R: First release [Dataset]. Online publication. Zenodo. doi: 10.5281/zenodo.160588

Kamvar, Z. N., Brooks, J. C., and Grünwald, N. J. 2015a. Novel R tools for analysis of genome-wide population genetic data with emphasis on clonality. Front. Genet. 6:208.

Kamvar, Z. N., Larsen, M. M., Kanaskie, A. M., Hansen, E. M., and Grünwald, N. J. 2015b. Spatial and temporal analysis of populations of the sudden oak death pathogen in Oregon forests. Phytopathology 105:982-989.

Kamvar, Z. N., Tabima, J. F., and Grünwald, N. J. 2014. *Poppr*: An R package for genetic analysis of populations with clonal, partially clonal, and/or sexual reproduction. PeerJ 2:e281.

Liese, J. 1939. The occurrence in the British Isles of the Adelopus disease of Douglas fir. Q. J. For. 33:247-252.

Linde, C. C., Zhan, J., and McDonald, B. A. 2002. Population structure of *Mycosphaerella graminicola*: From lesions to continents. Phytopathology 92:946-955.

Mantel, N. 1967. The detection of disease clustering and a generalized regression approach. Cancer Res. 27:209-220.

Manter, D. K., Bond, B. J., Kavanagh, K. L., Rosso, P. H., and Filip, G. M. 2000. Pseudothecia of Swiss needle cast fungus, *Phaeocryptopus gaeumannii*, physically block stomata of Douglas fir, reducing CO_2 assimilation. New Phytol. 148:481-491.

Marks, G. C. 1975. Swiss needle cast of Douglas fir. Australas. Plant Pathol. 4:24.

McCormick, F. A. 1939. *Phaeocryptopus gaeumannii* on Douglas fir in Connecticut. Plant Dis. Rep. 23:368-369.

Meinecke, E. P. 1939. The *Adelopus* needle cast of Douglas fir on the Pacific Coast. Department of Natural Resources, Division of Forestry, Sacramento, CA.

Ministry for Primary Industries. 2016. National Exotic Forest Description. Ministry for Primary Industries, New Zealand.

Morton, H. L., and Patton, R. F. 1970. Swiss needle cast of Douglas-fir in the Lake States. Plant Dis. Rep. 54:612-616.

Nei, M. 1972. Genetic distance between populations. Am. Nat. 106: 283-292.

Nei, M. 1978. Estimation of average heterozygosity and genetic distance from a small number of individuals. Genetics 89:583-590.

Oksanen, J., Guillaume, B., Friendly, M., Kindt, R., Legendre, P., McGlinn, D., Minchin, P. R., O'Hara, R. B., Simpson, G. L., Solymos, P., Stevens, M. H. H., Szoecs, E., and Wagner, H. 2017. vegan: Community Ecology Package. R package version 2.4-5. https://cran.r-project.org/web/packages/vegan/index.html

Osorio, M. 2007. Detección del hongo defoliador *Phaeocryptopus gaeumannii* en plantaciones de *Pseudotsuga menziesii* de Valdivia, Chile. Bosque (Valdivia) 28:69-74.

Peace, T. R. 1962. Pathology of Trees and Shrubs with Special Reference to Britain. Clarendon Press, Oxford.

Peakall, R., and Smouse, P. E. 2006. GenAlEx 6: genetic analysis in Excel. Population genetic software for teaching and research. Mol. Ecol. Notes 6: 288-295.

Peakall, R., and Smouse, P. E. 2012. GenAlEx 6.5: Genetic analysis in Excel. Population genetic software for teaching and research–an update. Bioinformatics 28:2537-2539.

R Core Team. 2017. R: A language and environment for statistical computing. R Foundation for Statistical Computing, Vienna, Austria. https://www.R-project.org

Ritóková, G., Shaw, D., Filip, G., Kanaskie, A., Browning, J., and Norlander, D. 2016. Swiss needle cast in western Oregon Douglas-fir plantations: 20-year monitoring results. Forests 7:155.

Rivas, G. G., Zapater, M. F., Abadie, C., and Carlier, J. 2004. Founder effects and stochastic dispersal at the continental scale of the fungal pathogen of bananas *Mycosphaerella fijiensis*. Mol. Ecol. 13:471-482.

Rogers, J. S. 1972. Measures of genetic similarity and genetic distances. Studies in Genetics, Univ. Texas Publ. 7213:145-153.

Rohde, T. 1936. *Adelopus gaeumannii* n. sp. und die von ihm hervorgerufene "Schweizer" Douglasienschütte. Forstliche Wochenschr. Silva 24: 420-422.

Shannon, C. E. 2001. A mathematical theory of communication. ACM Sigmobile Mob. Comput. Commun. Rev. 5:3-55.

Slowikowski, K. 2017. ggrepel: Repulsive text and label geoms for 'ggplot2'. R package version 0.7.0. https://cran.r-project.org/web/packages/ggrepel/index.html

Smith, J. M., Smith, N. H., O'Rourke, M., and Spratt, B. G. 1993. How clonal are bacteria? Proc. Natl. Acad. Sci. 90:4384-4388.

Stone, J. K., Capitano, B. R., and Kerrigan, J. L. 2008a. The histopathology of *Phaeocryptopus gaeumannii* on Douglas-fir needles. Mycologia 100: 431-444.

Stone, J. K., Coop, L. B., and Manter, D. K. 2008b. Predicting effects of climate change on Swiss needle cast disease severity in Pacific Northwest forests. Can. J. Plant Pathol. 30:169-176.

Stone, J. K., Hood, I. A., Watt, M. S., and Kerrigan, J. L. 2007. Distribution of Swiss needle cast in New Zealand in relation to winter temperature. Australas. Plant Pathol. 36:445.

Taylor, J. W., Jacobson, D. J., and Fisher, M. C. 1999. The evolution of asexual fungi: Reproduction, speciation and classification. Annu. Rev. Phytopathol. 37:197-246.

Temel, F., Stone, J. K., and Johnson, G. R. 2003. First report of Swiss needle cast caused by *Phaeocryptopus gaeumannii* on Douglas-fir in Turkey. Plant Dis. 87:1536.

Watt, M. S., Stone, J. K., Hood, I. A., and Palmer, D. J. 2010. Predicting the severity of Swiss needle cast on Douglas-fir under current and future climate in New Zealand. For. Ecol. Manage. 260:2232-2240.

Weston, G. C. 1957. Exotic forest trees in New Zealand. Statement prepared for the 7th British Commonwealth Forestry Conference, Australia and New Zealand No. 13. New Zealand Forest Service, Wellington, New Zealand.

Wickham, H. 2016. ggplot2: Elegant graphics for data analysis. Springer-Verlag, New York. http://ggplot2.tidyverse.org/

Wilson, M., and Waldie, J. S. L. 1928. Notes on new or rare forest fungi. Trans. Br. Mycol. Soc. 13:151-156.

Winton, L. M., Hansen, E. M., and Stone, J. K. 2006. Population structure suggests reproductively isolated lineages of *Phaeocryptopus gaeumannii*. Mycologia 98:781-791.

Winton, L. M., Stone, J. K., and Hansen, E. M. 2007. Polymorphic microsatellite markers for the Douglas-fir pathogen *Phaeocryptopus gaeumannii*, causal agent of Swiss needle cast disease. Mol. Ecol. Notes 7: 1125-1128.

Yu, G., Smith, D. K., Zhu, H., Guan, Y., and Lam, T. T.-Y. 2017. ggtree: An R package for visualization and annotation of phylogenetic trees with their covariates and other associated data. Methods Ecol. Evol. 8:28-36.